


ETD Archive

Winter 1-2019

Insights Into the Ribosomal, Extra-ribosomal And Developmental Role of Rp L13a In Mammalian Model

Ravinder Kour
Cleveland State University

Follow this and additional works at: <https://engagedscholarship.csuohio.edu/etdarchive>

 Part of the [Cell Biology Commons](#), [Developmental Biology Commons](#), and the [Molecular Biology Commons](#)

[How does access to this work benefit you? Let us know!](#)

Recommended Citation

Kour, Ravinder, "Insights Into the Ribosomal, Extra-ribosomal And Developmental Role of Rp L13a In Mammalian Model" (2019). *ETD Archive*. 1313.
<https://engagedscholarship.csuohio.edu/etdarchive/1313>

This Thesis is brought to you for free and open access by EngagedScholarship@CSU. It has been accepted for inclusion in ETD Archive by an authorized administrator of EngagedScholarship@CSU. For more information, please contact library.es@csuohio.edu.

INSIGHTS INTO THE RIBOSOMAL, EXTRA-RIBOSOMAL AND
DEVELOPMENTAL ROLE OF RP L13A IN MAMMALIAN MODEL

RAVINDER KOUR

Master of Science in Zoology
University of Jammu, Jammu & Kashmir, India
December 2011

submitted in partial fulfillment of requirements for the degree
DOCTOR OF PHILOSOPHY IN REGULATORY BIOLOGY
at the
CLEVELAND STATE UNIVERSITY

December 2019

© Copyright by Ravinder Kour 2019

We hereby approve this dissertation

For Ravinder Kour

Candidate for the Doctor of Philosophy in Regulatory Biology Degree for the Department
of Biological, Geological and Environmental Sciences

AND CLEVELAND STATE UNIVERSITY College of Graduate Studies by

Date: 08/19/2019

Dr. Barsanjit Mazumder, GRHD/BGES, Cleveland State University
Major Advisor

Date: 08/19/2019

Dr. Anton A. Komar, GRHD/BGES, Cleveland State University
Advisory Committee Member

Date: 08/19/2019

Dr. Crystal M. Weyman, GRHD/BGES, Cleveland State University
Advisory Committee Member

Date: 08/19/2019

Dr. William M. Baldwin, Department of Immunology, CCF
Advisory Committee Member

Date: 08/19/2019

Dr. Girish Shukla, GRHD/BGES, Cleveland State University
Internal Examiner

Date: 08/19/2019

Dr. William C. Merrick, Department of Biochemistry, Case Western Reserve
University

External Examiner

Student's Date of Defense: 08/19/2019

DEDICATION

I dedicate my work to my beloved parents, siblings and husband, who have been a source of inspiration and strength throughout my journey as a graduate student.

To my mentor and friends who shared their words of advice and encouragement to finish this study.

And lastly, I dedicate this thesis to the Almighty God, thank you for giving me the strength, knowledge, ability and opportunity to undertake this research study and complete it satisfactorily.

ACKNOWLEDGEMENTS

This thesis would not have been possible without the support and encouragement of my principal advisor, coworkers, my family and friends.

I am grateful to Professor Dr. Barsanjit Mazumder for giving me the opportunity to work in his research laboratory. His mentorship has been extremely valuable for my growth as a scientist, and I am thankful for the unwavering support he has shown throughout my graduate school career. His own zeal for perfection, unflinching courage, passion and conviction has always inspired me to do more.

I would take this opportunity to express my gratitude to all my advisory committee members, Dr. Weyman, Dr. Komar and Dr. Baldwin who helped me with their expert suggestions, constructive criticism and appreciation which led to the successful completion of this research work. Each committee meeting with them has been a great source of knowledge that I will carry with me forever and implement in future as well. I'd also like to thank Dr. Shukla and Dr. Merrick for agreeing to serve on my committee as an internal and external reviewer and for their time to read my thesis and evaluate my work.

In addition, I am privileged to have been able to work alongside so many wonderful people in Dr. Mazumder's lab. My coworkers have been a constant source of inspiration for me, and their input and advice have been crucial for the advancement of my research project as well as my overall scientific development. These dear colleagues include Dr. Abhijit Basu, Dr. Darshana Poddar, Maryam Pejman and Ante Curcic. I would like to thank them all for

their scientific and personal support over the years. In particular, the training that I received during my first year from Dr. Basu and Dr. Poddar was invaluable for getting my research project off the ground and moving in the right direction. Kuldeep Makwana, Amra Ismail, Sonal Patel, Anchal Aggarwal, Nikkhil Velingkaar, Richa Gupta, Amol Chaudhari and Artem Astafev are the friends in the BGES department who made this lengthy and difficult journey to be the one that I will cherish lifelong. They made the lows of graduate school bearable and were a large part of the reason why working in the lab could be both rewarding and fun.

Finally, I acknowledge the people who mean a lot to me, my parents, Mom and Dad, for showing faith in me and giving me the liberty to choose what I desired. I would never be able to pay back the love and affection showered upon by my parents. Also, I express my thanks to my brother and sisters for their support and valuable prayers, my lovely nieces and nephew for being a source of happiness. I owe thanks to a very special person, my husband, Gurpreet for his unconditional love and support that made the completion of thesis possible. I greatly value his contribution and deeply appreciate his belief in me. I would like to thank my father in law and mother in law for their constant love and support, which has made all the difference for me, and for which I am truly grateful. Thanks to the Almighty for blessing me with such a lovely family and giving me the strength and patience to work through all these years to achieve my goals.

INSIGHTS INTO THE RIBOSOMAL, EXTRA-RIBOSOMAL AND
DEVELOPMENTAL ROLE OF L13A IN MAMMALIAN MODEL

RAVINDER KOUR

ABSTRACT

Ribosomal protein L13a plays an extra-ribosomal function in translational silencing of GAIT (IFN-gamma-activated inhibitor of translation) element bearing mRNAs encoding inflammatory proteins but the underlying molecular mechanism of translational silencing and ribosomal incorporation of L13a remains poorly understood. Also, our laboratory showed that L13a acts as a physiological defense against uncontrolled inflammation in macrophage-specific knockout (KO) mice. However, the consequence of a total knockout of L13a in mammals remains unexplored. Therefore, our current study is focused on (i) identifying the amino acid residue(s) of L13a essential for incorporation and translational silencing of target mRNAs and (ii) studying the consequences of systemic loss of L13a in a mouse model. To address the first question, we compared prokaryotic L13 structure with human L13a, which depicted the presence of an α -helical extension of ~55 amino acids at the C-terminal end of human L13a. We observed that deletion of this helix impairs ribosomal incorporation and the translational silencing ability of L13a. We have identified the amino acids within this helix at position 159(K) and 161(K) that are essential for ribosomal incorporation. CryoEM studies of the human ribosome showed the interaction of the amino acids at position 185(V), 189(I) and 196(L) of L13a with RP L14. We found that mutating these residues abrogates the ribosomal incorporation of L13a. Importantly, we also showed that mutation of the amino acids at position 169(R), 170(K)

and 171(K) to Ala abrogate translational silencing activity, but not ribosomal incorporation, showing mutually exclusive ribosome incorporation and translational silencing domain. To address the second question, we generated heterozygous L13a mice (L13a^{+/-}). However, the homozygous KO (L13a^{-/-}) mice are embryonically lethal at an early stage. We have identified the KO embryos in the pre-implantation (morula) stage, suggesting an essential role of L13a in early embryonic development. Next Generation Sequencing (NGS) analysis of morula stage embryos harvested from L13a^{+/-} heterozygous parents, identified several potential targets with altered expression. Together, these studies provide a comprehensive analysis of the amino acid residues of L13a essential for ribosome incorporation and translational silencing activity and its essential role in early embryonic development in mammals.

TABLE OF CONTENTS

	Page
ABSTRACT.....	vii
LIST OF TABLES.....	xiii
LIST OF FIGURES.....	xiv
LIST OF ABBREVIATIONS.....	xviii
CHAPTER	
I. INTRODUCTION	
1.1. Ribosome Biogenesis.....	1
1.1.1. Ribosome Biogenesis in prokaryotes.....	2
1.1.2. Ribosome Biogenesis in eukaryotes.....	3
1.2. Nucleolar morphology and functions.....	9
1.2.1. Internal structure and regulation of nucleolar assembly.....	9
1.2.2. Role of nucleolar proteins in ribosome biogenesis.....	13
1.3. Translation mechanism and regulation.....	17
1.3.1. Steps in Protein synthesis.....	18
1.3.2. IFN- γ -activated inhibitor of translation (GAIT) pathway Mediated regulation of translation.....	24

1.4. Ribosomal and extra-ribosomal functions of RP L13a.....26

 1.4.1. Extra-ribosomal function of L13a in inflammation
 resolution in macrophages.....27

 1.4.2. Function of L13a within the ribosome.....29.

1.5. Role of Ribosomal proteins in embryonic development.....30

 1.5.1. Mouse: a model organism for embryology studies.....31

 1.5.1. Embryology of mouse.....31

II. EXISTENCE OF MUTUALLY EXCLUSIVE RIBOSOMAL

INCORPORATION AND TRANSLATIONAL SILENCING

DOMAIN IN RP L13A

2.1. Abstract.....38

2.2. Introduction.....40

2.3. Materials and Methods.....44

 2.3.1. Cell Culture.44

 2.3.2. Generation of Constructs.....44

 2.3.3. Ribosomal Incorporation Assay.....45

 2.3.4. Analysis of nuclear and nucleolar localization of
 L13a by Immunofluorescence Assay.....46

2.3.5. Determination of GAIT element dependent	
Translational silencing activity of L13a mutants.....	46
2.3.6. In vivo association of L13a with 28S rRNA.....	47
2.3.7. In vivo association of L13a with nucleolin.....	48
2.3.8. Structure and sequence analysis of human L13a with	
E. Coli L13 and yeast L16A.....	49
2.4. Results.....	50
2.5. Discussion.....	86

III. ROLE OF RIBSOMAL PROTEIN L13A IN EARLY EMBRYONIC

DEVELOPMENT IN MAMMALS

3.1. Abstract.....	97
3.2. Introduction.....	99
3.3. Materials and Methods.....	101
3.3.1. Generation of L13a heterozygous knock out	
(L13a ^{+/-}) Mice.....	101
3.3.2. Animal housing, breeding and timed mating.....	101
3.3.3. PCR- based genotyping strategy.....	102
3.3.4. Post-implantation embryo harvest and genotyping	

Assay.....	103
3.3.5. Induction of super-ovulation.....	104
3.3.6. Pre-implantation embryo harvest and genotyping	
Assay.....	104
3.3.7. Mouse embryonic fibroblast generation and culture....	105
3.3.8. Immunofluorescence assay of pre-implantation	
embryos and mouse embryonic fibroblasts.....	106
3.3.9. RNA extraction and purification.....	106
3.4. Result.....	107
3.5. Discussion.....	123
IV. CONCLUSION.....	125
REFERENCES.....	128

LIST OF TABLES

Table	Page
1. Table summarizing the results of ribosomal incorporation assay and subcellular Localization of L13a mutants.....	96
2. Screening of L13a ^{+/-} mice intercross for L13a ^{-/-} new borns.....	110
3. Screening of post-implantation embryos of L13a ^{+/-} mice intercross.....	113
4. Screening of pre-implantation embryos of L13a ^{+/-} mice intercross.....	114

LIST OF FIGURES

Figure	Page
1. Schematic organization of rRNA operon in Escherichia coli (E. coli).....	3
2. Schematic representation of human ribosomal genes	5
3. Eukaryotic ribosome biogenesis	8
4. Schematic representation of the nucleolar ultrastructure	11
5. Nucleolar organization of eukaryotic cells.....	12
6. Schematic representation of the Nucleolin structure.....	15
7. structures of Fibrillarin	17
8. Initiation of translation	20
9. Translation elongation cycle.....	23
10. L13a targets eIF4G for transcript-specific inhibition of translation.....	26
11. Assembly of L13a into GAIT complex	27
12. The preimplantation period of mouse embryonic development	35
13. Time course of mouse development summarizing 0-19 DPC embryonic development.....	37
14. sequence and structure alignments of E. coli L13 and human L13a	52
15. Schematic representation of ribosome incorporation assay.....	53

16. The eukaryote-specific C-terminal extension of L13a is essential for nucleolar translocation and ribosomal incorporation of L13a.....	55
17. Eukaryote-specific C-terminal extension alone retains the ability to translocate into the nucleolus but failed to incorporate into the ribosomes	56
18. Amino acid residues Lysine 159 and Lysine 161 within the C-terminal domain are essential for ribosomal incorporation of L13a.....	59
19. Modeling of the interaction between the C-terminal helices of human L13a and L14 protein.....	60
20. Amino acids of L13a (Val185, Ile189 and Leu196) involved in interaction with L14, are essential for ribosomal incorporation of L13a.....	61
21. Subcellular localization of ribosome incorporation defective triple mutant Lys159A-Arg160A-Lys161A	64
22. Subcellular localization of ribosome incorporation defective double mutant Val189A-Ile189A and triple mutant Val185A-Ile189A-Leu196A.....	65
23. Subcellular localization of ribosome incorporation defective mutants Lys(K) 159A and Lys(K) 161A	66
24. Subcellular localization of ribosome incorporation competent Arginine (R)160A mutant.....	67

25. subcellular localization of L13a variants lacking predicted NLSs `	69
26. Generation of His-tagged recombinant L13a WT/mutant proteins and in-vitro translation assay	72
27. The eukaryote-specific C-terminal extension of L13a harbors amino acid residues (R169-K170-K171) required for GAIT element mediated translational silencing	73
28. Schematic illustration of quantification of translation silencing activity of L13a proteins used in the in vitro translation silencing assay.....	75
29. Ribosomal incorporation and nuclear/nucleolar translocation assay of L13a mutant defective of translational silencing activity.....	76
30. Association of L13a and its mutant variants with 28S rRNA.....	78
31. Immunoblot of IP lysates input using anti-nucleolin antibody.....	81
32. In vivo association of L13a and its mutant variants with nucleolin.....	83
33. Amino acid Sequence alignment of uL13 proteins -CLUSTAL O (1.2.4).....	84
34. Proposed model for phosphorylation-induced conformational transition of the L13a C-terminal helix.....	94
35. Generation of L13a heterozygous knock out mouse.....	109
36. Screening uteri of L13a heterozygous females for resorption sites.....	112
37. Identification of L13a total KO embryos.....	115

38. Subcellular localization of L13a in pre-implantation embryos.....	117
39. Subcellular localization of L13a and L26 in pre-implantation stage embryos and L13a Localization in (post-implantation embryonic cells) MEFs.....	118
40. Alteration of gene expression in absence of L13a in early embryogenesis.....	121
41. RNA sequencing data revealed a negative correlation between cytokine and inflammatory pathway (indicated by blue arrow in the figure) and the regression scale of L13a.....	122

LIST OF ABBREVIATION

CHX	Cycloheximide
DAPI	4',6-diamidino-2-phenylindole
DFC	Dense Fibrillar Component
DPC	Days Postcoitum
EFs	Elongation factors
eIFs	Eukaryotic initiation factors
ETS	External transcribed spacer
FC	Fibrillar Center
FESEM	Field-emission scanning electron microscopy
FRT	Flippase recognition Target
GAIT	IFN- γ -activated inhibitor of translation
GAPDH	Glyceraldehyde-3 phosphate dehydrogenase
GC	Granular Component
HA tag	Hemagglutinin tag
HCG	Human chorionic gonadotropin
hnRNP	heterogeneous nuclear ribonucleoproteins
ICM	Inner cell mass

IP	Immunoprecipitation
IP injection	Intraperitoneal Injection
IRES	Internal Ribosome Entry Site
ITS	Internal transcribed spacer
KO	Knock out
LH	Leutinizing Hormone
LPS	Lipopolysaccharide
LSU	Large subunit
MEFs	Mouse embryonic fibroblasts
mRNA	Messenger RNA
NGS	Next generation sequencing
NLS	Nuclear localization signal
NSAP1	NS1-associated protein 1
PBS	Phosphate-Buffered saline
PIC	pre-initiation complex
PMS	Pregnant mare serum
PTC	Peptidyl transferase center
rDNA	Ribosomal DNA

RFs	Release factors
r-Protein	Ribosomal proteins
RNP complex	Ribonucleoprotein complex
rRNA	Ribosomal RNA
RNAi	RNA interference
RT-PCR	Reverse transcription-PCR
SnoRNPs	Small nucleolar ribonucleoproteins
SSU	Small Subunit
TCA	Trichloroacetic acid
TE	Trophectoderm
TEM	Transmission electron microscopy
WT	Wild-Type
ZP	Zona pellucida

CHAPTER I

INTRODUCTION

1.1 Ribosome Biogenesis:

Ribosomes have been described for the first time in 1955 by George E. Palade as small granular particles through microscopic observations of rat cells (Palade, 1955). Ribosomes are complexes of ribosomal RNA (rRNA) and ribosomal proteins (r-Proteins). Eukaryotic and prokaryotic ribosomes are different from each other because of divergent evolution. Prokaryotic ribosomes sediment as 70S particles and consists of a small subunit (30S) and a large subunit (50S). The small subunit is made of 16S rRNA and 21 ribosomal proteins whereas large subunit is made of two rRNAs, 23S and 5S rRNA and 33 ribosomal proteins. In eukaryotes, the 40S (SSU) small subunit contains 18S rRNA and 30-33 r-proteins while the 60S large subunit (LSU) contains three rRNA: 5S, 5.8S, and 25S (lower eukaryotes) or 28S (higher eukaryotes) rRNA as well as 40-50 r-proteins. 18S, 5.8S and 28S are transcribed by Pol I and 5S by Pol III. Synthesis of ribosomes, also known as ribosome biogenesis, is a complex, multi-step and one of the most energy-demanding activity of all the cellular processes. The biogenesis of ribosomes is a tightly regulated activity and defects in the biogenesis process are associated with several diseases (ribosomopathies). During protein translation, the larger and smaller subunit assembles on

the mRNA in a sequential manner and scan for start codon and thereafter ribosomes decode the nucleotide sequence and catalyze the addition of amino acids into a growing polypeptide.

1.1.1 Ribosome biogenesis in prokaryotes:

The assembly and maturation of ribosomal subunits in prokaryotes is a co-transcriptional process that involves a series of events marked by rRNA processing, modifications, folding and ordered binding of ribosomal proteins to the nascent rRNA transcript as the RNA polymerase moves through the operon. The biogenesis process begins with the transcription of the 16S, 23S and 5S rRNA as a single primary transcript (figure1). Maturation of the transcript begins before the transcription is completed and ribosomal proteins start binding as the binding sites emerge on the transcript. RNAase III is the first endonuclease that cleaves the rRNA transcript and the products of this cleavage are precursor 16S rRNA, precursor 23S rRNA and precursor 5S rRNA (Jemiolo, D. K. 1996). These precursor rRNAs undergo several processing events mediated by exo- & endonucleases such as RNAse P, RNAse T, RNAse E, RNAse G etc.(Li, Pandit and Deutscher, 1999). rRNAs (except 5S rRNA) undergo more than 80 chemical modifications like isomerization of uridine to pseudouridine or addition of carbonyl, methyl, amino, or thio groups during maturation. In 16S rRNA, some modifications are added to the nascent RNA while others are added during maturation of 30S rRNA. 23S rRNA undergoes chemical modifications mainly before maturation (DEL CAMPO, 2004). Some of these modifications in 23S rRNA (at least 17) are dispensable for both assembly and ribosomal

function (Green and Noller, 1996) 16S rRNA has three domains- I, II and III. Domain I is formed from the 5' end of the rRNA, domain II by central part and domain III by 3' end of the rRNA (Stagg, Mears and Harvey, 2003). Small subunit ribosomal proteins are divided into three groups- primary, secondary and tertiary binding proteins, wherein, binding of primary proteins initiates the nucleation of 30S subunit assembly and binding of secondary proteins. Binding of tertiary proteins require at least one primary and one secondary protein interaction for correct association (Powers, Daubresse and Noller, 1993). Ribosomal protein binding and assembly of the large subunit (50S) is much more complex than the 30S subunit. Five ribosomal proteins-L4, L13, L20, L22, L24 and L3 are especially important for proper assembly (Østergaard *et al.*, 1998). Proteins L5, L18 and L25 mediate the interaction between 23S and 5S rRNA(Kaczanowska and Ryden-Aulin, 2007)

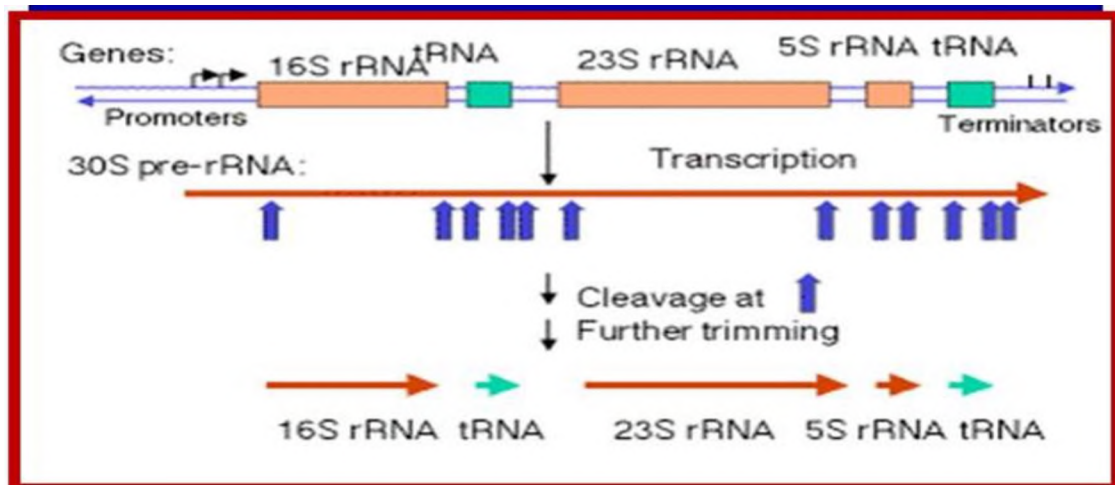


Figure1: Schematic organization of one of the rRNA operon in Escherichia coli (Kaczanowska M et al., 2007): The primary transcript contains all three rRNA species (16S, 23S and 5S), as well as one or more tRNAs transcribed from two promoters. The transcript is

1.1.2 Ribosome biogenesis in eukaryotes:

Ribosome biogenesis in eukaryotes is highly regulated and more complex process as compared to prokaryotes, which begins in the nucleolus with the transcription of rDNA into large primary RNA transcript and continues until the ribosomes are exported to the cytoplasm to form mature 40S and 60S ribosomal subunits. All three types of RNA polymerases are involved in process of ribosome synthesis. RNA polymerase I synthesizes 28S, 18S and 5.8S rRNA, RNA Pol III is dedicated for to the synthesis of 5S rRNA and small RNAs that are necessary for various steps of ribosome biogenesis. RNA Pol II synthesizes pre-mRNAs for (r-proteins) ribosomal proteins (Leary and Huang, 2001). The nucleolus that is the principle site for ribosome synthesis is subdivided into three compartments which are called Fibrillar Center (FC), Dense Fibrillar Component (DFC) and Granular Component (GC) respectively. The process of ribosome biogenesis starts with the transcription of ribosomal DNA (rDNA) repeats into a nascent 47S rRNA transcript (consisting of 18S, 5.8S, 28S) flanked by 5' and 3' external transcribed spacer (ETS) and two internal transcribed spacer (ITS) respectively (figure 2). It takes place at the borders of the FC and DFC region.

(i). Regulation of rDNA transcription

Ribosomal DNA (rDNA) is organized into repeated sequences, about 200 copies in yeast and 400 copies in human cells. Several factors regulate the transcription of rDNA repeats like chromatin remodeling (modulation of methylation, acetylation of histones). Histone deacetylation and hypermethylation are associated with the silencing of rDNA. Several Pol I transcription factors like UBF and SL-1 initiate rDNA transcription upon

acetylation. In addition, protein-protein interactions also play an active role in controlling transcription. Net1 is essential for positioning the Pol I at the transcription site. Net1 along with Sir2 and Cdc14 is required to maintain nucleolar structure and enhancement of rDNA transcription. Whereas binding of interferon-inducible protein p204 to UBF inhibits the transcription by preventing the transcription factor from binding to DNA by reducing DNA-binding affinity of UBF or by preventing the interaction between SL-1 and UBF. P53 is also known to bind to SL-1 and prevent SL-1 and UBF interaction, suppressing rDNA transcription.

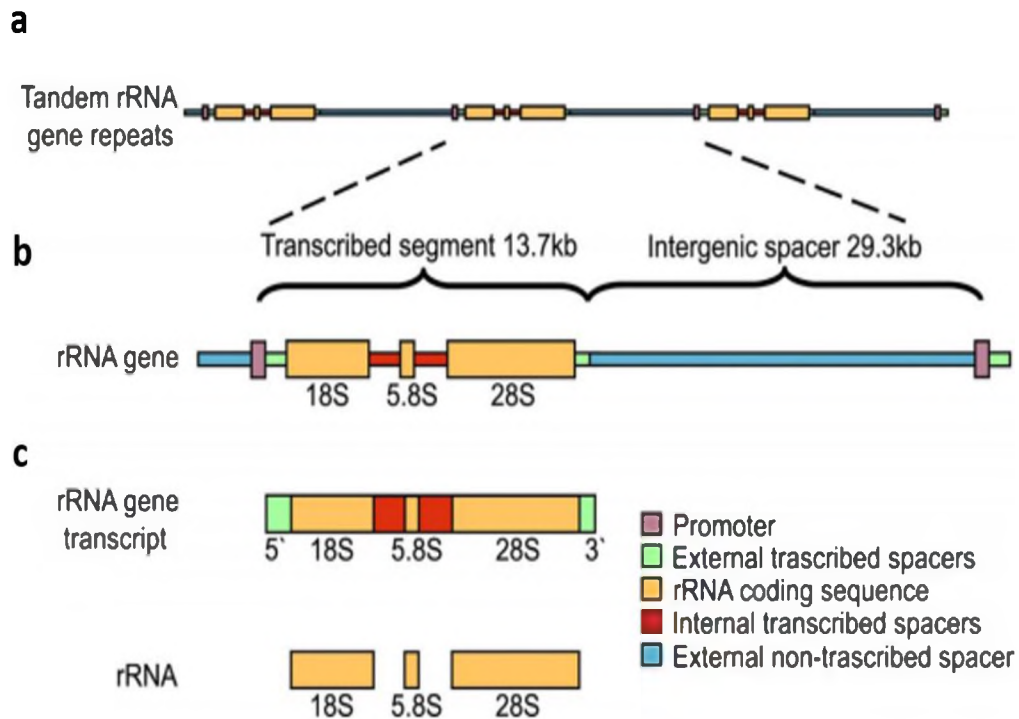


Figure 2: Schematic representation of human ribosomal genes (Raska et al., 2004). a. tandemly repeated ribosomal genes (rDNA) are organized in transcribed sequences and intergenic spaces. b. polycistronic rRNA transcribed from one gene of rDNA. C. maturation of rRNA leads to production of 18S, 5.8S and 28S rRNA.

(ii). Formation of the 90S precursor ribosome

Nascent precursor rRNA is assembled into an 90S pre-ribosomal particle, which is then processed into 18S, 5.8S and 28S rRNAs respectively (Granneman, 2004). Packaging of precursor rRNA into a pre-ribosome particle is accompanied by transient association of numerous trans-acting factors including nucleolar proteins and rRNA processing endo and exo-nucleases which cleave the nascent pre-rRNA. Two types of nucleotide modifications: methylation and pseudouridylation take place in the 90S complex by two classes of modification enzymes- 2'-O-ribose methylation by conserved methyltransferases or C/D box small nucleolar ribonucleoproteins (SnoRNPs) and pseudo-uridylation by H/ACA box snoRNPs. Human rRNA contain 91 pseudouridines and 106 2'-O-methyl residues. In yeast, there are 43 pseudouridines and 55 methylations (Maden, 1990) (Tollervey and Kiss, 1997)(Ofengand and Bakin, 1997)(Lafontaine *et al.*, 1998). In addition to nucleotide modifications, several ribosomal proteins (known as early binding proteins) also incorporate early into the pre-ribosome complex. These ribosomal proteins are S1, S4, S6, S7, S8, S9, S11, S15, S17, S24, S28 and L1, L3, L4, L6, L7, L8, L9, L13a, L16, L18, L20, L32 and L33. These early ribosomal proteins most likely stabilize the local RNA secondary structure. L13a is known to be one of the early binding proteins. Studies from our laboratory have experimentally shown that ribosomal protein L13a incorporates into the 90S precursor ribosome in the nucleolus. (Das *et al.*, 2013).

(iii) Formation of mature 60S and 40S ribosome subunits

Cleavage reactions by nucleases occur at positions A0, A1, and A2 in the 90S precursor ribosome complex. These cleavage events are well studied in yeast. These early cleavages result in the separation of the 20S pre-rRNA (precursor to 18S), which remains part of the early pre-40S particle and the 27S/32S pre-rRNA (precursor to 25S/28S and 5.8S) moiety in yeast and higher eukaryotes respectively (Kornprobst *et al.*, 2016). The majority of ribosomal proteins are also incorporated in a cooperative manner as 60S and 40S pre-ribosomal particles move from the DFC to GC component of the nucleolus, traverse the nucleoplasm and exit the nucleus through nuclear pores to become mature 40S and 60S ribosomal subunits in the cytoplasm. The final steps of assembly occur in the cytoplasm and include the processing of 6S pre-rRNAs to mature 5.8S rRNAs and the assembly of few r-proteins, among them are L10, L24, L29 etc. (Espinar-Marchena *et al.*, 2018). Various steps of ribosome biogenesis in eukaryotes have been summarized in figure 3.

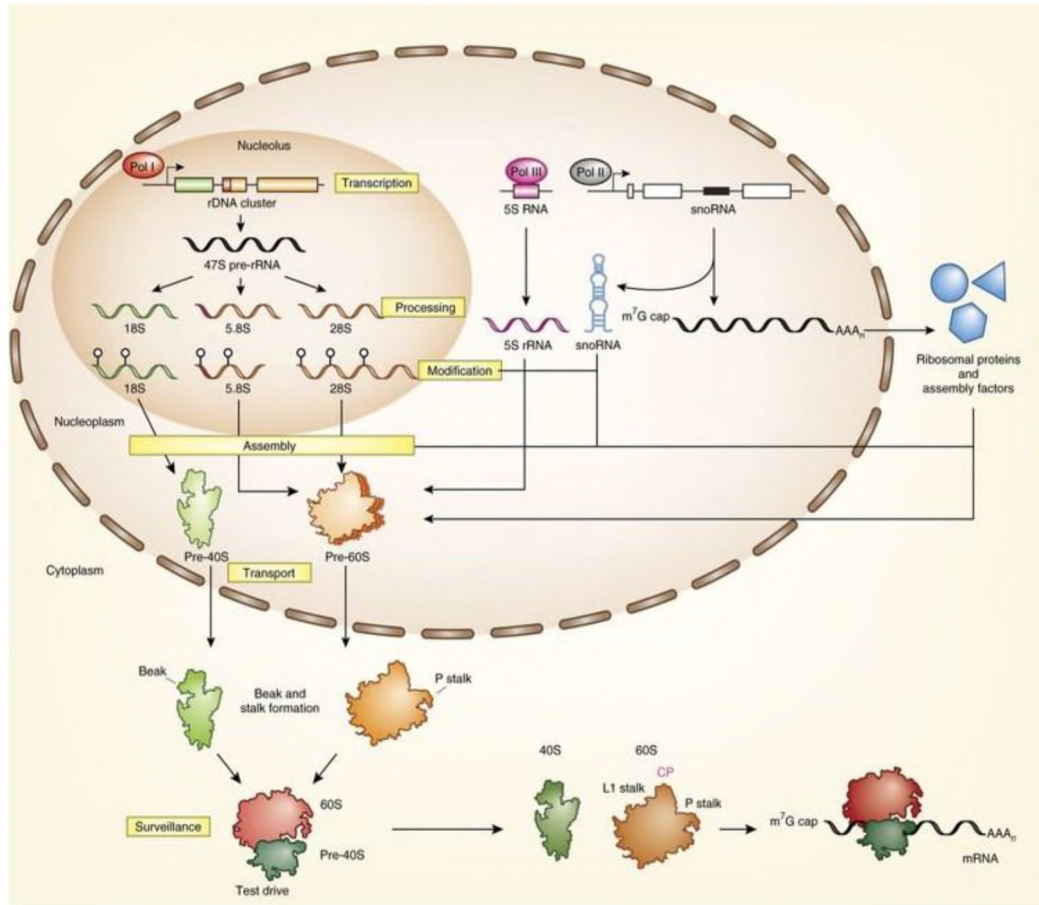


Figure 3: Eukaryotic ribosome biogenesis (figure adapted from Lafontaine et al., 2015).

Ribosome biogenesis encompasses six important steps (yellow boxes): (i) transcription of components (rRNAs, mRNAs encoding ribosomal proteins (RPs) and snoRNAs); (ii) processing (cleavage of pre-rRNAs); (iii) modification of pre-rRNAs, RPs and RBFs; (iv) assembly; (v) transport (nuclear import of RPs and RBFs; pre-ribosome export to the cytoplasm); and (vi) quality control and surveillance. Three out of four rRNAs are transcribed in the nucleolus by Pol I as a long 47S precursor (47S pre-rRNA), which is then processed and modified to yield the 18S, 5.8S and 28S rRNAs that are assembled into the pre-40S (green) and pre-60S (orange) ribosomal subunits. 5S rRNA (pink) is transcribed by Pol III in the nucleoplasm and incorporated into maturing 60S subunits, forming the central protuberance (CP). 80 RPs, more than 250 RBFs and 200 snoRNAs are transcribed by Pol II. Pre-40S subunits are exported to the cytoplasm more rapidly than pre-60S subunits, which require numerous nuclear maturation steps.

1.2 Nucleolar Morphology and functions:

Nucleolus is the most prominent intranuclear structure in the cell, being the site of rRNA transcription, processing and ribosome assembly (Olson, Hingorani and Szebeni, 2002). It assembles around the rDNA repeats during late telophase, persists throughout the interphase and disassembles when the cells enter mitosis. High density and ability to purify nucleoli makes it easier to study nucleolar protein composition using high-throughput mass-spectrometry based proteomic techniques. These studies have been conducted on human cells, continuously expanding the number of nucleoli proteins close to 700 (Andersen *et al.*, 2002) (Scherl *et al.*, 2002) (Andersen *et al.*, 2005). Studies have revealed that more than one-third of the nucleoli proteome is involved in different steps of ribosome biogenesis (Anderson *et al.*, 2005). In addition, there are proteins that have no relationship with the classical nucleoli function i.e., ribosome synthesis. These proteins play a role in cell cycle regulation (3.5% of nucleoli proteome), DNA damage repair (1%) and pre-mRNA processing (5%), RNA editing, telomere metabolism, tRNA processing and regulation of protein stability ((Olson, Hingorani and Szebeni, 2002)(Pederson, 1998) (Sansam, Wells and Emeson, 2003). This gives the idea that the nucleoli are the dynamic organelles that function beyond ribosome biogenesis.

1.2.1 Internal Structure and regulation of nucleolar assembly:

a. Internal structure.

Nucleolus: a membrane-less structure in the cell is composed of filamentous and granular material. The internal structure of the nucleolus has been studied by both

transmission electron microscopy (TEM) and field-emission scanning electron microscopy (FESEM). Field-emission scanning electron microscopy has revealed the high resolution (~ 1 nm) view of the 3D contour of the nucleolar surface and the interface between the nucleolus and the nucleoplasm in HeLa cells (Lam, 2005). TEM studies have revealed three subcompartments within the nucleolus in higher eukaryotes- fibrillar center (FC), dense fibrillar centre (DFC) and granular center (GC) whereas, in lower eukaryotes (yeast), only FC and GC components are present in the nucleoli. FC and DFC are made up of 0.1 to 1µm fibrils and GC is made of granules of 15-20 nm diameter. Each region has distinct protein compositions and functions. For example, FC contains RNA polymerase I, DNA topoisomerase I, and the transcription factor UBF(Scheer, Thiry and Goessens, 1993) (Zatsepina *et al.*, 1993). Fibrillarin is the marker protein for DFC. This protein is known to be a part of the snoRNA methylation complex, involved in ribose 2'-O-methylation of rRNA during ribosome biogenesis (Tollervey *et al.*, 1993). B23 accumulates in the granular center. Whereas, nucleolin can be seen throughout the GC and DFC regions. Hence, nucleolin serves as a marker for nucleolus (Schwarzacher and Mosgoeller, 2000).

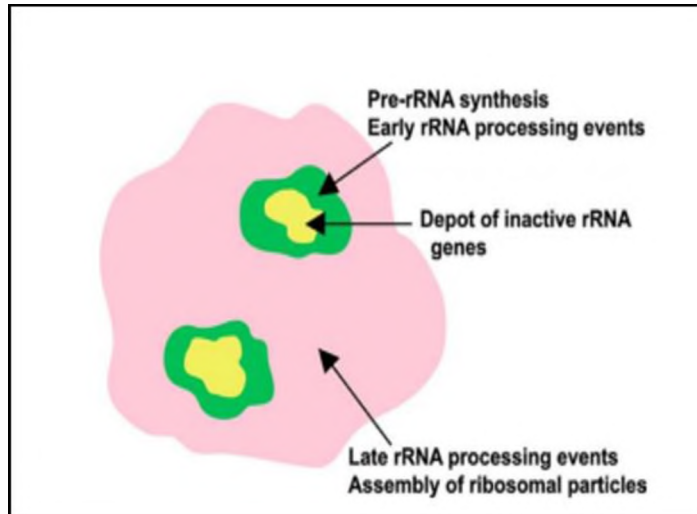


Figure 4: Schematic representation of the nucleolar ultrastructure depicting the respective functions (Figure adapted from Raska et al., 2004): fibrillar centers (yellow): rRNA genes are localized in this region, dense fibrillar components (green): site of rRNA synthesis and processing, and granular components (pink): rRNA processing and assembly of ribosomal subunits.

Usually nucleoli can be found in the central nuclear region but may also be close to the nuclear membrane. A nucleolus is built by a nucleolus organizing region (NOR) of a specific chromosome. NOR is known to contain the genes for ribosomal RNA subunits. In a diploid human cell, a total of 10 chromosomes (13,14,15,21 and 22) containing NORs exist. Therefore, in principal, 10 nucleoli per nucleus could be present. Usually, only one or two nucleoli are found, since NORs from several chromosomes build a common nucleolus (Hernandez-Verdun *et al.*, 2010). rDNA transcription by RNA Pol I takes place at the boundary between the fibrillar center and dense fibrillar center (Dundr and Raška, 1993). The early processing (formation of the 90S pre-ribosome particle and association with several ribosomal and non-ribosomal factors/proteins) occurs in the DFC and late

processing (formation of 28S, 5.8S, 18S rRNA transcripts) takes place in the GC component of the nucleoli in a vectoral manner.

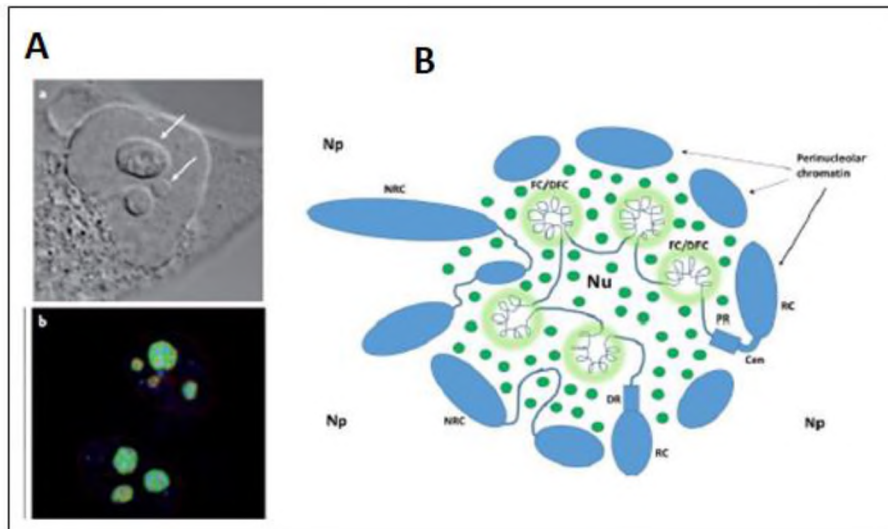


Fig 5: Nucleolar organization of eukaryotic cells (figure adapted from Smirnov et al 2014). A. Visualization of nucleolar morphology: (a) Differential interference contrast images of HeLa cells showing prominent nucleoli (white arrows). (b) Immunofluorescent labeling of HeLa cells with specific antibodies against proteins in the GC (B23 in green), DFC (Fbl in red) and FC (RPA39 in blue) (Boisvert et al., 2007). C. Schematic representation of nucleolus associated DNA. Nu nucleolus, Np nucleoplasm, RC chromosomes carrying ribosomal genes, Cen centromere, PR proximal flanking region, DR distal flanking region, NRC non-ribosomal chromosome. FC/DFC-rDNA transcription center consists of fibrillar center (FC) surrounded with dense fibrillar component (DFC). Green dots: granular component.

b. Regulation of nucleolar assembly

Cellular metabolic activity determines the size, number, and position of the nucleoli within the nuclear volume. In G1 and G2 phase, volume of the nucleoli increases and the number of FC (fibrillar center) doubles during G2 (Junera HR, Masson C and Hernandez-

verdum D, 1995). In quiescent cells when ribosome biogenesis stops, ring-shaped nucleoli or nucleolar remnants are observed characterized by a clear area made up of chromatin and dense fibrils at the periphery. At the beginning of mitosis, rRNA transcription and processing machinery is repressed but remains attached with the rDNA within the NORs and activates only when the telophase is approached (Roussel, 1996). This repression is controlled in part by the CDK1-cyclin B-directed phosphorylation of components of the Pol I transcription machinery. Nucleoli assembly at the end of mitosis is accompanied by the resumption of Pol I activity, inactivation of CDK1-cyclin B and traffic of rRNA processing factors to the site of rDNA transcription.

1.2.2. Role of nucleolar proteins in ribosome biogenesis

Each nucleolar subcompartment has a subset of proteins that regulates rRNA transcription, processing, incorporation of ribosomal proteins, maturation and assembly of ribosome subunits (Chen and Huang, 2001). The two most abundant nucleolar proteins are nucleolin and fibrillarin.

Nucleolin is a ubiquitously expressed 100-110 kDa acidic phosphoprotein that represent as much as 10% of total nucleolar protein in CHO cells (BUGLER *et al.*, 2005). It actively participates in the ribosome biogenesis by regulating chromatin structure, rDNA transcription, ribosome assembly and nucleo-cytoplasmic export (P. Bouvet *et al.*, 1999). Nucleolin is one of the non-ribosomal proteins that transiently interact with rRNA and pre-ribosomal particles and is not detectable in the mature ribosomes. Structurally, nucleolin has three regions: N-terminal domain, central domain and C-terminal domain. The N-terminal domain is made up of highly acidic regions interspersed with basic sequences and

contain multiple phosphorylation sites for kinases such as Casein Kinase II (CK2), P34^{cde2} etc. (Caizergues-Ferrer *et al.*, 1987). This phosphorylation of nucleolin by CK2 and p34^{cde2} regulates nucleolin function during the cell cycle. The central region has four RNA-binding domains called RBD and is involved in the association of nucleolin with 5' ETS (external transcribed region) of nascent pre-ribosomal RNA in the DFC region of nucleolus (Herrera and Olson, 1986). The C-terminal domain is rich in glycine, arginine and phenylalanine repeats of variable lengths and is called the GAR or RGG domain. Studies have shown that this domain is involved in RNA-protein interactions during ribosome biogenesis, facilitating the binding of nucleolin RBD with rRNA (GHISOLFI *et al.*, 1992)(Heine, Rankin and DiMario, 1993). In addition, nucleolin has a remarkable ability of shuttling between nucleus and cytoplasm, enabling nucleolin to act as a carrier of ribosomal proteins from the cytoplasm to the nucleolus, i.e. the site of incorporation of ribosomal proteins. Nucleolin interacts with 18 rat and 16 human ribosomal proteins (13 large subunit and 5 small subunit r-proteins). Ribosomal protein L13a is one the proteins that shows an interaction with nucleolin. It has been shown that these proteins are among the initial proteins that assemble within the pre-ribosomal particles and remain tightly associated with the rRNA (Bouvet *et al.*, 1998). This L13a-nucleolin association has been utilized in the previous studies in our lab to track the subcellular localization of WT/ mutant L13a protein and nucleolin in immunofluorescence-based studies, using nucleolin as a marker. These studies have further confirmed that L13a binds with nucleolin in vivo and can be seen co-localized with the nucleolin protein in the nucleolus (Das *et al.*, 2013). Therefore, nucleolin serves an important role in the rRNA processing, r-proteins incorporation and dissociates

from ribosomes as evidenced by the absence of nucleolin in the mature cytoplasmic ribosomes.

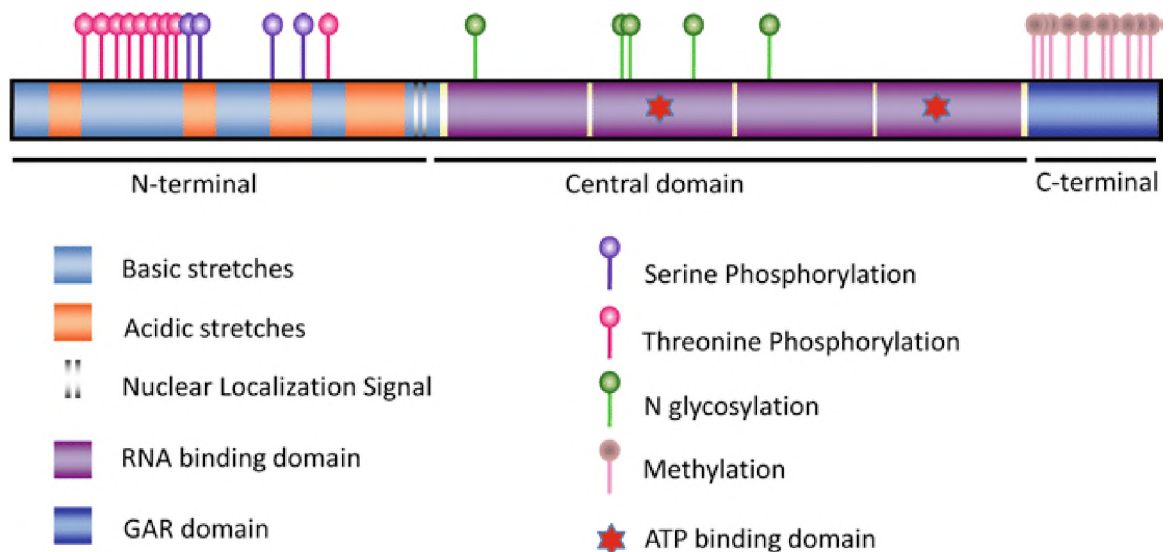


Figure 6: Schematic representation of the Nucleolin structure (figure adapted from Sadhan Das, 2011). Showing three functional domains and target sites of posttranslational modifications known thus far are shown at the upper side of the protein structure. The phosphorylation sites are threonine residues 58, 75, 83, 91, 98, 105, 120, 128, and 219 and serine residues 143, 156, 187, and 209. Methylation sites are 655, 659, 665, 669, 673, 679, 681, 687, 691, and 694 in the C-terminal GAR domain. Glycosylation sites are 317–319, 399–401, 403–405, 477–479, and 491–493. Two potential ATP binding sites have been also located in the RNA binding domains.

Another essential nucleolar protein is fibrillarin that participates in ribosome biogenesis. This 34-36 kDa protein is primarily localized in the DFC compartment of the nucleolus. The structure and function of fibrillarin is conserved in yeast and human. Yeast Nop1 is 70% identical to fibrillarin in humans. A salient feature of fibrillarin is the presence of amino-terminal sequence of about 80 amino acids, consisting of glycine and arginine rich repeated motifs, similar to the other nucleolar proteins such as nucleolin (Jansen, 1991). This high degree of structural conservation among eukaryotes suggest an important function for these proteins. The central domain of fibrillarin consists of approximately 90 amino acids long RNA binding domain-like motif. The C-terminal consists of a small domain that forms alpha helices.

In DFC of the nucleolus, fibrillarin acts like a methyltransferase enzyme and is a part of C/D class of snoRNP (small nucleolar ribonucleoprotein) complex. Fibrillarin belongs to the superfamily of the Rossmann-fold-S-adenosylmethionine (SAM) methyltransferases (MTases). Within the snoRNP complex fibrillarin transfers the methyl group of SAM to the 2-hydroxyl group of ribose targets, that utilizes methyl donor S-adenosyl-L-methionine to carry out the 2'-O-methylation of the pre-rRNA in the 90S precursor ribosomes during ribosome biogenesis. These post-transcriptional modification sites lie within the functionally important regions of the ribosome and facilitate the folding and stability of rRNA. Previously published studies from our laboratory has shown that cells deficient in L13a showed significant reduction of ribosomal RNA methylation and a subsequent defect in cap-independent translation of Internal Ribosome Entry Site (IRES) element containing mRNAs such as P27, P53 and SNAT2 (Chaudhuri *et al.*, 2007). We

have further shown that this inhibition of IRES mediated translation in L13a depleted cells result from lack of rRNA methylation. L13a as a part of fibrillar and snoRNA containing C/D box snoRNP complex is essential to carry out rRNA methylation of 90S pre-ribosomes in the nucleolus of mammalian cells (Das *et al.*, 2013).

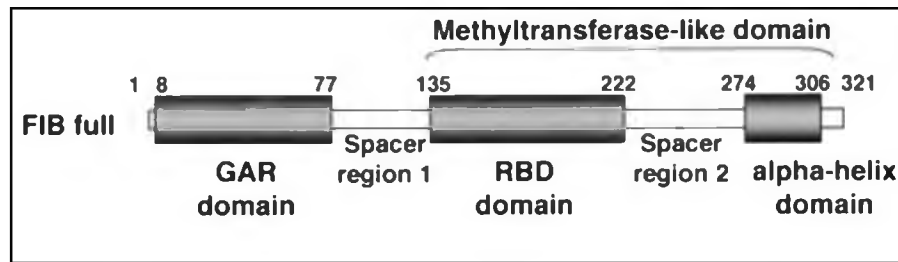


Figure 7: Structures of Fibrillar (figure adapted from Yanagida M *et al.*, 2004). The N-terminal glycine- and arginine-rich (GAR) domain, RNA-binding domain (RBD), and α -helix domain are shaded in gray, and the spacer regions 1 and 2 are indicated. The methyltransferase-like domain is composed of the RBD, spacer region 2, and α -helix domain.

1.3. Translation mechanism and regulation.

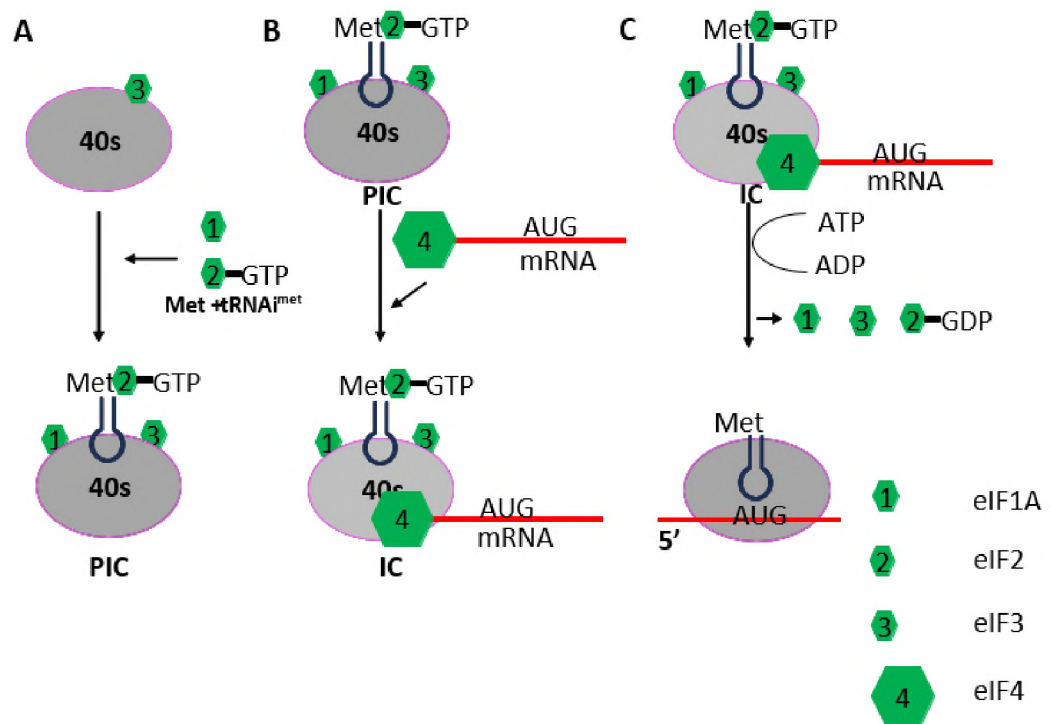
Most of the biological activities are performed by the proteins. The information to generate a protein molecule is stored in the DNA molecule. This information is conveyed through messenger RNA (mRNA) and the process by which a protein is synthesized by the ribosomes from the information contained in the messenger RNA (mRNA) is known as translation. Protein synthesis involves the formation of peptide bonds that link the carboxyl group of one amino acid to the amino group of another to form a chain. Peptide bond formation is a chemical process that involves a nucleophilic attack by

an amino group of one amino acid on the carboxyl group of another. The synthesis of proteins in cells involves a very complex machinery comprising ribosomes, numerous RNAs and proteins, and amino acids. In eukaryotic cells, translation occurs in the cytoplasm. Three types of RNAs participate in protein synthesis: rRNA, mRNA, tRNA.

1.3.1. Steps in protein synthesis:

i) Initiation: The ribosomal subunit assembly happens with the help of a set of proteins known as eukaryotic initiation factors (eIF). Some of these initiation factors are coupled to GTP and the hydrolysis of GTP to GDP provides a proofreading step to allow the next step in protein synthesis process to proceed only if the preceding step was correct. Additionally, phosphorylation of some of these initiation factors can block the translation process (Sonenberg and Hinnebusch, 2009). Formation of a pre-initiation complex (PIC) is the first step of translation initiation. The PIC is formed when the smaller subunit of ribosome (40S) associates with eIF3, eIF1A, and a ternary complex composed of eIF2.GTP.Met- tRNA_i. The 5' m⁷G cap of the mRNA is bound by the eIF4 cap-binding complex which then associates with the PIC. The eIF4 complex is made up of different subunits: eIF4A (helicase activity during scanning), eIF4B (architectural role), eIF4G (binds to eIF3 in PIC), and eIF4E (binds to 5' cap of mRNA). This complete association of PIC, eIF4 complex and mRNA is called an initiation complex. The multicomponent initiation complex (IC) then scans the mRNA in the 5' -3' direction to find the start codon AUG. Recognition of the correct start codon leads to eIF2-GTP hydrolysis to GDP form (proofreading step) followed by dissociation of eIF1, 2, 3 and eIF4 complex. This is an irreversible step which prevents further scanning. The Kozak consensus sequence

ACCAUGG facilitates the selection of the correct start codon. The small subunit unites with the large (60S) subunit in a process catalyzed by the eIF5B and 6, forming the 80S ribosome, accompanied by hydrolysis of eIF5-GTP to GDP (another proofreading, irreversible step). The whole complex is recruited to the P-site of the ribosome. This is the predominant form of eukaryotic translation initiation which depends on the m⁷G cap structure, present at the 5' end of the mRNA, known as cap-dependent translation initiation (figure 8).



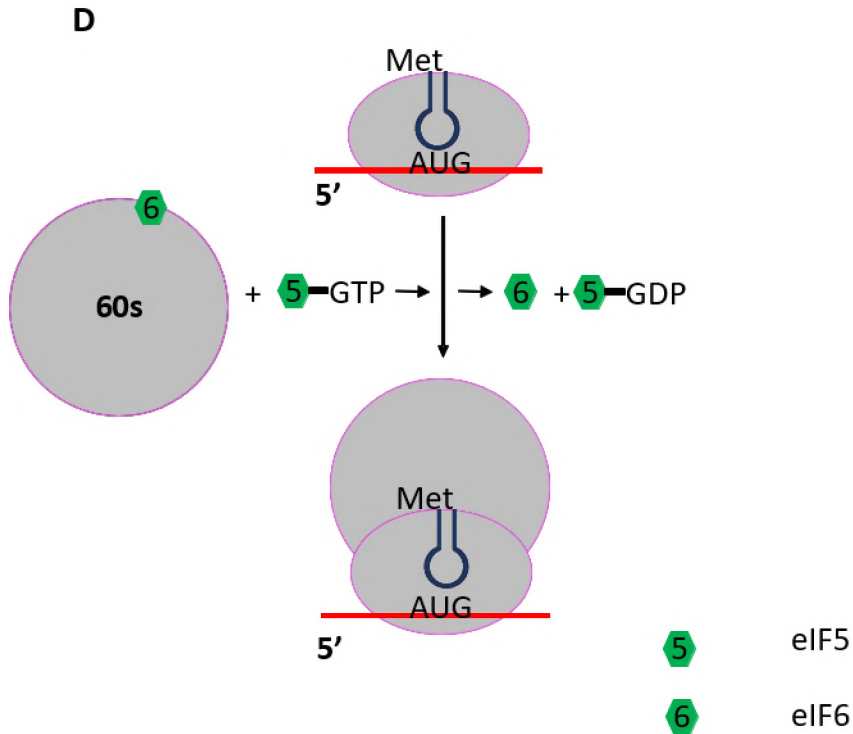


Figure 8: Initiation of translation. A) 40S subunit associated with eIF3 joins eIF1A and ternary complex of eIF2.GTP.Met- tRNA_i to form a preinitiation complex (PIC). B) PIC binds to 5'cap structure of mRNA with the help of eIF4 complex. C) PIC scans for the start codon AUG. As the start codon is recognized correctly, there follows hydrolysis of eIF2-GTP to the GDP form. This is the first proofreading step which is irreversible. D) After the correct recognition of start codon and correct binding of Met- tRNA_i to its complementary codon on mRNA, the 60s subunit associated with eIF6 unites with 40S subunit. This step is catalyzed by eIF5B-GTP which is hydrolyzed at the end of this reaction to eIF5B-GDP and dissociated along with eIF6 to form the ribosome.

IRES-dependent initiation:

Studies of viral gene expression in the late 1980s led to the discovery of an alternative mode of translation initiation in eukaryotic cells that bypasses the requirement for cap-dependent scanning. This mode of translation initiation allows the 40S ribosome to be directly recruited to the vicinity of the initiation codon. The mRNA regions required for this direct recruitment of the small subunit were termed Internal Ribosome Entry Sites (IRESs) to emphasize that the process is independent of 5'-end recognition. The location of cellular IRES elements is within the 5'-UTRs immediately upstream of the initiation codon. Numerous IRES have been discovered in viruses (Jackson, Hellen and Pestova, 2010). Importantly, IRES-containing mRNAs can also be translated by the cap-dependent mechanism, however how the switch between these two modes of initiation is regulated needs to be investigated further. Interestingly, it has been demonstrated that inhibition of cap-dependent translation by physiological, pathophysiological and stress conditions lead to a substantial increase in cellular IRES-mediated translation (Komar and Hatzoglou, 2005). Such conditions include endoplasmic reticulum stress, hypoxia, nutrient limitation, mitosis and cell differentiation.

Previous studies in our lab have shown that ribosomal protein L13a is a component of a methyl transferase complex that catalyzes 2'-O-methylation during ribosome biogenesis (Das *et al.*, 2013). Decrease of 2'-O-methylation leads to a decrease in IRES-dependent translation of a subset of mRNAs such as p53, p27 and SNAT2 while global translation is not affected (Chaudhuri *et al.*, 2007).

(ii) **Elongation:** chain elongation process requires the translation elongation factors (EFs). Based on the codon present in vacant A site, the second aminoacyl-tRNA (aa-tRNA) enters the A site of the ribosome as a ternary complex of aa-tRNA and eEF1A-GTP. This ternary complex enters the A site upon correct binding of aa-tRNA binds its anticodon in A site there occurs hydrolysis of GTP bound to eEF1A, another proofreading step which occurs only if the correct aa-tRNA bind to the A-site. As the initiating Met-tRNA_i is at the P site and the second aminoacyl-tRNA is bound at the A site, amino group of second amino acid (at A site) forms a peptide bond with the methionine present on initiator tRNA (tRNA_i). This reaction is catalyzed by rRNA of the large subunit. Following peptide bond synthesis, the ribosome is translocated along the mRNA a distance equal to one codon. This step requires eEF2A-GTP. Translocation is followed by the hydrolysis of eEF2A-GTP and release of eEF2A-GDP. This is an irreversible step which prevents backward movement of ribosome. This results in the shift of the second tRNA with a dipeptide in the P site. This leaves the A site vacant for the next aa-tRNA and empty tRNA_i shift to E site (Dever and Green, 2012). At the end of the translocation, the A site is again vacant and ready to accept a new aa-tRNA (figure 9).

iii) **Termination:** Termination is the final stage of translation that requires a set of proteins known as release factors (RFs). Two types of RFs have been discovered: eRF1 (similar in shape to tRNA) and eRF3 which is a GTP binding protein. eRF1 binds to the A site of the ribosome and recognizes stop codon. eRF3-GTP works in concert with eRF1 to facilitate the cleavage of the peptidyl-tRNA from ribosome and thus releasing the completed polypeptide chain (Hellen, 2018).

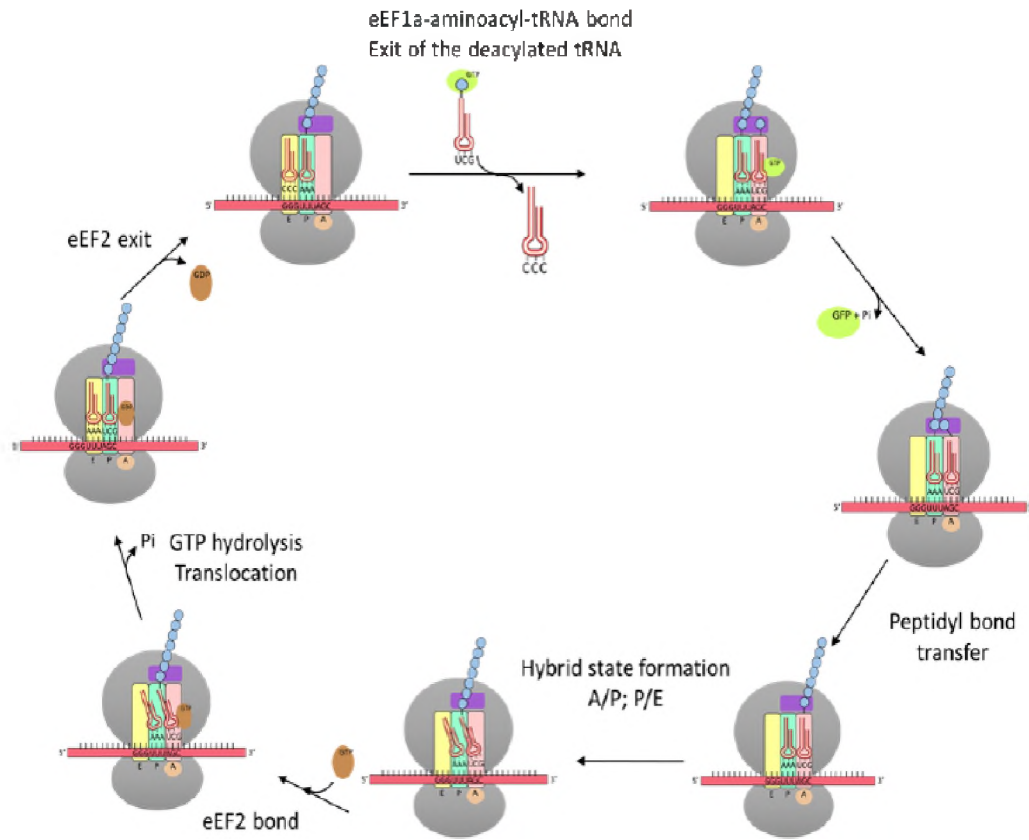


Figure 9: Translation elongation cycle. During the translation of mRNA, the ribosome first recruits an aminoacyl-tRNA in the A site and binds to the elongation factor eEF1A (green disc). Following this first crucial step, the tRNA hybridizes by complementarity its anticodon to the mRNA codon, releasing eEF1A. The peptide bond is transferred to the pre-existing polypeptide chains. The tRNA is translocated to the P sites after an intermediate hybrid state with the help of the eEF2 (brown disc). The deacylated tRNA located in the E site exits from the ribosomes and a new cycle begins

1.3.2. IFN- γ -activated inhibitor of translation (GAIT) pathway mediated regulation of translation.

Translational regulation can be global or mRNA specific. Global control of translation usually operates by regulating the phosphorylation or availability of initiation factors. Two of the most well-known examples are the regulation of eukaryotic initiation factor eIF4E availability by 4E-binding proteins (4E-BPs), and the modulation of the levels of active ternary complex by eIF2 α phosphorylation. mRNA-specific translational control is driven by RNA sequences and/or structures that are commonly located in the untranslated regions (3' or 5') of the transcript (Mazumder *et al.*, 2003) (Sonenberg and Hinnebusch, 2009). These features are usually recognized by heterogeneous nuclear ribonucleoproteins (hnRNP) and other pre-mRNA/mRNA-binding proteins (mRNP) or micro RNAs (miRNAs) that bind to the RNA through special RNA binding domains (Glisovic *et al.*, 2008). One such transcript-specific translation control has been discovered and elaborated by our lab and a group of other researchers. This pathway is called Gamma-Interferon Activated Inhibitor of Translation mechanism or the GAIT pathway, which has possibly evolved as an endogenous mechanism to limit inflammation.

IFN- γ -activated inhibitor of translation (GAIT) pathway:

The IFN- γ induced delayed translational silencing pathway was first studied in cells of myeloid origin, primarily monocytes and macrophages and related cell lines where it regulates the expression of several inflammatory genes e.g. chemokines and chemokine receptors. The GAIT complex is a multi-subunit protein complex which is composed of

four protein constituents: ribosomal protein L13a, glutamyl-prolyl-tRNA synthetase (EPRS), NS1-associated protein 1 (NSAP1) and glyceraldehyde-3 phosphate dehydrogenase (GAPDH) which results in delayed translational silencing of GAIT element bearing mRNA transcripts (Vyas *et al.*, 2009) (Mazumder and Fox, 1999), (Sampath *et al.*, 2003)(Mazumder *et al.*, 2003)(Sampath *et al.*, 2004) (Kapasi *et al.*, 2007)(Arif *et al.*, 2011). This regulatory system of eukaryotic gene expression relies upon the presence of a minimal 29 nucleotide long structural element in the 3' untranslated region (3'-UTR) of the target mRNA, called the GAIT element made up of a 5-nt terminal loop, a weak 3-bp helix, an asymmetric internal bulge, and a proximal 6-bp helical stem (Sampath *et al.*, 2003). In this pathway, the GAIT complex forms in two stages. An inflammatory trigger such as IFN- γ treatment results in sequential phosphorylation (Ser886 and Ser999 in the noncatalytic linker connecting the synthetase cores) mediated release of EPRS from the parent tRNA multisynthetase complex in the initial hours (2 hr) post IFN- γ treatment. Ser886 phosphorylation is required for the interaction of EPRS with another GAIT component NSAP1 to form an inactive pre-GAIT complex (incapable of binding to the GAIT element in the 3' UTR of selective mRNAs). In the second step, after another 12-14 hours, L13a is phosphorylated and released from the 60S subunit and joins GAPDH and then binds to the pre-GAIT complex to form tetrameric GAIT complex. Ser999 phosphorylation of EPRS is essential for the conformationally correct interaction with phospho-L13a and GAPDH to generate the active GAIT complex that binds to the GAIT element in the 3' UTR of target mRNA. Upon binding, the GAIT complex interacts with eIF4G of the translation initiation machinery and blocks the recruitment of 43S pre-initiation complexes, thereby inhibiting translation initiation (Arif *et al.*, 2011)(Kapasi *et*

al., 2007). This blocking of formation of 48S initiation complex, requires circularization of mRNAs mediated via the eIF4E–eIF4G–polyA-binding-protein (PABP) interaction (figure 10). Such interactions between the 5' and 3' ends of mRNAs could provide a spatial framework for the action of regulatory factors like the GAIT complex that binds to the 3' untranslated region (Mazumder *et al.*, 2003). This GAIT mediated translational silencing mechanism was first studied in monocytes expressing ceruloplasmin in response to IFN- γ treatment.

A genome-wide approach identified a cohort of mRNAs encoding proteins having a role in inflammation and were identified to be the direct target of the L13a-dependent GAIT translational silencing pathway (Vyas *et al.*, 2009). Most of these targets were identified as chemokines and chemokine receptors.

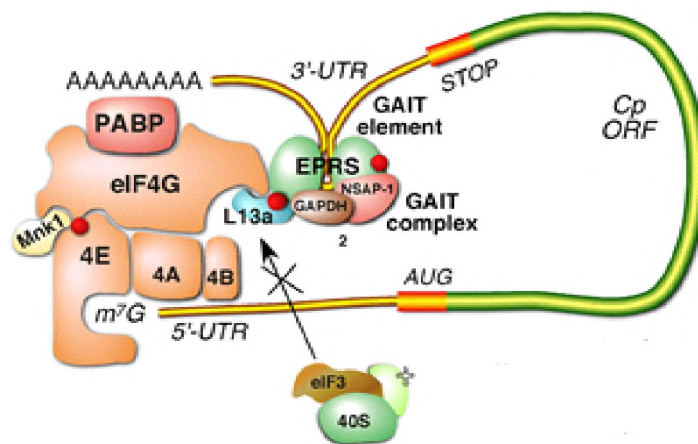


Figure 10: L13a targets eIF4G for transcript-specific inhibition of translation (Kapasi P et al., 2007). L13a in the 3' UTR bound GAIT complex targets eIF4G without cleavage of eIF4G or disruption of cap-binding eIF4F complex. Binding of the phospho-L13a to the eIF3 binding site of eIF4G blocks interaction of 43S ribosomal complex and represses translation initiation.

1.4. Ribosomal and extra-ribosomal function of RP L13a:

Mammalian ribosomal protein L13a is a member of conserved ribosomal L13 protein family (uL13). L13a is a component of the 60S ribosomal subunit and is a component of the GAIT complex explained above. Many ribosomal proteins have been shown to possess ribosomal and extra-ribosomal functions. L13a is one of the ribosomal proteins which is known to play an essential extra-ribosomal function discussed below.

1.4.1. Extra-ribosomal function of L13a in inflammation resolution in macrophages.

After phosphorylation at Ser77 by DAPK/ZIPK pathway and release from 60S subunit, L13a binds GAPDH which shields and protects free L13a from degradation. L13a,

as a component of GAIT complex, can bind the translation initiation factor eIF4G and prevent the formation of 48S preinitiation complex thereby inhibiting the translation initiation of a subset of inflammatory proteins (Jia *et al.*, 2012) (figure 11).

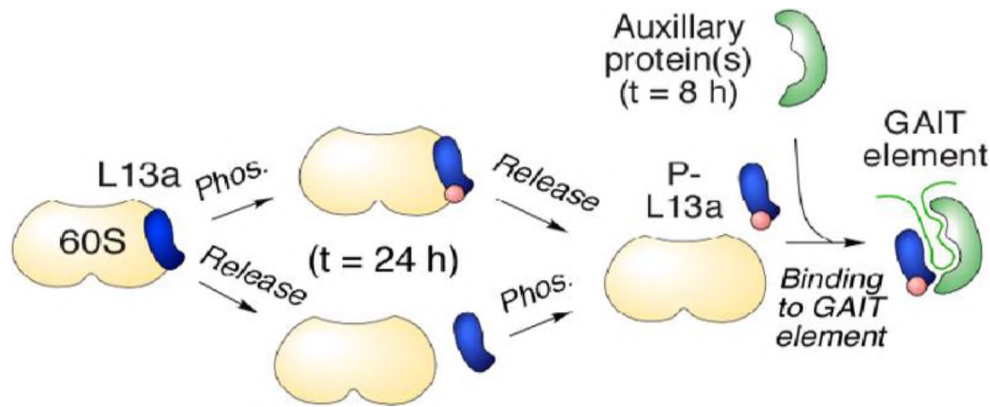


Figure 11: Assembly of L13a into the GAIT complex (Mazumder et al. 2003).

Phosphorylation mediated release and delayed assembly of L13a into pre-GAIT complex to form a functional GAIT complex, capable of binding to Cis-acting GAIT element in 3' UTR of target mRNA transcripts.

Infectious events are marked by the recruitment of monocytes and macrophages, key effector cells in an immune response, to the site of inflammation where synthesis of chemokines and cytokines serves as a weapon against the invading microorganisms. However, uncontrolled inflammation can have detrimental effects and inflamed tissues need to be restored back to the normal tissues. Based on the notion that GAIT-mediated translational silencing of several chemokines and its receptors could serve as an endogenous defense against inflammation and a deficiency of L13a in macrophages may promote uncontrolled inflammation, our lab generated a novel macrophage-specific L13a knock out animal model (L13a flox/flox LysMCre⁺) where impact of abrogation of ribosomal protein L13a-dependent translational silencing mechanism was studied in detail

by challenging the WT and KO animals with inflammatory stimuli such as LPS (lipopolysaccharide). These studies demonstrated that macrophage-specific L13a KO mice showed a lower survival rate, more invasion of myeloid cells in the peritoneal cavity and in the major organs suggesting signs of organ damage in comparison to the control mice. Moreover, macrophages harvested from these KO animals also showed elevated expression of several previously identified target proteins of GAIT pathway such as CCL22, CXCL13 and CCL8 etc., suggesting abrogation of inflammation resolution in KO animals in the absence of L13a-mediated GAIT complex assembly and translational silencing (Poddar *et al.*, 2013). Subsequent studies have been conducted by our laboratory to understand the extra-ribosomal function of L13a and GAIT complex in inflammation resolution in several pathological conditions such as ulcerative colitis and atherosclerosis (Poddar *et al.*, 2016) (Basu *et al.*, 2014).

However, the mechanism of assembly of L13a into the GAIT complex remain poorly understood. As discussed earlier, arginine at position 68 is essential for ribosomal incorporation. However, L13a with arginine at 68 mutated to alanine still retains the ability to play its extra-ribosomal function i.e. translational silencing of GAIT element bearing mRNAs, suggesting existence of an independent ribosomal incorporation and translational silencing domain in L13a (Das *et al.*, 2013). Therefore, our current study aims at identifying the specific domains of L13a essential for ribosomal incorporation and GAIT-mediated translational silencing activity.

1.4.2. Function of L13a within the ribosomes.

As discussed above, a series of studies by our group has deciphered an important extra-ribosomal function of L13a. To gain insights into the role of L13a within the ribosome, we have shown that depletion of L13a by RNA interference (RNAi) in monocytic cells abrogates GAIT element-mediated translational silencing but, interestingly, it doesn't affect rRNA processing, ribosome assembly and primary function of ribosomes i.e. protein synthesis. However, rRNA methylation and translation of several IRES (internal ribosome entry site) containing mRNAs such as P⁵³ and SNAT2 requires L13a. Therefore, depletion of L13a compromises the translation of these mRNAs (Chaudhuri *et al.*, 2007). Further, we have shown that L13a incorporates into the ribosomes in the 90S precursor ribosome in the nucleolus. This is the site where the L13a as a component of the methyltransferase complex and participates in the rRNA methylation. Previous studies have demonstrated that reduced translation of IRES containing mRNAs in L13a depleted cells is a consequence of reduced rRNA methylation (Das *et al.*, 2013).

So far, we have shown that complete loss of L13a in cultured cells and tissue-specific loss of L13a in mammalian model (mouse) is tolerable and doesn't interfere with the cell proliferation and survival of mice under normal condition.

Since we have studied the role of GAIT pathway in inflammation resolution in macrophage-specific knockout mice and we have demonstrated that depletion of L13a in cultured cells of myeloid origin is tolerable, we decided to investigate the consequences of L13a knockout at systemic level in mammals. For this purpose, we have generated the heterozygous L13a knock out (L13a^{+/-}) mice which could be crossed to get L13a total knockout mice. Unfortunately, we didn't identify any knockout genotypes among the new born pups. Interestingly, L13a heterozygous mice are breeding competent and show no

visible abnormality under standard animal housing conditions. However, the mice harboring the homozygous KO allele (L13a^{-/-}) are found to be embryonically lethal as we failed to identify any knockout among offspring of L13a heterozygous parents. This suggests an essential role of this protein in embryonic development in mammals. In this regard, I shall discuss the role of ribosomal proteins in mammalian embryonic development and the process of pre-implantation embryonic development in mice to obtain a better understanding of the experimental strategies that we pursued further to study the role of L13a in the embryonic development of mice.

1.5. Role of ribosomal proteins in embryogenesis:

In addition to their essential roles in ribosome biogenesis and protein translation, ribosomal proteins are also known to play developmental roles in various organisms. e.g. mice homozygous for small subunit protein S19 shows defect in early embryonic development where the homozygous knock out zygote fails to transition into a blastocyst, suggesting a role of S19 in blastocyst formation. The role of ribosomal proteins in mammalian development is discussed further in chapter III.

1.5.1. Mouse: a model organism for embryology studies.

Mouse (*Mus musculus*) has been a model organism of choice for molecular biologists inclined to study the outcome of gene knockouts in mammals. Mouse is also the mammal of choice to understand how genes control growth and differentiation of the mammalian embryo because of its small size, resistance to infection, large litter size (4-14)

and their short gestation period, about 21 days. The genome of about 17 inbred strains has been sequenced. The most remarkable feature is the ability to experimentally manipulate the mouse germline either by genetic modifications of embryonic stem (ES) cells, spermatogonial stem cells or by direct injection of cloned DNA into zygotes.

Mouse development can be divided into preimplantation and post-implantation stages. Preimplantation stage embryos are not attached to the maternal tissue and can be located in the oviduct and uterus, whereas, post-implantation embryos are attached to the maternal tissue through placenta tissues. Mouse embryos are staged by days postcoitum (dpc).

1.5.2. Mouse embryonic development.

(i) Oocyte maturation and ovulation

Mouse oocyte are in the diplotene stage of the prophase of the first meiotic division. Therefore, they are diploid but contain four times the haploid amount of DNA (4C). Oocyte is surrounded by follicle or granulosa cells and are called primordial follicles. Primordial follicles are then recruited to differentiate into preovulatory or antral follicles. Gradually, zona pellucida starts developing between the follicle cells and the oocyte. Zona pellucida is made up of three acidic glycoproteins- Zp1, Zp2, Zp3 synthesized by growing oocyte and reaching about 7 μ m in thickness (Dean, 1992). Zp3 is required for acrosome reaction during fertilization. In response to LH (luteinizing hormone), follicles grow and acquire competence for ovulation by undergoing a first meiotic division to exclude one polar body. 8-12 eggs are released in a span of 2-3 hours. After ovulation follicular cells differentiate to form corpora lutea, which help to maintain pregnancy.

(ii) Spermatogenesis

Seminiferous tubules are the site of spermatogenesis. Testes contain prospermatogonia in the mitotic arrest at the time of birth that develop into primary spermatocytes after a series of changes in size and transitions. These primary spermatocytes undergo meiosis to form secondary spermatocytes. Spermatids are formed after second meiotic division which differentiate to form mature spermatozoa.

(iii) Fertilization:

Fertilization occurs in the oviducts. Zona pellucida component ZP3 triggers the acrosome reaction in which the acrosome fuses with the plasma membrane of the sperm head. Fusion of the sperm head with the oocyte membrane is followed by a cascade of reactions known as fertilization. The head, mid piece and tail of the sperm enters the oocyte cytoplasm. Fertilization triggers a second meiotic reaction and extrusion of a second polar body. The fertilized oocyte is known as zygote.

(iv) Morulation:

Twenty-four hours post fertilization, the mouse embryo forms a two-cell stage in the oviduct and keeps moving towards the uterus. Four to eight cell embryos can be retrieved from the oviduct at 2.5 dpc. After pairing male and female, a vaginal copulation plaque is observed in the female next morning, it is counted as 0.5 dpc. The eight cell stage is known as morula. The cells inside the embryo undergo cleavage divisions without cell growth, keeping the embryo volume constant. This results in increase in number of cells only. Each cell within the 2-cell to 8-cell stage embryo is equipotent, capable of giving rise to a blastocyst.

(v) Blastocyst formation:

As the cleavage divisions reach the 16-cell stage, two distinct lineages are formed: the trophoctoderm (TE) and the inner cell mass (ICM). At this stage the blastomeres flatten and increase their contact with each other, developing an apical and basal membrane and cytoplasmic domains. Inner cell mass arises from the cells that lie on the inside of compacted embryo, whereas the outer cells form trophoctoderm. After about the fifth cleavage division, a fluid filled cavity appears, called the blastocoel cavity. As the blastocyst expands and forms a “fully expanded” blastocyst, the blastocoel cavity also enlarges. The blastocyst (32-80 cells) is made up of single layer of trophoctoderm surrounding a fluid-filled cavity with a small group of cells called ICM, attached to the trophoctoderm (TE) at one region. The TE overlying the ICM is known as polar TE (embryonic pole) and the cells surrounding the blastocoel constitute the mural TE (abembryonic pole). Blastocysts can be retrieved from the uterus at 3.5 dpc.

(vi) Implantation in the uterus:

A blastocyst is ready for implantation when it escapes or hatches from the zona pellucida. The first event of implantation is the adherence of the blastocyst to the uterine wall by its abembryonic pole, forming a uterine crypt and stimulates the uterine stroma to form a spongy cell mass known as the decidual tissue/deciduum. Usually implantation takes place at 4.5 dpc. The progression of pre-implantation embryos is summarized in figure 12.

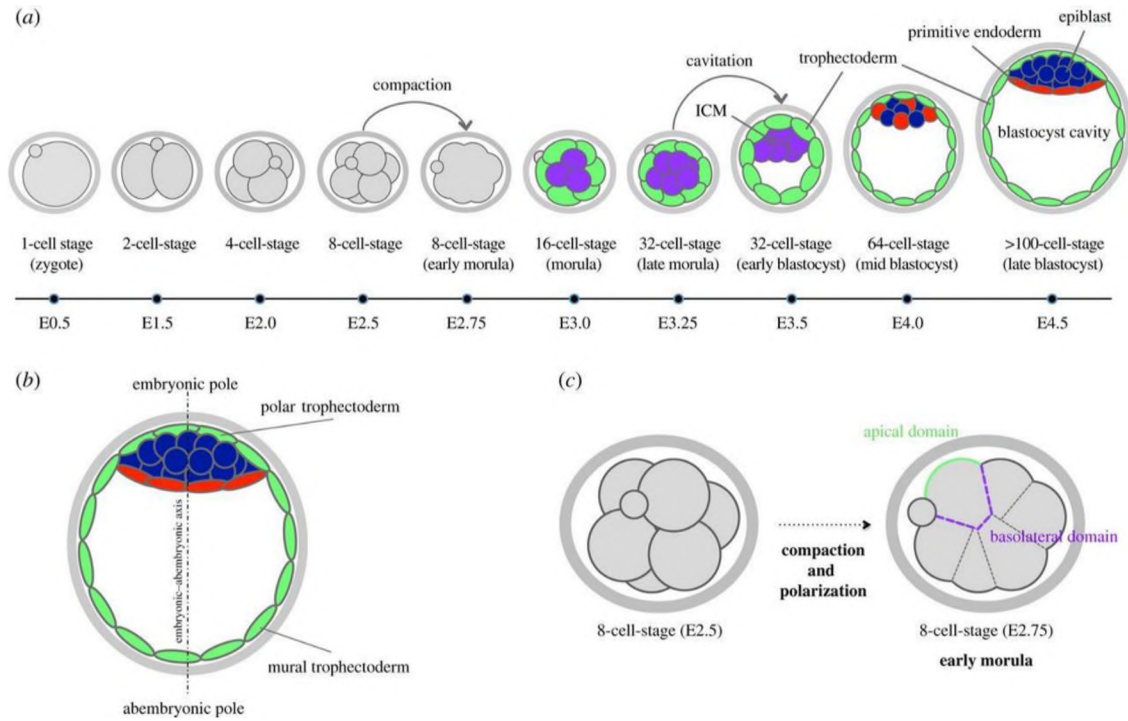
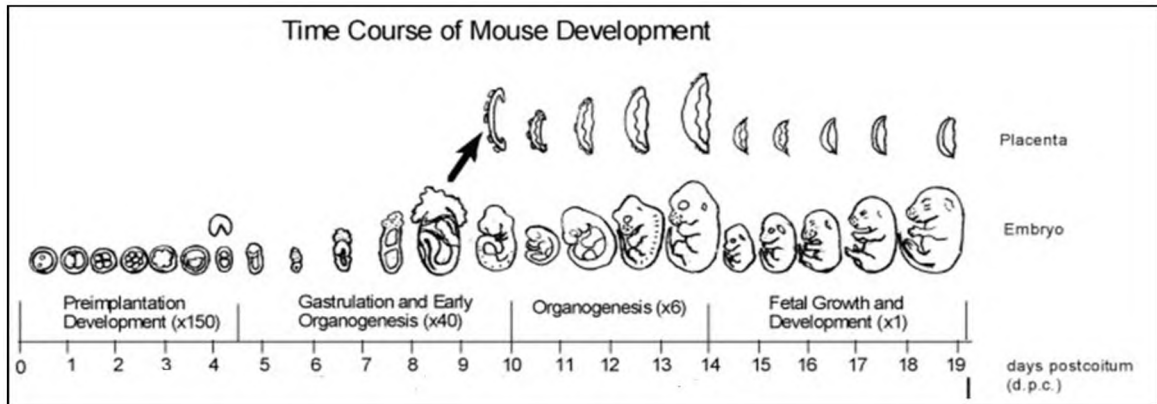


Figure 12: The preimplantation period of mouse embryo development (figure adapted from Aleksandar I et al., 2017): (a) The sequence of events throughout the preimplantation mouse embryo development with relevant embryonic stages and cell lineages generated through the first and the second cell-fate decisions. (b) Orientation of the embryonic–abembryonic axis in the late blastocyst stage (4.5 dpc). The position of mural and polar trophectoderm at abembryonic and embryonic poles of the embryo is shown. (c) A non-compacted 8-cell-stage embryo undergoing the first morphogenetic event (compaction) to develop into an early morula-stage embryo. Concomitantly, intracellular polarization is established as exemplified by the apical (green), and basolateral (purple) membrane domains of individual blastomeres.

(vii) Post-implantation development:

Shortly after implantation, a differentiation event results in formation of a primitive endoderm and epiblast or primitive ectoderm from inner cell mass. Therefore, an implanted blastocyst is made up of three layers: trophoctoderm, primitive endoderm and epiblast. A proamniotic cavity starts forming at around 5.5 dpc from epiblast cells. Cells of epiblast start dividing rapidly between 5.5-6.5 dpc from 120 cells to 660 cells (Snow, 1977). This is the time when gastrulation begins, a process in which blastocysts transform into a multilayered embryo. Extra-embryonic mesoderm and definitive endoderm is also formed during gastrulation. This is followed by organogenesis marked by events like germ line origin, limb formation, sex determination, tail bud, neurulation, gut formation etc. Birth of fully formed pups takes place around 20-21st day of gestation. The different stages of mouse development are shown in the figure 13 below:

a



b

Mouse (GD)	Event
0	Fertilization
1-2.5	Cleavage
2-4	Blastocyst stage
4.5-5	Implantation
6-14	Placentogenesis
14	Organogenesis complete
14-17	Fetal and Placental growth
17-birth	Accelerated Fetal Growth
19-21	Birth

Figure 13: (a) Time course of mouse development summarizing 0-19 DPC embryonic development. (b). The table based on the Theiller stages of mouse development (The House Mouse: Atlas of Mouse Development by Theiler Springer-Verlag, NY (1972, 1989).

CHAPTER II

EXISTENCE OF MUTUALLY EXCLUSIVE RIBOSOMAL INCORPORATION AND TRANSLATIONAL SILENCING DOMAIN IN RP L13A

2.1 ABSTRACT

Ribosomal protein L13a is essential for transcript-specific translational silencing of mRNAs encoding several inflammatory proteins e.g. chemokines and chemokine receptors. A series of studies from our laboratory has shown that phosphorylation-dependent release of L13a from 60S ribosomal subunit and its assembly into the IFN- γ -activated inhibitor of translation (GAIT) complex is essential for translational silencing of target mRNAs. Our current study is focused on identification of amino acid residue(s) essential for translation silencing of target mRNAs and the residue(s) important for ribosomal incorporation. Structurally, eukaryotic L13a differs from prokaryotic L13 by an α -helical extension of ~55 amino acids at the C-terminal end. Interestingly, we observed that deletion of this helix impairs the extra-ribosomal function of L13a i.e. translational silencing of inflammatory genes as well as its incorporation into the ribosomes. We have identified the amino acids within this helix at position 159(K) and 161(K) that are required

for nucleolar import of L13a and incorporation into the ribosome. Cryo EM studies of the human ribosome showed the interaction of the amino acids at position 185(V), 189(I) and 196(L) of L13a with another ribosomal protein L14. We found that mutating these residues abrogates the ribosomal incorporation of L13a. Importantly, we also showed that mutation of the amino acids at position 169(R), 170(K) and 171(K) to Ala abrogate GAIT-mediated translational silencing, but not L13a incorporation into ribosomes. Moreover, we show that the C-terminal helix (149-203 amino acids) alone can silence translation of GAIT element-containing mRNAs. This demonstrates the presence of mutually exclusive domains for ribosome incorporation and translational silencing.

2.2 INTRODUCTION

Ribosomes are complex ribonucleoprotein (RNP) complexes that catalyze the synthesis of the cell's proteome. However, there are several unanswered questions about the mechanism of ribosome biogenesis and its regulation in concert with the role of ribosomal proteins (RP) and assembly factors. One of the important questions is: how and when do ribosomal proteins associate with rRNA and their roles as a part of functional ribosomes? In yeast, many ribosomal proteins are co-transcriptionally incorporated as soon as the nascent rRNA starts emerging from the RNA polymerase or in the nucleolus, some others incorporate late cytoplasmic pre-ribosomes. Many ribosomal proteins are known to play an important role in rRNA processing and ribosome biogenesis e.g. L33 in yeast (Martin-Marcos, Hinnebusch and Tamame, 2007). However, the functions of many RPs remain unexplored. Previous studies in our laboratory have demonstrated the ribosomal and extra-ribosomal functions of one of the large subunit (LSU) protein i.e. ribosomal protein L13a (RP L13a). A series of studies have shown that the arginine residue at position 68 in human L13a is essential for L13a binding to rRNA and subsequent incorporation into the ribosomes. Arginine 68 was predicted to be a potential candidate for anchoring the protein to rRNA based on the yeast L16a where arginine at position 68 interacts with the cytosine at position 2988 (C2988). Yeast L16 is the structural homolog of human L13a. Arginine at position 68 is highly conserved among eukaryotes ranging from yeast, *Drosophila*, pig, mice, monkey and human. Furthermore, our group has experimentally shown that precursor 90S ribosome is the site of ribosomal incorporation of L13a. WT L13a but not the R68A mutant incorporates into the 90S pre-ribosome complex in the DFC region of nucleolus. Nucleolin is an important nucleolar protein which is known to interact

with several ribosomal proteins and nucleolar factors and acts as a shuttle for nucleocytoplasmic traffic. Based on this, it is believed that nucleolin might be involved in the import of ribosomal proteins to the nucleolus and act as an adaptor for binding of RPs to the rRNA. L13a has been identified as one of the proteins that interacts with nucleolin (Bouvet *et al.*, 1998). Therefore, the ability of WT and mutant L13a protein were tested for their ability to bind to nucleolin and translocate to the nucleolus (site of L13a incorporation). We have shown that ribosomal incorporation of a defective mutant R68A binds to the nucleolin, translocates to the nucleolus but fails to incorporate into the ribosomes, suggesting that successful nucleolar import of L13a doesn't necessarily ensure its ribosomal incorporation. As aforementioned, L13a plays an extra-ribosomal function in translational silencing of GAIT element bearing mRNAs encoding inflammatory proteins, it was also tested if the ribosomal incorporation defective (R68A) mutant retains the ability to become phosphorylated at S77 residues and silence the translation of GAIT element bearing mRNAs in an in vitro experiment. Interestingly, mutation of arginine 68 to ala (R68A) doesn't interfere with the S77 phosphorylation and translational silencing ability. Therefore, ribosomal incorporation of L13a is not a prerequisite for phosphorylation and extra-ribosomal function of L13a. Previous studies by our lab and other groups have shown that the DAPK-ZIPK pathway mediated phosphorylation at S77 and release of L13a is essential for its extra-ribosomal function (Mukhopadhyay *et al.*, 2008). Moreover, our group has demonstrated that L13a is dispensable for ribosome biogenesis and the primary function of ribosomes (protein synthesis). Depletion of L13a in somatic cells doesn't affect ribosomal RNA processing, polysome formation, global translational activity, translational fidelity, and cell proliferation. However, depletion of L13a caused significant reduction of

methylation of ribosomal RNA and of cap-independent translation mediated by Internal Ribosome Entry Site (IRES) elements such as p53 and SNAT2. Further, we have shown that the ribosome incorporation defective L13a mutant (R68A) but not WT L13a shows reduced rRNA methylation in the 90S precursor ribosome, suggesting that L13a is a part of rRNA methylation complex and ribosomal incorporation of L13a is essential for rRNA methylation (Chaudhuri *et al.*, 2007)(Das *et al.*, 2013).

So far, we know that arginine at position 68 is essential for ribosomal incorporation of L13a. Disrupting ribosomal incorporation of L13a by mutating R68 resulted in reduced rRNA methylation and translation of IRES-containing mRNAs. However, it doesn't interfere with ribosome independent function of L13a i.e. the GAIT pathway mediated translational silencing.

Analysis of eukaryotic ribosome structure using X-ray crystal structures of the yeast 80S ribosome at 3.0 Å showed that bacterial and eukaryotic ribosomes evolved from a common structural (RNP) core with inclusion of extra rRNA (expansion segments) and additional ribosomal proteins enveloping the core on the solvent side of the ribosome. The 80S yeast ribosome contains 79 proteins, of which 46 are eukaryote-specific and thirty-four proteins are conserved. Many of the conserved ribosomal proteins have evolved eukaryote-specific N-terminal and C-terminal extensions, the functional significance of which is largely unknown. It has been proposed that these eukaryote-specific extensions might have evolved to play a role in complex translation mechanisms in eukaryotes, involved in protein-protein interactions and/or specific extra-ribosomal functions. Several ribosomal proteins are known to possess N-terminal or C-terminal eukaryote-specific extensions. For example, ribosomal protein uS2 has eukaryote-specific N- and C-terminal

extensions and is known to play a role as cell surface receptor for laminin (Ghosh and Komar, 2015). N-terminal terminal extension of yeast L8 (eL8) protein is necessary for late nuclear stages of 60S subunit assembly (Tutuncuoglu *et al.*, 2016).

In our current study, we have also identified a eukaryote-specific C-terminal extension in human ribosomal protein L13a. Structure and sequence alignment of prokaryotic L13 and human L13a protein has revealed the evolution of a C-terminal helix of ~55 amino acids long. We have investigated the role of this C-terminal extension in nuclear/nucleolar translocation of L13a, ribosomal incorporation and extra-ribosomal function.

2.3 MATERIAL AND METHODS

2.3.1 Cell Culture

HEK 293T cells were grown in DMEM medium containing 4.5 g/L glucose supplemented with 10% fetal bovine serum (FBS), 2 mM glutamine, 1% penicillin and streptomycin. The cell culture was maintained in an incubator at 37° C and 5% CO₂. Sf9 (insect cells) cells were maintained as adherent cells in Sf-900 II SFM (1X) serum-free media in a non-humidified incubator at 27° C. DMEM media was purchased from Corning Cellgro (cat#10-017-CV), Sf-900 II SFM (1X) from Gibco (Cat#10902-096).

2.3.2 Generation of constructs

Hemagglutinin (HA)-tagged L13a plasmids were generated by cloning the human wild type L13a cDNA or its different mutant variants in-frame with the HA tag in the pcDNA3.1(+) mammalian expression vector (Invitrogen) using BamHI and NotI restriction sites. The resulting constructs were expressed in HEK 293T cells for various cell-based assays discussed in this study. His-tagged recombinant L13a bacmid DNAs were generated by cloning human L13a cDNAs (wild type or different mutant variants) into pFastBac HT A vector using EcoRI and SalI restriction sites. The resulting recombinant his-tagged bacmids were transformed into Max efficiency DH10bac competent *E. coli* cells using the Bac-to-Bac Baculoviral Expression System kit according to the manufacturer's protocol (Invitrogen, Cat# 10359-016). Mutations in the HA-tagged and His-tagged plasmids were introduced by site directed mutagenesis using the Quick-Change II Site-Directed Mutagenesis Kit (Agilent Technologies, Cat# 200524). L13a deletion mutants

were generated by PCR of different length L13a fragments using L13a specific primers flanking restriction site sequences of choice followed by cloning into pcDNA3.1(+) and pFastBac HTA vector. HA and (6X) His tags were placed at the N-terminus of the L13a open reading frame.

2.3.3 Ribosomal Incorporation assay

Wild-type (WT) and mutant variants of HA-tagged L13a proteins were tested for their ability to co-sediment with polyribosomes. HEK293T cells were transfected with HA-tagged pcDNA3.1(+) plasmids expressing either WT or mutant human L13a protein. 18 hours post-transfection, polyribosomes were harvested from the transfected cells by our previously published method (Das et al. 2013). Briefly, transfected cells were treated with cycloheximide (CHX) (100 μ g/ml) for 15 minutes at 37 $^{\circ}$ C, washed once and harvested in PBS containing CHX at 100 μ g/ml concentration. Cells were lysed in polyribosome buffer (100 mM KCl, 2.5 mM MgCl₂, 1mM DTT, 10 mM HEPES pH 7.5, 100 μ g/ml CHX) containing 0.1% Igepal-CA630 (NP-40), 50 U of recombinant RNasin (Promega) and protease inhibitor cocktail (Roche). Cytoplasmic lysates (20 Optical density units) were layered over a 10-50% linear sucrose gradient in polyribosome buffer and then centrifuged at 17,000 RPM in a Beckman SW32.1 Ti rotor for 18 hours at 4 $^{\circ}$ C. Gradients were fractionated to get lighter RNP fractions (40S, 60S and 80S) and heavier polyribosomal fractions using an ISCO Gradient Fractionation System by monitoring the continuous UV absorption profile at A₂₅₄. The total protein in each fraction was recovered by TCA

(trichloroacetic acid) precipitation and analyzed by SDS-PAGE (12% gel) followed by immunoblotting with a rabbit polyclonal anti-HA antibody (Abcam, cat#ab9110).

2.3.4 Analysis of nuclear and nucleolar localization of L13a by immunofluorescence

HEK 293T cells cultured on cover glass were transfected with pcDNA3.1(+)-constructs expressing HA-tagged WT or mutant human L13a. optimal confluency at the time of transfection of HEK cells for immunostaining and confocal microscopy is 60-65% to avoid overlapping/overgrowth of cells to get clear images. Approximately twenty-four hours post-transfection, cells were fixed with ice-cold methanol, permeabilized with 0.1% Triton X-100, and blocked in 1% BSA for 1 hour at room temperature. Cells were then incubated with mouse monoclonal antibody against the HA tag (Abcam, Cat# ab18181) or rabbit polyclonal antibody against human nucleolin (as an endogenous marker of nucleoli; Abcam, Cat# ab22758) for 3 hours. Antibodies used were diluted (1:200) in 1x PBS containing 0.5% triton X-100. After incubation with the primary antibodies, cells were washed with PBS three times (five minutes each wash) and incubated with Alexa Fluor 488 (green) conjugated donkey anti-mouse antibody (Cat# A21202, Invitrogen; for anti-HA stained cells) or Alexa Fluor 594 (red) conjugated donkey anti-rabbit antibody (Cat# A21207, Invitrogen; for anti-nucleolin stained cells) for 1 hour at room temperature in dark. All cells were co-stained with 4',6-diamidino-2-phenylindole (DAPI, blue) to visualize nuclei. After washing three times with PBS, cover glass were mounted in a drop of prolong gold antifade reagent (Cat# P36930, Invitrogen) on glass slides. Next day, the antibody-stained cells were subjected to confocal microscopy using a Nikon TE inverted fluorescent microscope.

2.3.5 Determination of the GAIT element-dependent translational silencing activity of L13a mutants

His-tagged recombinant WT and different mutant variants of L13a proteins were expressed in Sf9 (insect cells) using the Bac-to-Bac baculoviral expression system following manufacturer's protocol (Invitrogen). Briefly, Sf9 insect cells were transfected with WT or mutant L13a bacmids to generate baculoviral stocks: P0, P1, P2. Baculoviral stocks were stored in -80° C after adding 2% FBS. Sf9 cells were further infected with the baculoviral particles, lysed at the time point optimized initially to obtain maximum protein yield. His-tagged L13a proteins were purified using HisPur Ni-NTA purification Kit (Thermo Fisher Scientific, Cat#88227) and tested by doing a Western blot using mouse anti-His antibody (Invitrogen, Cat#37-2900). Purified proteins were tested using an in vitro translational silencing assay. 200 ng GAIT element bearing chimeric RNA transcript containing a GAIT element (Cap-Luc-GAIT-PolyA) and a cRNA transcript encoding T7 gene 10 (used as a loading and specificity control) were translated in rabbit reticulocyte lysate (RRL) in the presence of purified WT or mutant L13a proteins, 20 µM methionine-free amino acid mixture, 20 µCi translation grade [³⁵S] methionine, and 40U of RNasin in a total volume of 50 µl reaction at 30° C for 1 hour. An aliquot was resolved by 10% SDS-PAGE. The gel was fixed, dried and radiolabeled bands were detected by autoradiography.

2.3.6 In vivo association of L13a with 28S rRNA

HEK 293T cells were transfected with pcDNA3.1(+) plasmids expressing HA-tagged WT or mutant L13a proteins. Twenty four hours post transfection, cell lysates were

prepared and subjected to immunoprecipitation using mouse anti-HA antibody coupled agarose beads (Sigma, Cat#IP0010-1KT) or non-antibody-coupled beads as a control in the buffer 150 mM NaCl, 1 mM EDTA, 1.5 mM MgCl₂, 0.05% Triton X-100, 50 mM HEPES (pH 7.5) (Mazumder et al. 2003). Total L13a-bound RNA was extracted from the immunoprecipitates using TRIzol. The extracted RNA was reverse transcribed using random hexamers and reverse transcriptase (superscript) following manufacturer's protocol (Invitrogen). The synthesized first-strand cDNA was subjected to reverse transcription-PCR (RT-PCR) using human 28S rRNA specific primer pairs. Forward primer sequence 5'-GAAGTTTCCCTCAGGATAGCT-3' and reverse primer sequence 5'-GCAGGTGAGTTGTTACACACT-3' were used. The PCR product of 355 base pair was analyzed by agarose gel electrophoresis. Immunoblotting with anti-HA antibody was used to confirm presence of L13a in the immunoprecipitate.

2.3.7 In vivo association of L13a with nucleolin

HEK 293T cells were transfected with plasmids expressing HA-tagged WT or mutant L13a proteins. 24 hours post transfection, cells were lysed in lysing buffer supplied with the IP kit and 100 µg of lysates were immunoprecipitated with mouse anti-HA antibody coupled agarose beads (Sigma, Cat# IP0010-1KT) or non-antibody-couple beads as a control in the buffer 150 mM NaCl, 1mM EDTA, 1.5 mM MgCl₂, 0.05% Triton X-100, 50 mM HEPES (pH 7.5). 10 µg of lysates before immunoprecipitation were used as an input for nucleolin. Total protein from the immunoprecipitates was subjected to SDS-PAGE, followed by immunoblot analysis with mouse monoclonal anti-nucleolin antibody (Millipore, Catalog# MABC587). An immunoblot with rabbit anti-HA antibody (Abcam)

was also performed to confirm the equal efficiency of immunoprecipitation in all the samples.

2.3.8 Structural and sequence analysis of human L13a with E. coli L13a and with east (L16A) and the molecular environment of the proteins on ribosome surface

Visualization and analysis of L13a and L14 structures were performed using CryoEM data of the human ribosome at 3.6 Å resolution (Protein Data Bank code 5T2C) and X-Ray data of the yeast ribosome at 3.0 Å resolution (Protein Data Bank code 4V88). Ribosome and protein structures were visualized and analyzed using Swiss-Pdb Viewer V4.1.0 and/or PyMOL v1.5.0.5. The PyMOL interface residues script was used to select interface residues involved in interaction between L13a and L14. Structural alignment of the human L13a and a yeast homologue (L16A) was done using interactive fit (all atom) alignment option of the Swiss-Pdb Viewer. Alignments of amino acid sequences of ribosomal proteins was done using Clustal Omega (1.2.4) <https://www.ebi.ac.uk/Tools/msa/clustalo/> that uses seeded guide trees and hidden Markov models (HMM) profile-profile techniques to generate alignments between three or more sequences. Structure alignment of E. coli L13 and human L13a depicted as ribbon diagrams was done using X-ray structure of the E. coli ribosome at 3.1 Å (Protein Data Bank code 4v7u) and the CryoEM structure of the human ribosome at 3.6 Å resolution (Protein Data Bank code 5T2C).

2.4 RESULTS

2.4.1. Human L13a harbors a eukaryote-specific C-terminal extension

As aforementioned, previous studies in our lab have identified arginine at position 68 essential for ribosomal incorporation of L13a. This amino acid lies within one of the predicted RNA binding domains (aa 53-75) based on the homology modeling using crystal structure of yeast L16a (structural homolog of human L13a) as a template and a web-based server, RNABindR (<http://einstein.cs.iastate.edu/RNABindR>). RNABindR predicts the probable candidate amino acids to contact RNA. This predicted RNA binding domain lies in the N-terminal globular domain of L13a. RNABindR also predicted one more RNA binding domain (aa 169-179) in the C-terminal region of L13a. In our present study, the sequence and structure alignment of prokaryotic L13 (homolog of mammalian L13a) and human L13a showed a conserved N-terminal globular domain, whereas human L13a has C-terminal extension that is not present in its prokaryotic homolog (Fig. 14). E. coli L13 is 142 amino acids long and has a histidine at position 80 at the tip of a protruding loop which shows Vander walls interactions with G2642 of the 50S rRNA. The C-terminal helix in human L13a is about 55 amino acids long (Tyr140-Val203 amino acids). Yeast L16 also has a C-terminal helix and its role in growth and ribosome biogenesis has been studied previously (Espinar-Marchena *et al.*, 2016). However, in higher eukaryotes such as mammals, the evolutionary significance of this eukaryote-specific C-terminal helix remains unknown. Therefore, in this study, we did structural and functional analysis of C-terminal extension of human L13a using human cell lines as a model and in vitro assays. Interestingly, the other predicted RNA binding domain (aa 169-179) and the predicted nuclear localization signal (NLS) by NLStradamus

(<http://www.moseslab.csb.utoronto.ca/NLStradamus/>)] sequence also lies within the C-terminal extension spanning the sequence from Lys159 to Lys 188. Therefore, we hypothesized that this C-terminal domain could have evolved in eukaryotes to perform additional functions that are absent in their prokaryotic counterparts. It is important to mention here that in yeast, the C-terminal domain had been dissected at molecular level to show its important role in rRNA processing and stabilization of 60S particles. However, the role of this domain in higher eukaryotes like mammals is largely unknown.

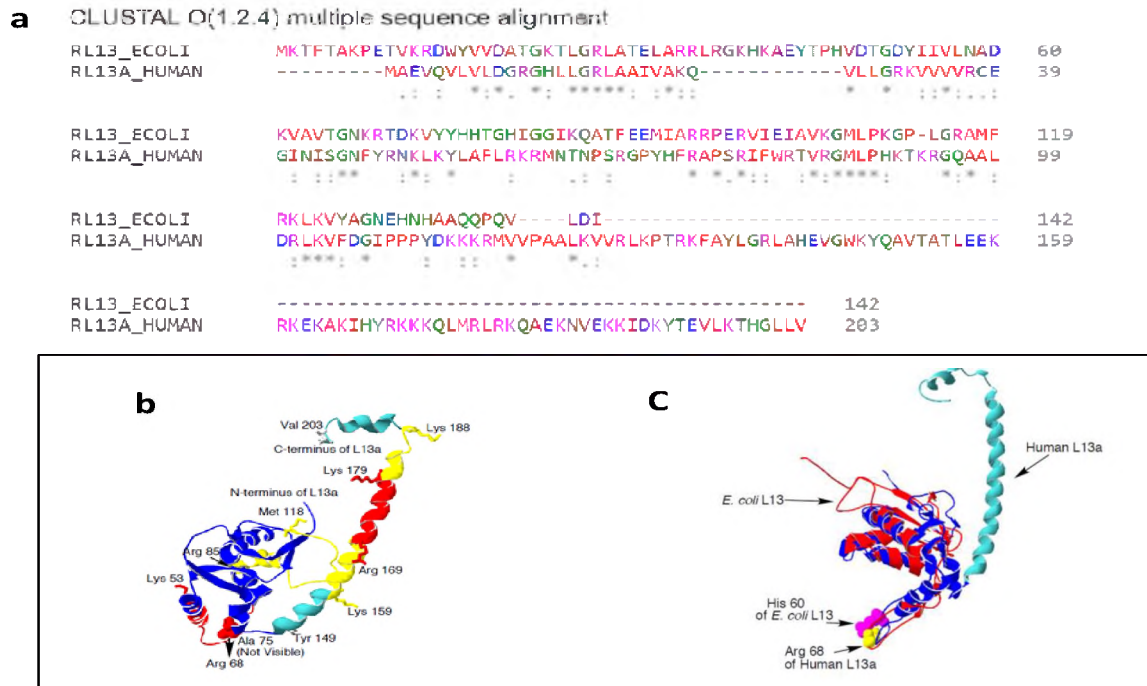


Figure 14: sequence and structure alignments of *E. coli* ribosomal protein L13 and human L13a. (a) CLUSTAL O (1.2.4) sequence alignment; (b) Human L13a structure depicted as a ribbon diagram based on the CryoEM structure of the human ribosome at 3.6 Å resolution (Protein Data Bank code 5T2C). The conserved globular core domain is shown in dark blue. Predicted NLSs (Arg84 to Met118 and Lys159 to Lys188) are shown in yellow. Predicted RNA-binding sites (Lys53 to Ala75 and Arg169 to Lys179) are shown in red. The eukaryote-specific C-terminal extension (Tyr149 to Val203) is shown in sky blue. Side chains are shown as sticks for Lys53, Lys159, Lys179, Lys188, Ala75, Arg85, Arg169, Met118, Tyr149 and Val203. (c) Structure alignment of *E. coli* L13 (red) and human L13a (blue) depicted as ribbon diagrams based on the X-ray structure of the *E. coli* ribosome at 3.1 Å (Protein Data Bank code 4v7u) and the CryoEM structure of the human ribosome at 3.6Å resolution (Protein Data Bank code 5T2C). The eukaryote-specific L13a C-terminal extension is shown in sky blue. *E. coli* His60 and human Arg68 residues previously shown to be important for ribosome incorporation are indicated. Structure alignment was done using Swiss-Pdb Viewer V4.1.0 iterative magic fit subroutine.

2.3.2. Eukaryote-specific C-terminal extension is essential for nucleolar import and incorporation of L13a into the ribosomes.

To understand the function of this C-terminal domain of human L13a, we started with deleting the whole C-terminal domain to investigate the ability of the remaining N-terminal globular domain to incorporate into the ribosomes. To accomplish this objective, we made a construct expressing HA-tagged version of L13a 148 Δ 149-203 (amino acids 149 to 203 deleted).

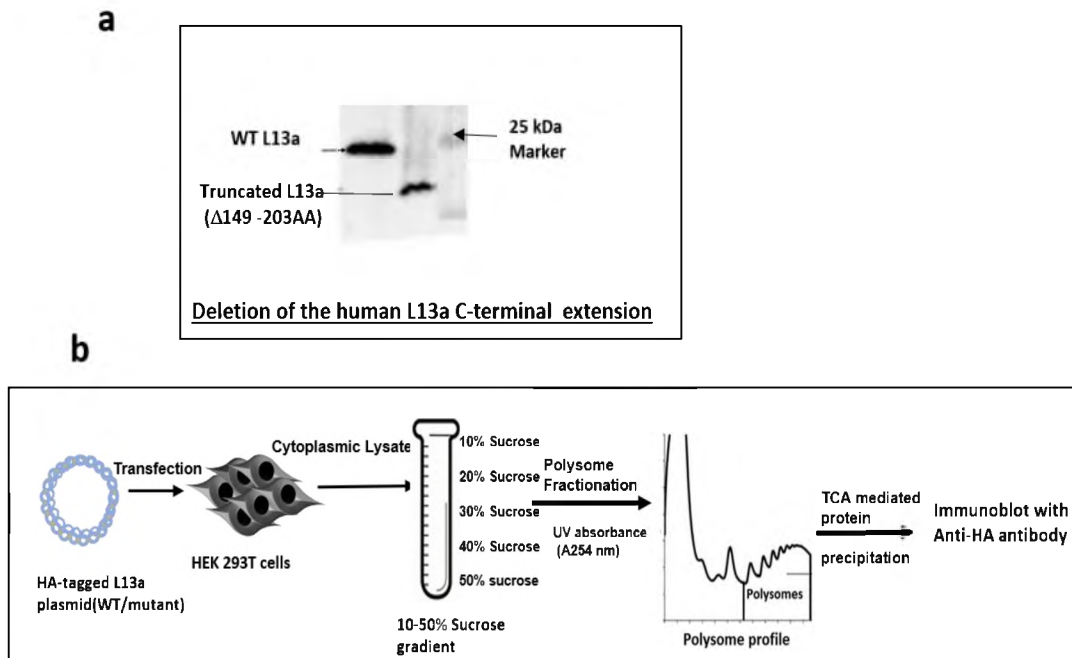


Figure 15: Schematic representation of ribosome incorporation assay: (a) Immunoblot of HA-tagged WT and truncated L13a (Δ 149-203 AA). (b) Ribosome profiling of HEK293T cells expressing HA-tagged L13a protein: Cell lysate of transfected cells was layered over 10-50% sucrose gradient. Ribosomal fractions were resolved by sucrose density gradient centrifugation, protein from each fraction was precipitated using trichloroacetic acid (TCA) followed by immunoblotting with anti-HA antibody to test the co-sedimentation of L13a variants with fractions corresponding to free fractions, 40S, 60S, 80S and polyribosomes.

The ability of the plasmid to express truncated version of L13a was tested by Western blot using anti-HA antibody (figure 15 a). We expressed this truncated form of L13a in human cell line and performed ribosome incorporation assay (figure 15 b). Results show that HA tagged WT L13a (used as positive control) significantly incorporated in to the ribosome and was present in the translationally active polysomes. WT L13a was found to be co-sedimented with lighter fractions (40S, 60S and 80S) and heavier polyribosome fractions. Whereas, truncated form of L13a with c-terminal domain deletion failed to co-sediment with the polyribosomes. We could detect the truncated protein only in lighter fractions (figure 16a.)

Based on the previous studies where we have shown that translocation of L13a from cytoplasm to the nucleolus is essential. The nucleolus is the site where L13a incorporates into the 90S precursor ribosome during ribosome biogenesis. Next, to investigate whether the C-terminal domain is essential for translocation of L13a into the nucleus and nucleolus, we studied the subcellular localization of WT and truncated L13a protein lacking C-terminal extension. We followed our previously published approach where nucleolin was used a marker for the nucleolus to check the colocalization of L13a protein with the nucleolin. The results showed that WT L13a could successfully translocate to the nucleolus, evident by its localization with the nucleolin protein. L13a1-148 Δ 149-203 also successfully enters the nucleus but shows a defect in trafficking of the protein to the nucleolus- the site of ribosomal incorporation. This experiment suggested that one of the functions of evolution of C-terminal extension in human L13a might be in the trafficking of the protein from cytoplasm to the nucleolus and incorporation into the ribosomes. This coincides well with fact that ribosome biogenesis in prokaryotes has a

different mechanism from eukaryotes where nucleolus is the main site of ribosome biogenesis. This subcellular organelle is absent in prokaryotes (figure 16b).

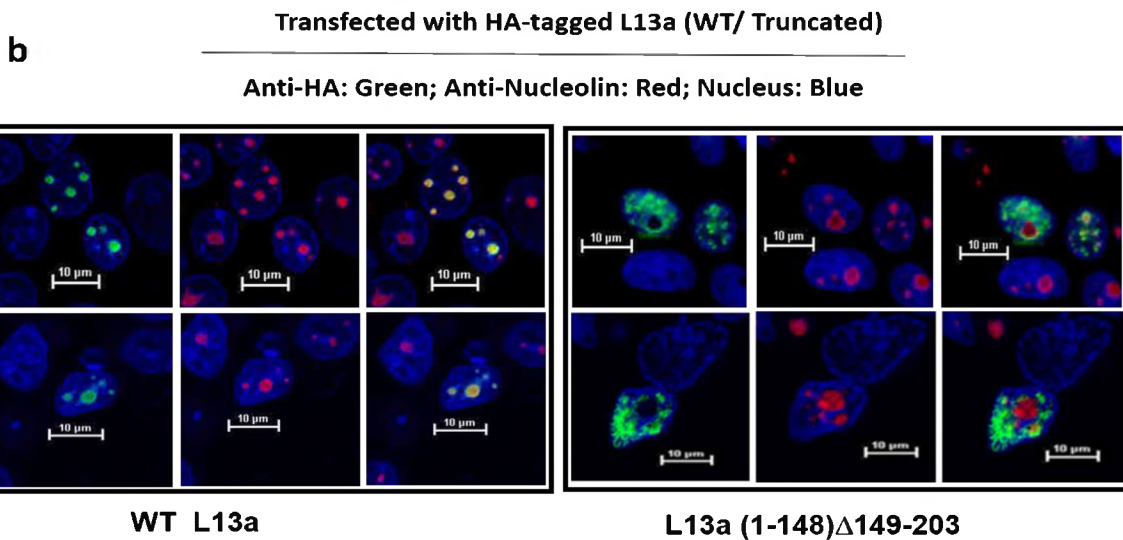
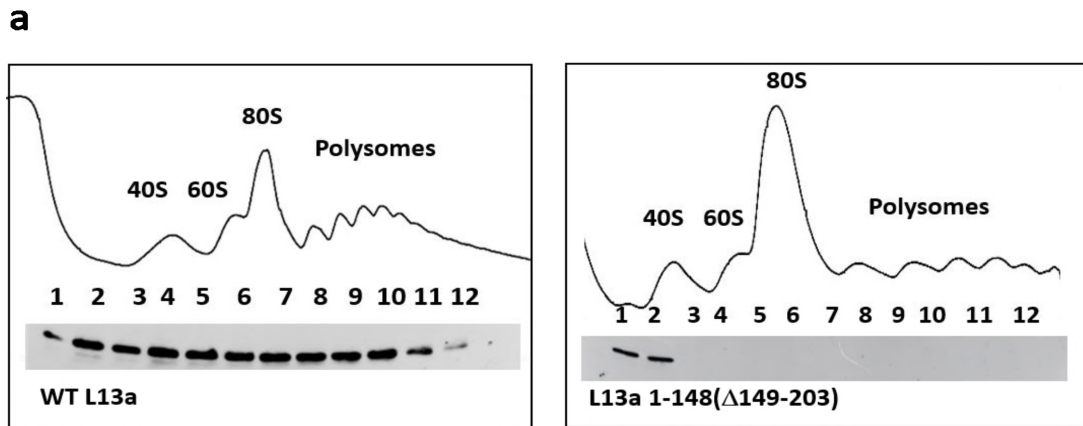


Figure 16: The eukaryote-specific C-terminal extension of L13a is essential for nucleolar translocation and ribosomal incorporation of L13a. (a) absorption profiles during ribosome fractionation of WT L13a and L13a (1-148) Δ 149-203 is shown. Density gradient co-sedimentation analysis of L13a WT/mutant protein was done by following ribosome incorporation assay elaborated in figure 15b. The sedimentation of 40S, 60S and 80S ribosome subunits and polysomes is indicated at the top of the figure. (b) Subcellular localization of L13a protein: HEK 293T cells were transfected with plasmids expressing HA-tagged WT or L13a (1-148) \square 149-203 protein. Cells were fixed, stained with anti-nucleolin (red), anti-HA (green) and DAPI (blue; to visualize nucleoli) and viewed under fluorescence microscope.

We also tested the C-terminal domain alone (L13a 149-203 Δ 1-148) for its ability to incorporate into the ribosomes and nucleolar translocation. Surprisingly, the C-terminal L13a protein consisting of amino acid sequence of 149-203 doesn't show any defect in the nuclear and nucleolar translocation but failed to incorporate into the polyribosomes (figure 17a and b). This protein behaved in a way similar to the R68A mutant (Das et al., 2013) that could accumulate in the nucleolus but failed to incorporate into the ribosomes.

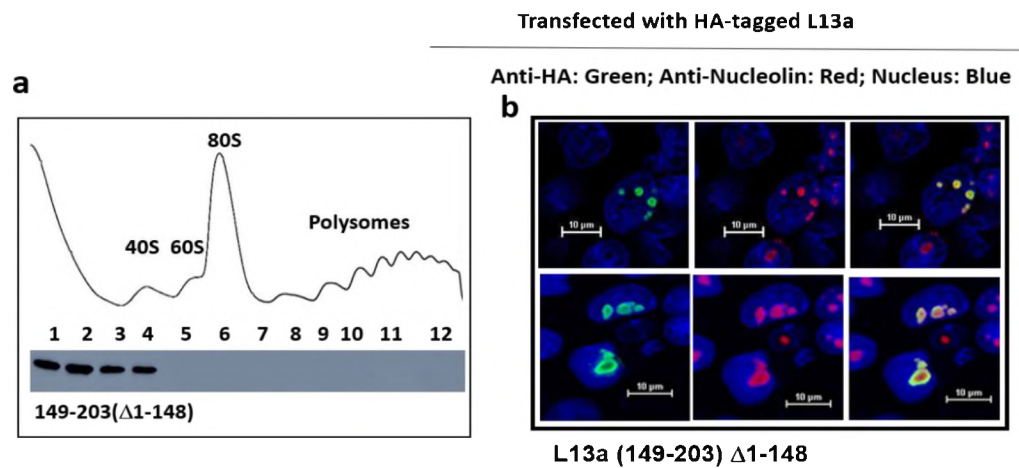


Figure 17: Eukaryote-specific C-terminal extension alone retains the ability to translocate into the nucleolus but failed to incorporate into the ribosomes. (a). absorption profile of sucrose density ribosome fractionation of (HA-tagged C-terminal only) L13a 149-203 (Δ 1-148). L13a lacking N-terminal domain fails to incorporate into the ribosomes. (b). Subcellular localization of L13a 149-203 (Δ 1-148). Cells expressing HA-tagged L13a 149-203 (Δ 1-148). L13a were fixed, stained with anti-HA (green), anti-nucleolin (red) antibody and nuclear stain DAPI (blue). Images were captured with confocal microscope to determine co-localization of nucleolin and L13a in the nucleolus.

We have also tested the in vivo association of both N-terminal L13a protein (1-148 Δ 149-203) and C-terminal L13a protein (149-203 Δ 1-148) with 28S rRNA (constituent RNA of 60S subunit) to further confirm their inability to incorporate in 60S ribosomal subunits (see figure 30).

2.3.3. Eukaryote-specific C-terminal extension of L13a harbors ribosomal incorporation domain:

Previously, we have experimentally demonstrated that arginine (R) at position 68 within the predicted RNA binding domain (53-75) is essential for ribosomal incorporation and occupies the same position as His60 in *E. coli* and arginine 68 in yeast L16a i.e. the tip of protruding loop. According to current study, the C-terminal domain is also essential for ribosomal incorporation but the specific amino acid residue (s) critical for ribosomal incorporation within this extension are unknown. Since the second RNA binding domain lies within this C-terminal extension, we substituted several amino acids encompassing the whole C-terminal domain and performed ribosomal incorporation assay. We tested several point, double and triple mutants namely K159A-R160A-K161A, E186A-K187A-K188A, K172A, Q173A, M175A, R176A, L177A, K179A-Q180A and I166A-H167A-Y168A by expressing them in HEK293T cells followed by polysome fractionation and immunoblot to detect L13a co-sedimentation with polyribosomes. Surprisingly, L13a mutants E186A-K187A-K188A, K172A, Q173A, M175A, R176A, L177A, K179A-Q180A and I166A-H167A-Y168A co-sediment well with the polysomes just like WT L13a (figure 18). Therefore, mutating these amino acids doesn't interfere with ribosomal incorporation. However, the triple mutant K159A-R160A-K161A failed to retain its ability to incorporate into 60S ribosomal subunits, 80S ribosomes and polyribosomes. Instead the

protein can be seen in free fractions only, suggesting a role of these amino acid residues in the ribosomal incorporation of L13a. To gain more insights, we made HA-tagged constructs harboring point mutation for each of these three amino acids followed by ribosomal incorporation assay. Mutant R160A retains ability to incorporate into the ribosomes. In contrast, L13a variants with single K159-A and K161A mutation entirely abrogated the ribosomal incorporation similar to the triple mutant K159A-R160A-K161A shown in figure 18. This experiment shows that in addition to R68, there are other amino acid residues of L13a that are indispensable for ribosomal incorporation.

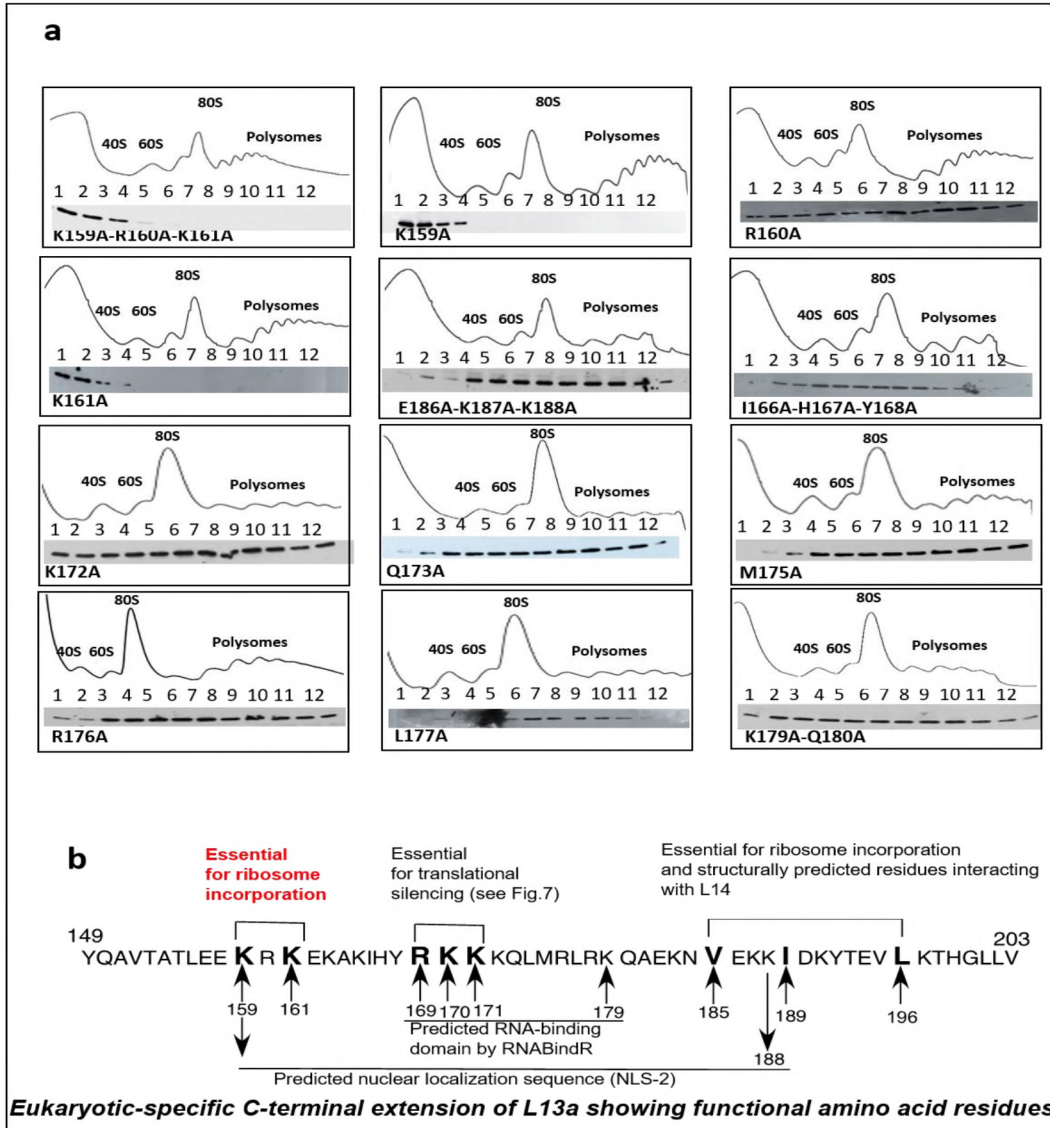


Figure 18: Amino acid residues Lysine 159 and Lysine 161 within the C-terminal domain are essential for ribosomal incorporation of L13a. (a). absorption profiles of sucrose density ultracentrifugation-based ribosome fractionation of HA-tagged mutant L13a proteins are shown in this figure. Twelve fractions corresponding to 40S, 60S 80S and polyribosomes were collected followed by immunoblot with anti-HA antibody to detect co-sedimentation of L13a proteins with ribosomes. L13a mutants for lysine 159 and lysine 161 failed to incorporate into the ribosomes. (b). Schematic diagram of the human L13a amino acid sequence indicating residues Lys 159 and 161 (red-within the eukaryote-specific C-terminal extension of L13a) essential for ribosomal incorporation of L13a.

2.3.4. Eukaryote-specific C-terminal extension mediated interaction between ribosomal proteins L13a and L14 is essential for ribosomal incorporation of L13a

Several ribosomal proteins are known to interact with each other resulting in the formation of complex networks of ribosomal protein interactions on the outer shell of the ribosome in eukaryotes. Cryo EM studies of the human ribosome showed the interaction of the amino acids at positions 185(Valine), 189 (Isoleucine) and 196(Leucine) within the C-terminal extension of L13a with another ribosomal protein L14. The C-terminal domain of L13a forms a long α helix that bends and interacts with a long C-terminal helix of human ribosomal protein L14 (figure 19).

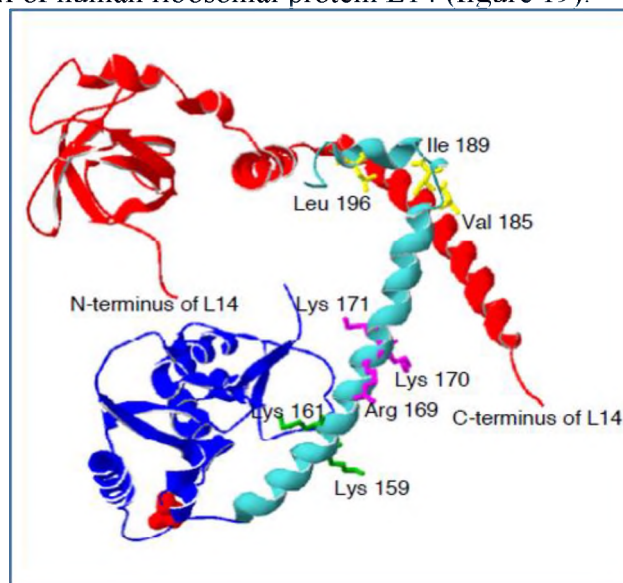


Figure 19: Modeling of the interaction between the C-terminal helices of human L13a and L14 protein. L13a (blue and sky blue) and L14 (red) protein structures are depicted as ribbon diagrams based on the CryoEM structure of the human ribosome at 3.6 Å resolution (Protein Data bank code 5T2C). Side chains of L13a residues Val185, Ile189 and Leu196 interacting with the L14 C-terminal helix are shown in yellow. Side chains of the L13a residues experimentally determined to affect L13a ribosomal incorporation (Arg68, Lys159, Lys161, Arg169, Lys170, and Lys171) are also shown.

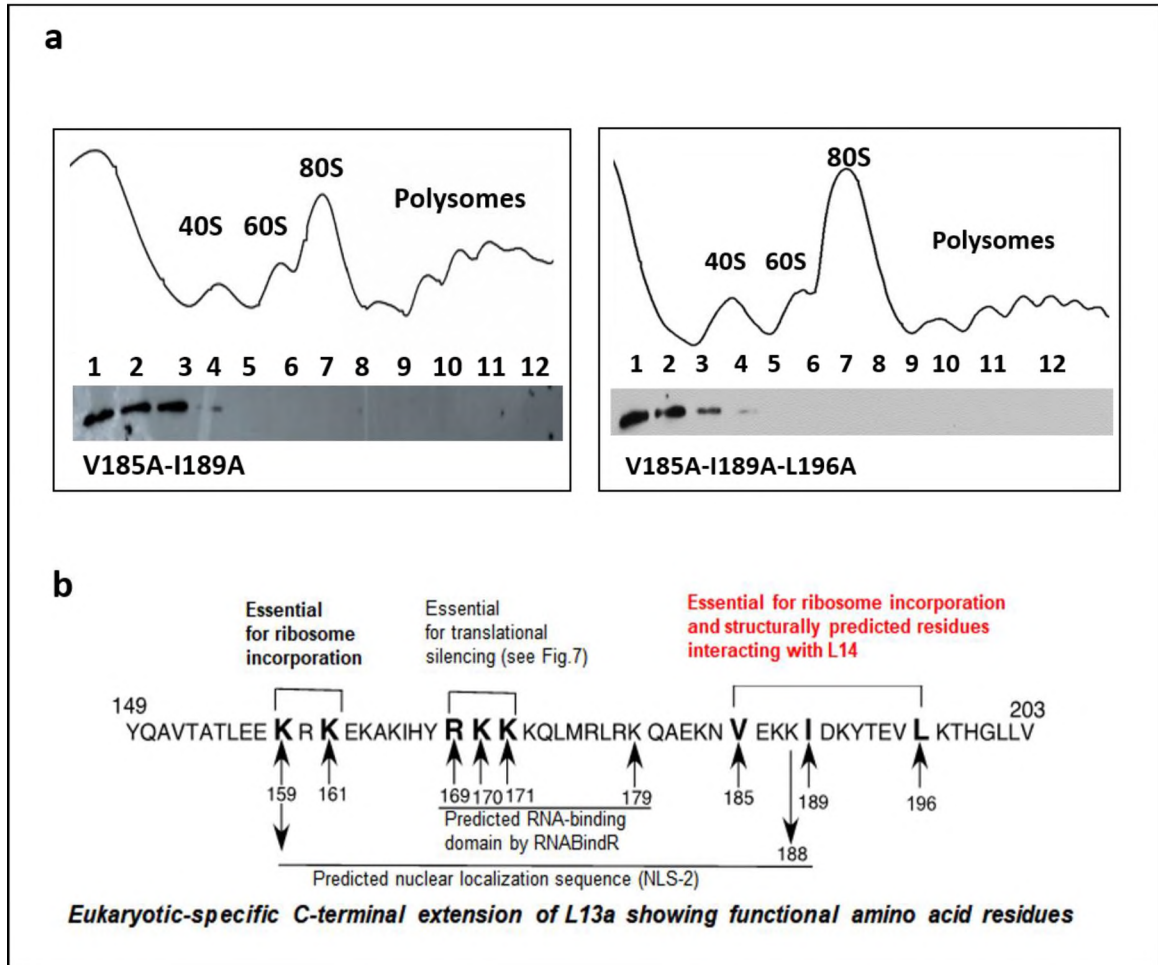


Figure 20: Amino acid residues of L13a (Val185, Ile189 and Leu196) within the C-terminal extension and involved in interaction with L14, are essential for ribosomal incorporation of L13a. (a). absorption profiles of ribosome fractionation of cells expressing HA-tagged Val185A-Ile189A and Val185A-Ile189A-L196A L13a mutants. Both the double and triple mutants failed to co-sediment with the polyribosomes. (b) Schematic diagram of amino acid sequence of C-terminal extension of L13a showing amino acids Val185, Ile189 and L196 (red) essential for ribosomal incorporation of L13a.

We proposed that this interaction could be important for L13a ribosomal attachment and mutating the indicated amino acids within L13a could interfere with the ribosomal incorporation or stability of L13a within the ribosomes. To further test the role of the residues involved in interaction between two ribosomal proteins of the large subunit, we have generated a double mutant (V185A-I189A) and a triple mutant (V185A-I189A-L196A), followed by ribosome incorporation assay.

Both the L13a variants (double and triple mutant) failed to incorporate into the polyribosomes (figure 20). It is noteworthy that a similar interaction between L14 and L16 (homolog of mammalian L13a) exists in yeast.

2.3.5. Sub-cellular localization of ribosomal incorporation competent and defective L13a mutants:

In order to understand the molecular mechanism underlying the ribosomal incorporation and association of L13a with rRNA, it's important to study the structural features of L13a that governs its trafficking from the cytosol to nucleus, nucleolus and hence into the ribosomes. Since nucleolus is the site of incorporation of L13a into rRNA, it is essential for the protein to traffic to this specific organelle. Therefore, we decided to test if ribosomal incorporation defective mutants K159A-R160A-K161-A and V185A-I189A-L196A can translocate to the nucleus and nucleolus. We followed previously used immunofluorescence-based assay in which we expressed L13a mutant proteins in a human cell line, followed by detection of the transfected HA-tag L13a and nucleolin with dye conjugated antibodies Alexa fluor-488 and Alexa fluor-594 respectively. We tested WT

and several other ribosome incorporation competent mutants such as E186A-K187A-K188A, K172A, Q173A, M175A, R176A, L177A, K179A-Q180A and I166A-H167A-Y168A etc. As expected, WT and ribosome incorporation competent L13a mutants can completely translocate into the nucleolus (data not shown). No protein was retained in the nucleus. Interestingly, all three ribosomal incorporation defective L13a mutants K159A-R160A-K161A, double mutant V185A-I189A and triple mutant V185A-I189A-L196A successfully translocated into the nucleus but failed to translocate into the nucleolus (figure 21 and 22). Therefore, we showed that these incorporation defective mutants failed to incorporate into the ribosomes due to their inability to enter the nucleolus. We also tested the nuclear and nucleolar trafficking ability of single mutants K159A, R160A and K161A. K159A and K161A mutants failed to translocate to the nucleolus like the triple mutant K159A-R160A-K161A. whereas, R160A retains the ability to accumulate in the nucleolus (figure 23,24). Therefore, we concluded that the amino acid residues K159 and K161 are essential for nucleolar import and ribosomal incorporation of L13a. However, our previous studies have shown that the ribosome incorporation of the defective R68A mutant showed no defect in nucleolar trafficking, suggesting that nucleolar translocation is a prerequisite but not sufficient for incorporation of L13a into the 90S pre-ribosomes (Das. P et al., 2013).

Transfected with HA-tagged L13a mutants

Anti-HA: Green; Anti-Nucleolin: Red; Nucleus: Blue

L13a K159A-R160A-K161A

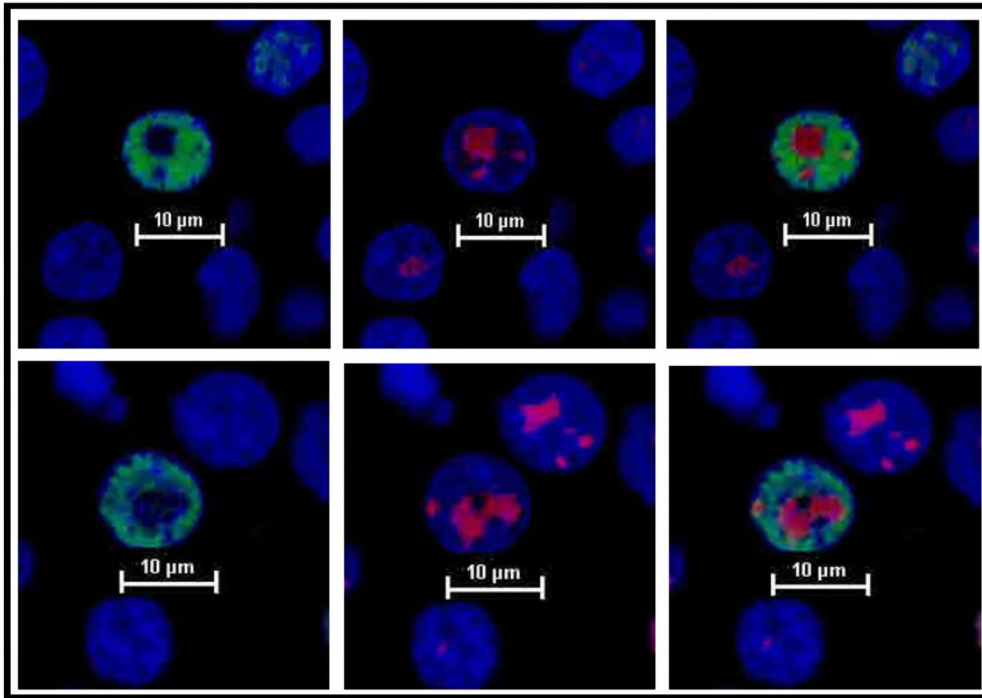
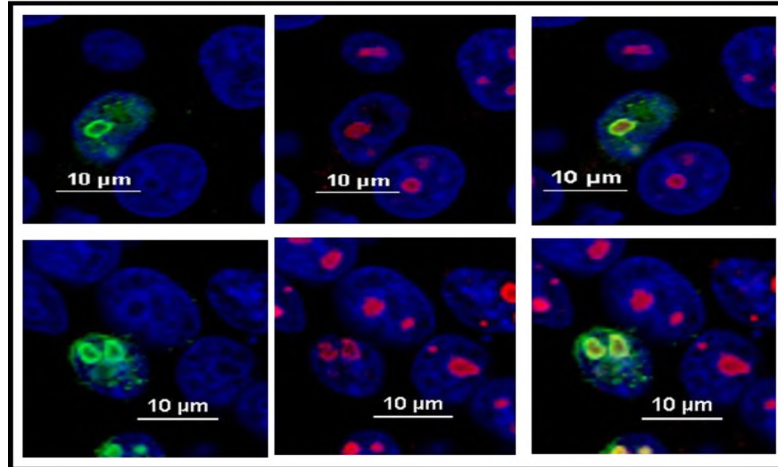


Figure 21: Subcellular localization of ribosome incorporation defective triple mutant Lys159A-Arg160A-Lys161A: The nuclear and nucleolar localization of triple mutant Lys159A- Arg160A -Lys161A was studied by immunofluorescence-based analysis of HEK 293T cells expressing HA-tagged triple mutant L13a. Twenty four hours post-transfection, cells were fixed and stained with anti-HA antibody (green), anti-nucleolin antibody (endogenous nucleolin protein: marker for nucleolus) and nuclear stain DAPI. Cells were viewed under fluorescent microscope (2 replicates).

Transfected with HA-tagged L13a mutants

Anti-HA: Green; Anti-Nucleolin: Red; Nucleus: Blue

L13a V185A-I189A



L13a V185A-I189A-L196A

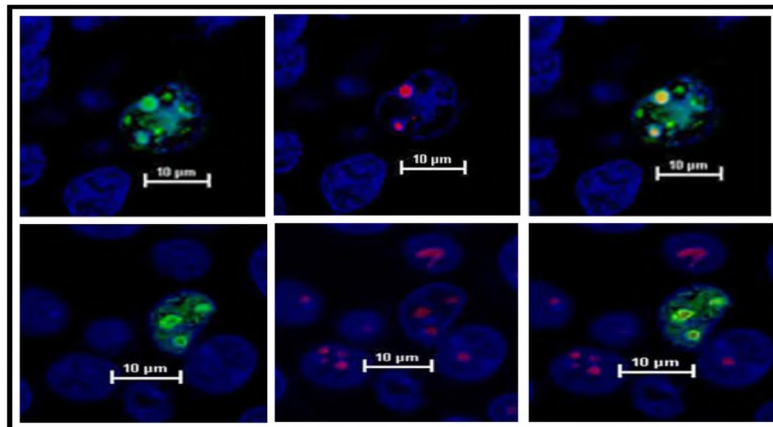
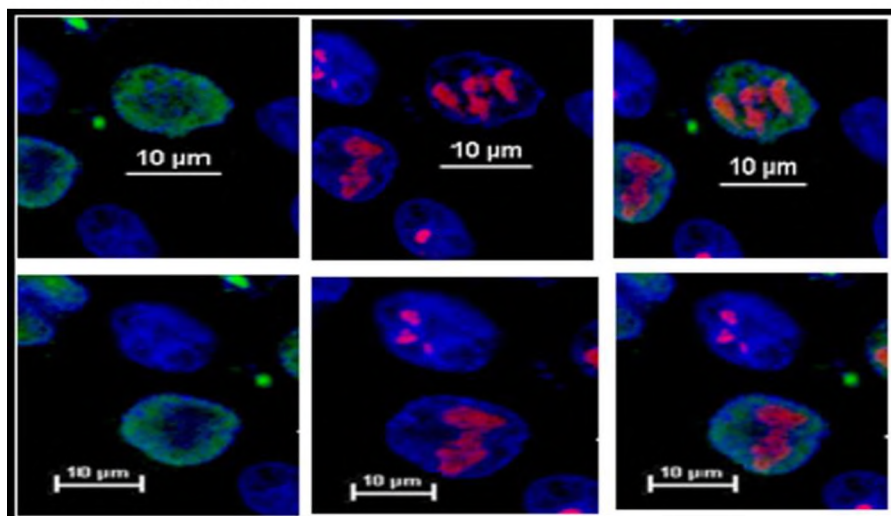


Figure 22: Subcellular localization of ribosome incorporation defective double mutant Val189A-Ile189A and triple mutant Val185A-Ile189A-Leu196A: The nuclear and nucleolar localization of double and triple mutant Val185A-Ile189A and Val185A-Ile189A- was studied by immunofluorescence-based analysis of HEK 293T cells expressing HA-tagged mutant L13a proteins (green in above images). Twenty-four hours post-transfection, cells were fixed and stained with anti-HA antibody (green), anti-nucleolin antibody (endogenous nucleolin protein: marker for nucleolus) and nuclear stain DAPI. Cells were viewed under fluorescent microscope (2 replicates of each mutant).

Transfected with HA-tagged L13a mutants

Anti-HA: Green; Anti-Nucleolin: Red; Nucleus: Blue

L13aK159A



L13aK161A

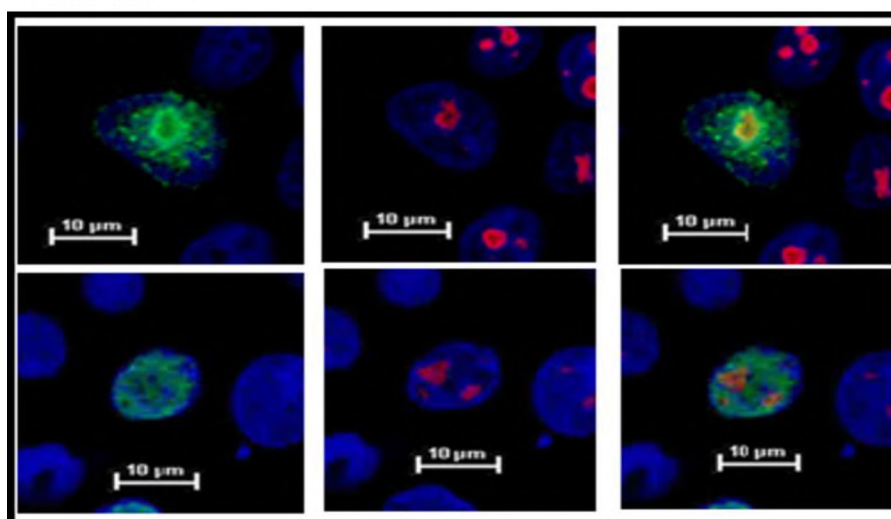


Figure 23: Subcellular localization of ribosome incorporation defective mutants Lys(K) 159A and Lys(K) 161A: The nuclear and nucleolar localization of the Lys159A mutant was studied by immunofluorescence-based analysis of HEK 293T cells expressing HA-tagged mutant L13a protein (green in above images). Twenty-four hours post-transfection, cells were fixed and stained with anti-HA antibody (green), anti-nucleolin antibody (endogenous nucleolin protein: marker for nucleolus) and nuclear stain DAPI. Cells were viewed under a fluorescent microscope.

Transfected with HA-tagged L13a mutants

Anti-HA: Green; Anti-Nucleolin: Red; Nucleus: Blue

L13aR160A

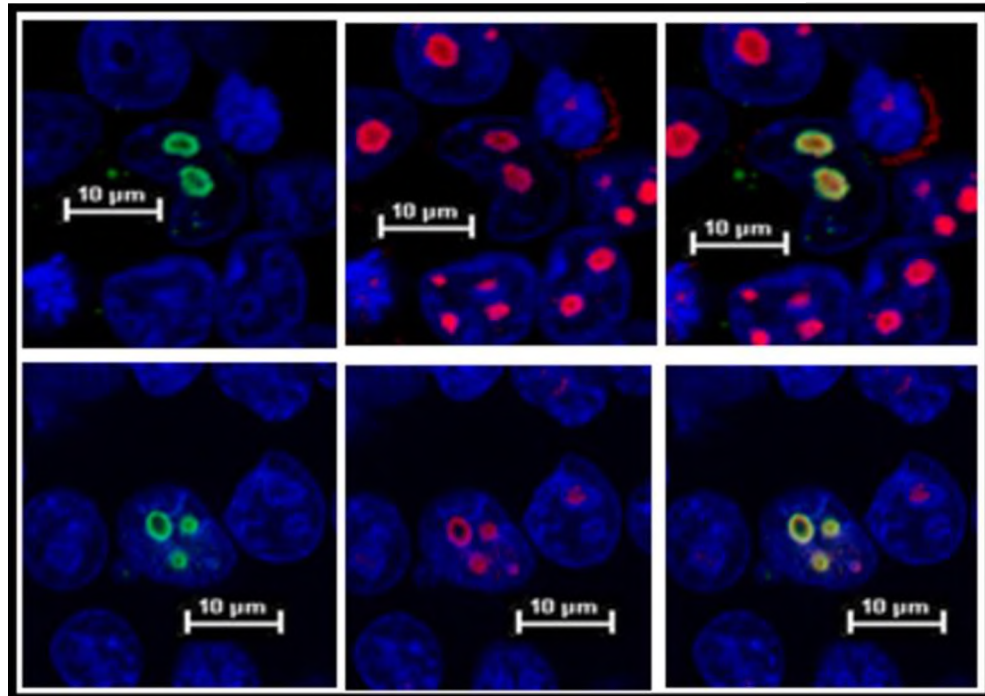


Figure24: Subcellular localization of ribosome incorporation competent Arginine (R)160A mutant: The nuclear and nucleolar localization of single mutant R160A was studied by immunofluorescence-based analysis of HEK 293T cells expressing HA-tagged mutant L13a protein (green in above images). Twenty-four hours post-transfection, cells were fixed and stained with anti-HA antibody (green), anti-nucleolin antibody (endogenous nucleolin protein: marker for nucleolus) and nuclear stain DAPI. Cells were viewed under fluorescent microscope (2 replicates).

2.3.6. Mutations in the predicted NLS sequences in C-terminal and N-terminal domains of L13a affect nucleolar, but not nuclear translocation of the L13a protein.

In eukaryotes, ribosome assembly requires an intricate trafficking of ribosomal proteins which are produced in the cytoplasm. The proteins first enter the cell nucleus and accumulate in the nucleolus before they associate into nascent ribosomes. Therefore, eukaryotic ribosomal proteins are thought to harbor nuclear/nucleolar localization signals (NLSs) which are usually short, predominantly basic stretches of amino acids that trigger active transport of proteins to the nucleus. Many conserved ribosomal proteins such as uL4, uL5, uL9 have evolved nuclear localization signals in their globular domains by undergoing structural rearrangements. These NLS sequences are absent in their prokaryotic counterparts, since ribosomal proteins in prokaryotes doesn't need a NLS due to lack of nucleus/nucleolus (Melnikov *et al.*, 2015).

The mechanism of trafficking of L13a to the nucleus/nucleolus and existence of NLS sequences for human L13a have not been explored yet. Therefore, we used two web-based programs to search for potential nuclear localization signals (NLSs) within L13a sequence: NLS mapper (http://nls-mapper.iab.keio.ac.jp/cgi-bin/NLS_Mapper_form.cgi) and NLStradamus (<http://www.moseslab.csb.utoronto.ca/NLStradamus/>). Both the programs identified separate NLS sequences, one in globular domain (Arginine 84 to Methionine 119), which we called NLS1 and the other one in eukaryote-specific C-terminal domain (Lysine 159 to Lysine 188), which we named as NLS2 (figure 25a).

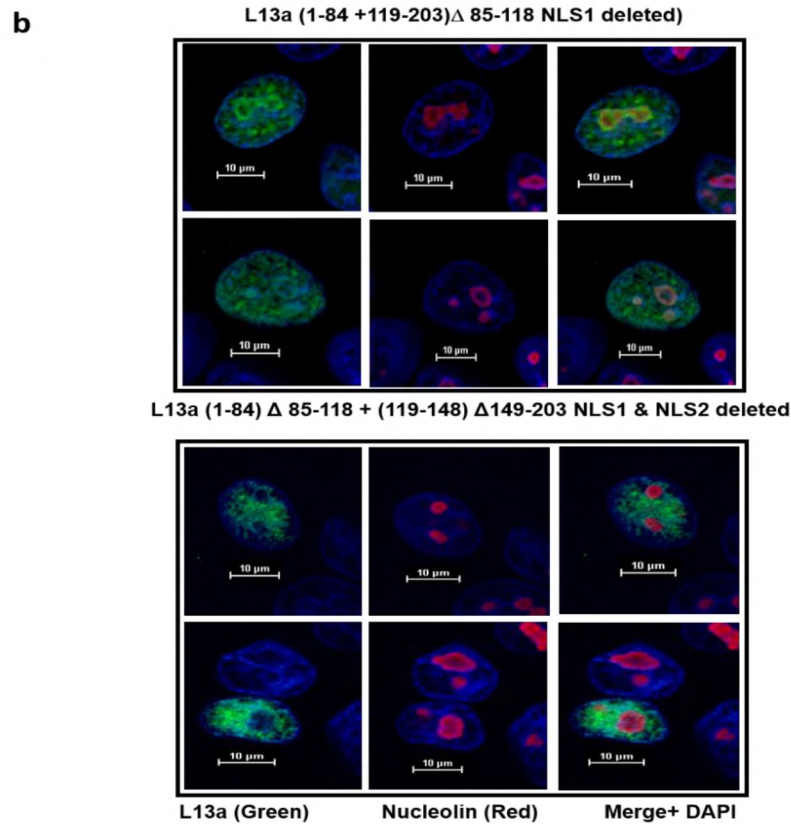
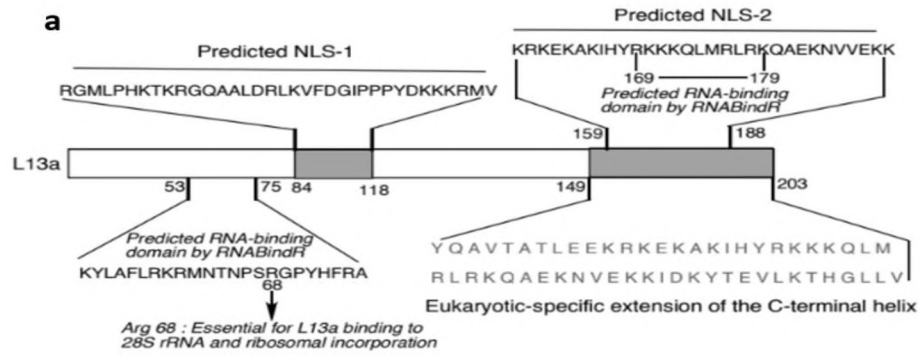


Figure 25: subcellular localization of L13a variants lacking predicted nuclear localization signal (NLSs): (a) Schematic diagram of the human L13a amino acid sequence with predicted NLSs (Arg84 to Met118 and Lys159 to Lys188) indicated. (b) nuclear and nucleolar localization of L13a variants (1-84+119-203) Δ 85-118; predicted NLS1 deleted), (1-84) Δ 85-118+119-148 Δ 149-203; predicted NLS1 and NLS2 deleted) analyzed by immunofluorescence-based assay. HEK 293T cells expressing HA-tagged L13a proteins (green in above images) were fixed and stained with anti-HA antibody (green), anti-nucleolin antibody and nuclear stain DAPI. Cells were viewed under fluorescent microscope.

In order to experimentally validate these predicted NLSs, we generated HA-tagged L13a constructs: one with NLS1 internally deleted (1-84) Δ 85-118+119-203 and the other one with both NLS1 and NLS2 deleted (1-84) Δ 85-118 + (119-148) Δ 149-203. The ability of these specific deletion versions of L13a proteins to translocate to the nucleus was examined by the same immunofluorescence-based assay. Contrary to our expectations, both the mutant L13a proteins lacking either NLS1 or both NLS1 &2 showed no defect in nuclear import. We observed that no protein was retained in the cytoplasm, whereas, nucleolar import of L13a was compromised in both the mutants. Mutant L13a failed to translocate into the nucleolus and the defect is more severe in the L13a protein lacking both NLS1 and NLS2 as evident from the confocal microscopy pictures in the figure 25b.

Therefore, these studies show that the nuclear translocation of the human L13a protein is more refractory to the amino acid alterations as compared to nucleolar translocation.

2.3.7. R169-K170-K171 residues within the eukaryote-specific C-terminal extension are essential for GAIT-mediated translational silencing.

Our lab and other groups have demonstrated an important ribosome independent function of mammalian L13a elaborated in the introduction (chapter I). Briefly, inflammatory stimulus results in phosphorylation mediated release of L13a from the 60S subunit and incorporation into a cis-acting GAIT complex, which is known to inhibit translation initiation of GAIT element bearing target inflammatory mRNAs. While L13a is an important component of this GAIT complex, amino acid residue (s) of L13a critical for this extra-ribosomal function remains unknown. Previous studies have also shown that ribosome incorporation defective L13a mutant R68A retains the ability to silence the

translation of GAIT element bearing reporter mRNA (Das *et al.*, 2013). Therefore, we have examined the importance of this C-terminal extension for its role in GAIT mediated silencing activity.

We have followed our previously established *in vitro* translational assay in which we tested the purified recombinant WT or mutant His tagged L13a protein for their ability to silence the translation of a GAIT-element bearing reporter luciferase mRNA (Cap-Luc-GAIT-PolyA) and a control T7gene10 mRNA (lacking the GAIT element) in rabbit reticulocyte lysate. We expressed WT or mutant versions of His-tagged L13a proteins (mutations confined to C-terminal domain) in insect cell lines, purified the proteins to be used in the *in vitro* translation assay. We tested the expression of full length and truncated purified protein by immunoblot with anti-His antibody (figure 26).

First, we compared translational silencing ability of WT L13a with different length truncations in the C-terminal extension: L13a 1-195 Δ 196-203, L13a 1-180 Δ 181-203, L13a 1-62 Δ 163-203 and L13a 1-148 Δ 149-203. Results summarized in figure 27 show that deletion of the last 5 amino acids and 23 amino acids doesn't interfere with translational silencing ability of L13a. Both of these truncated L13a proteins shows silencing ability equivalent to WT L13a, while deletion mutants L13a 1-162 Δ 163-203 and L13a 1-148 Δ 149-203 failed to silence the translation of the reporter mRNA. These results identified a region within the C-terminal extension ranging from Tyr149-Val203 as essential for translational silencing.

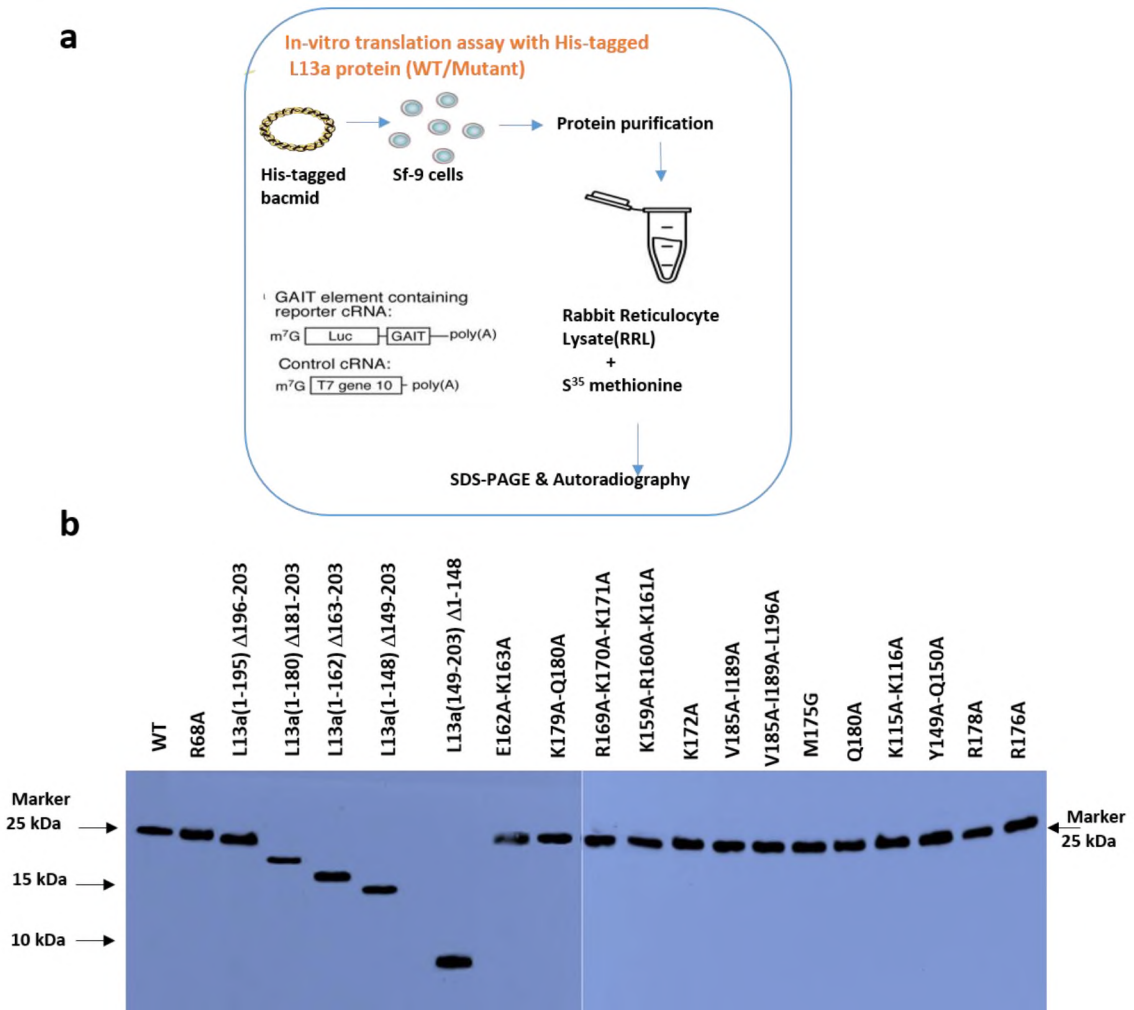


Figure 26: Generation of His-tagged recombinant L13a WT/mutant proteins and in vitro translation assay: (a). Schematic representation of transfection of Sf-9 cells with bacmid DNA expressing L13a variants, protein purification. The purified recombinant L13a proteins were used in an in vitro translation assay of a luciferase reporter RNA (bearing GAIT element) and a control RNAT7 gene 10 (Lacking GAIT element) in cell-free (rabbit reticulocyte lysate) RRL system. The S^{35} -radiolabeled translated proteins were visualized by 10% SDS-PAGE followed by autoradiography. **(b)** Immunoblot of His-tagged recombinant L13a variants with anti-His antibody.

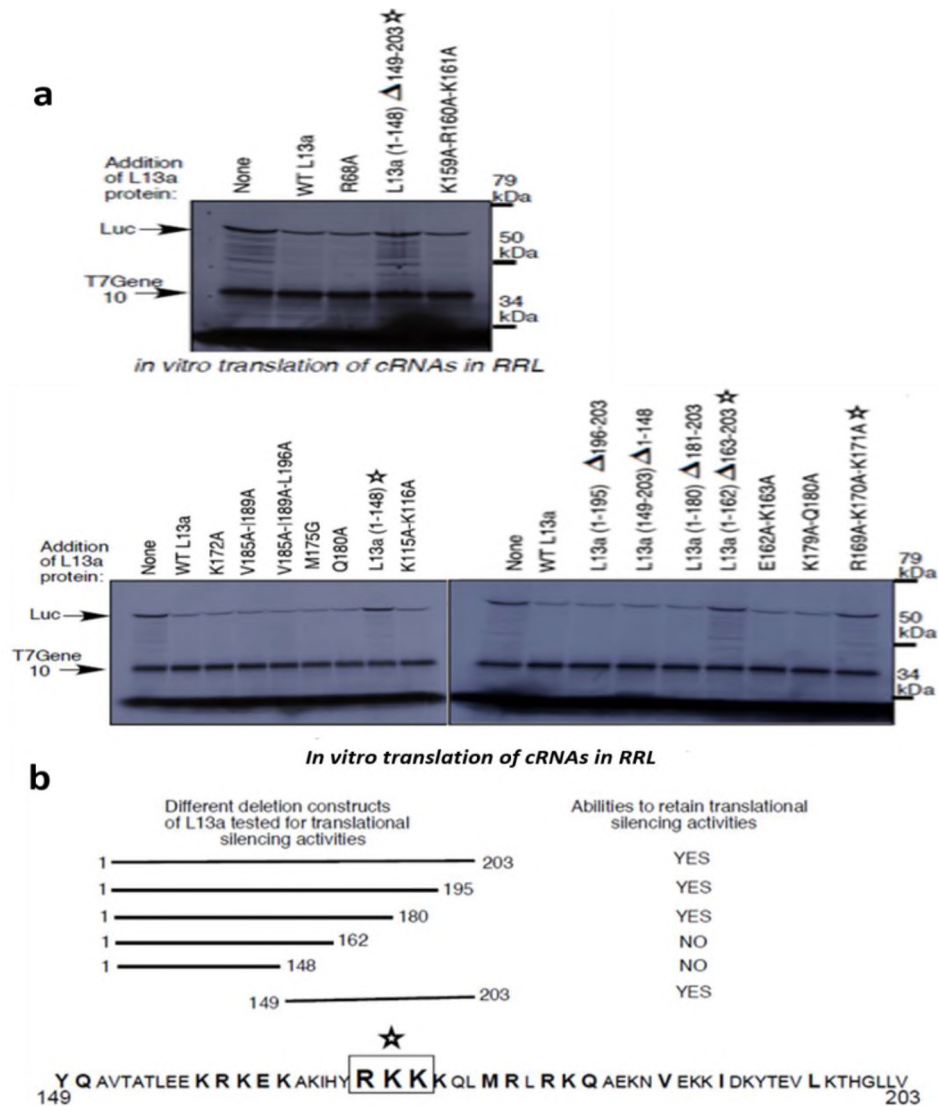


Figure 27: The eukaryote-specific C-terminal extension of L13a harbors amino acid residues (R169-K170-K171) required for GAIT element mediated translational silencing: (a) Effect of L13a variants on in vitro translation of luciferase reporter RNA and control RNA as described in the figure above. The L13a variants that do not induce GAIT element-dependent translational silencing are marked with a star (L13a (1-148) Δ 149-203, L13a (1-162) Δ 163-203 and R169A-K170A-K171A- these three amino acids critical for silencing activity are indicated by a box with a star at the bottom of the figure. (b) Schematic representation of L13a deletion constructs tested in translation silencing assay and a summary of results.

We expressed various L13a mutant proteins by inducing point, double or triple mutations specifically targeting the amino acids between 149-203 region with the intention to pinpoint the amino acids critical for silencing activity. Various L13a mutants such as Y149A-Q180A, E162A-K163A, K172A, M175G, R176A, R178A, Q180A, K179A-Q180A and ribosome incorporation defective K159A-R160A-K161A and V185A-I189A-L196A, V185A-I189A showed translational silencing ability comparable to WT L13a. In contrast, the triple mutant R169A-K170A-K171A L13a failed to show translation silencing of the GAIT-element bearing mRNA transcript. In this assay, the translation of control mRNA (without GAIT element) remains unaffected in presence of L13a variants (figure 27). The quantification of extent of translation inhibition of reporter mRNA by various L13a protein is presented in the figure 28 below.

This experiment has identified a short region of L13a (169-171 AA) as the translational silencing domain of L13a, that is essential for extra-ribosomal function of this ribosomal protein.

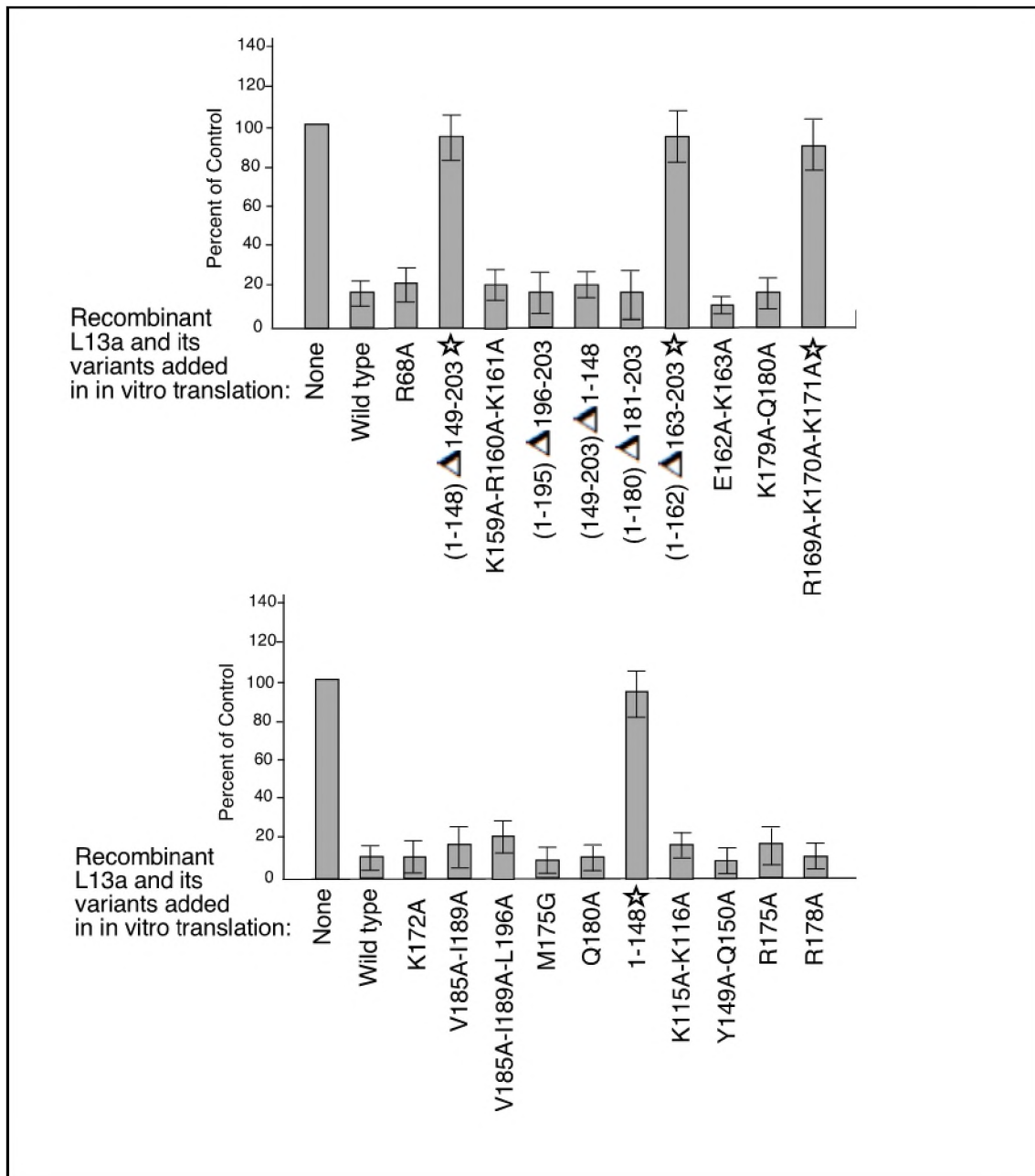


Figure 28: Schematic illustration of quantification of translation silencing activity of WT/mutant/truncated L13a proteins used in the in vitro translation silencing assay.

2.3.8 Translational silencing domain of human L13a retains nucleolar translocation and ribosome incorporation ability.

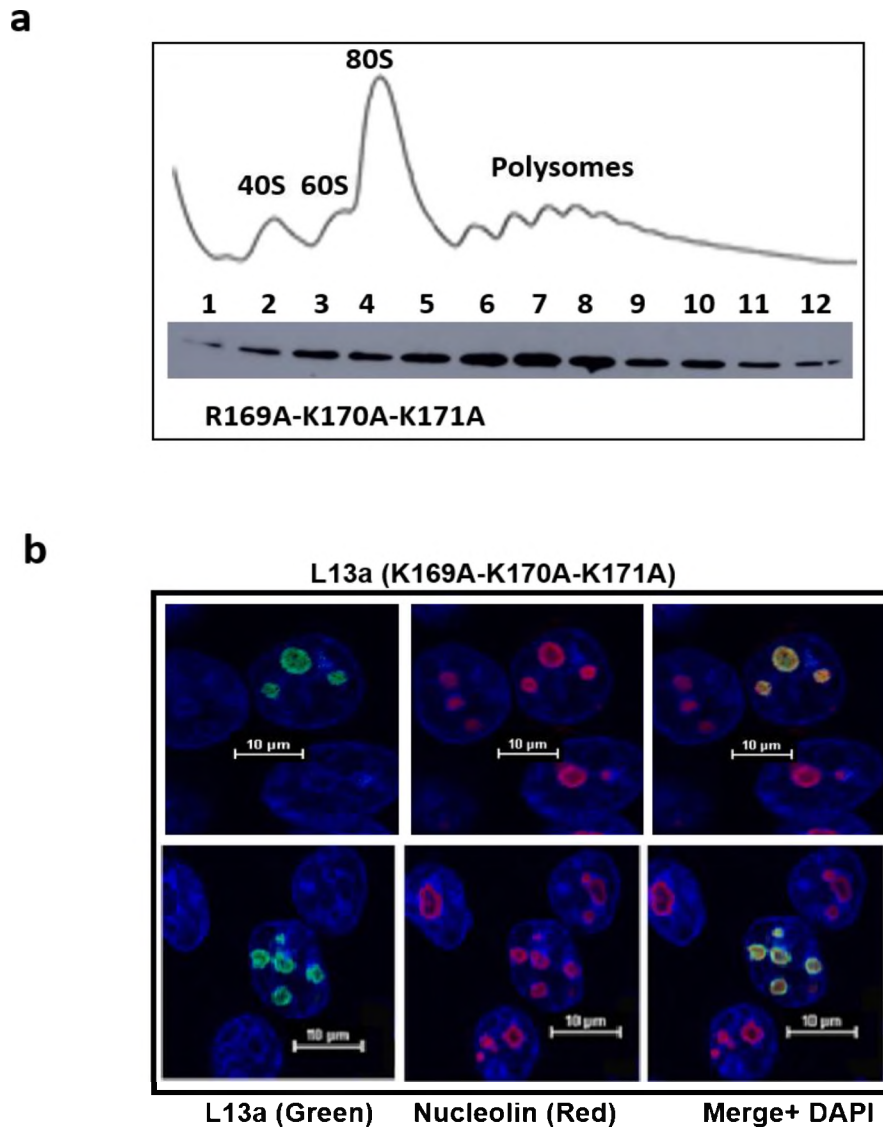


Figure 29: Ribosomal incorporation and nuclear/nucleolar translocation assay of L13a mutant defective of translational silencing activity. (a) ribosome fractionation absorption profile and immunoblot of triple mutant R169A-K170A-K171A showing its co-sedimentation with polyribosomes. and (b) localization within the mammalian cells (translocation to the nucleolus and colocalization with nucleolin protein (2 replicates)).

In order to check if amino acid residues arginine169, lysine 170 and 171 are also essential for ribosomal incorporation of L13a in addition to their role in GAIT-mediated translational silencing pathway, we tested this triple mutant in nuclear/nucleolar translocation assay and ribosome incorporation assay.

Interestingly, the R169A-K170A-K171A mutant doesn't show any defect in nuclear/nucleolar translocation. The protein can be seen colocalized with the nucleolin in the figure (figure29b). Also, this triple mutant successfully co-sediments with polyribosomes, suggesting successful incorporation into the ribosomes (figure 29a). This is further confirmed by RNA-immunoprecipitation assay to check the association of R169A-K170A-K171A with 28S rRNA (shown in fig30.).

2.3.9. Ribosome incorporation defective L13a mutants fail to associate with 28S rRNA in vivo.

The ribosomal incorporation assay used in this study is based on co-sedimentation of the WT or mutant L13a protein with the ribosomal subunits and polyribosomes. Therefore, we further tested the ability of various ribosome incorporation defective and competent mutants to bind 28S rRNA in vivo. In this experiment, we expressed HA-tagged WT, ribosome incorporation defective mutants, nucleolar translocation defective mutant (NLS mutant) and few ribosome incorporation competent mutants of L13a in HEK 293T cells followed by immunoprecipitation of L13a proteins using HA-antibody coated agarose beads.

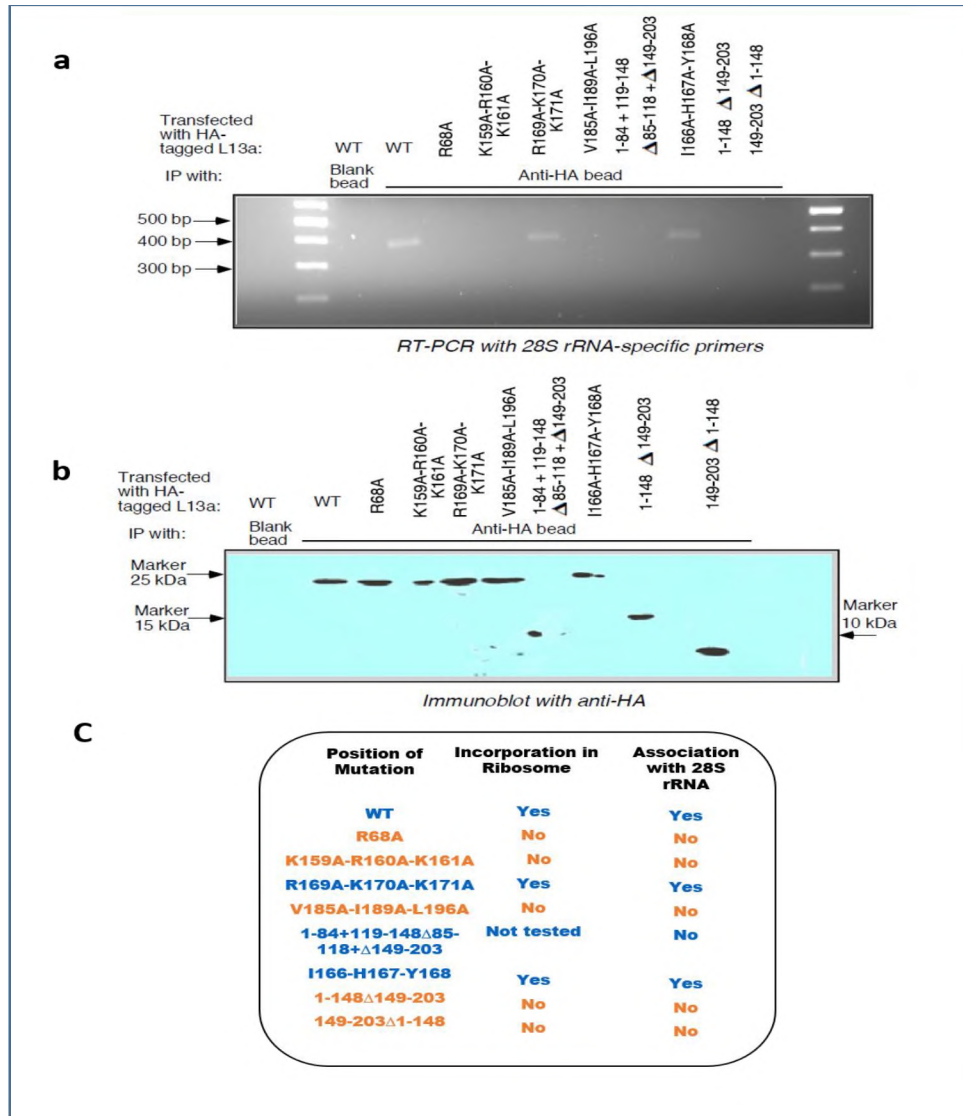


Figure 30: association of L13a and its mutant variants with 28S rRNA. Lysates prepared from HEK 293T cells expressing HA-tagged L13a (wild type or mutant as indicated above each lane) were used for immunoprecipitation with anti-HA-coated agarose beads (or non-antibody-coated blank beads as a control, 1st lane from left). (a) Total RNA was extracted from the immunoprecipitates and analyzed by RT-PCR with primers specific for 28S rRNA. RT-PCR products were visualized on an ethidium bromide stained agarose gel. (b) Equal volumes of the immunoprecipitate from each reaction were run on an SDS-PAGE gel and immunoblotted with anti-HA antibody to confirm the presence of equivalent amounts of HA-tagged protein. (c) Summary of results of ribosomal incorporation and association with 28S rRNA of L13a variants.

Association of immunoprecipitated L13a protein with 28S rRNA was confirmed by isolating the RNA from immunoprecipitates and RT-PCR with 28S rRNA specific primers. we tested eight different L13a variants e.g. ribosome incorporation defective K159A-R160A-K161A, V185A- I189A-L196A, L13a (1-148) Δ 149-203, L13a (149-203) Δ 1-148 and previously tested R68A and WT L13a as controls (Das et al., 2013), incorporation competent R169A-K170A- K171A and I166A-H167A-Y168A and a single variant without predicted NLS-1 and NLS-2 (1-84) Δ 85-118 + (119-148) Δ 149-203. Consistent with the results of the ribosomal incorporation assay, we have not detected 28S rRNA in the immunoprecipitates of K159A-R160A-K161A, V185A-I189A-L196A, L13a (1-148) Δ 149-203, L13a (149-203) Δ 1-148, R68A and of the variant without NLS-1 and NLS-2 i.e. (1-84) Δ 85-118 + (119-148) Δ 149-203 (nucleolar translocation defective mutant (Fig.30a). In the same experiment, we could detect 28S rRNA in the immunoprecipitates of ribosome incorporation competent L13a mutants R169A-K170A-K161A and I166A-H167A-Y168A. We also performed the Immunoblot analysis with anti-HA antibody of the same immunoprecipitates to confirm the equal efficiency of immunoprecipitation for different L13a variants (Figure 30b). The specificity of the 28S rRNA immunoprecipitation was confirmed by the absence of the PCR product from 28S rRNA obtained using HA-tagged wild-type L13a-transfected cells and beads without coupling with the antibody. Results of this experiment are summarized in figure 30c.

2.3.10. Testing in vivo association of L13a variants with nucleolin protein.

We have used nucleolin as a nucleolar marker in our previous as well as current study. Nucleolin is a protein abundant in the nucleolus and is known to play several important functions including ribosome biogenesis. Nucleolin has been shown to bind

several ribosomal proteins. However, the role of such interactions is not clear yet (Bouvet et al., 1998). In the results discussed above, we have found that the outcomes of our ribosome incorporation assay coincide well with nucleolar translocation assay. These results show that ribosome incorporation defective mutants K159A-R160A-K171A, L13a 1-148 Δ 149-203, V185A-I189A-L196A also fail to translocate to the nucleolus except one mutant 149-203 Δ 1-148 which retains nucleolar retention ability but still fails to incorporate into ribosomes. Also, ribosome incorporation competent L13a mutants such as R169A-K170A-K171A, E186A-K187A-K188A, I166A-H167A-Y168A showed no defect in nucleolar translocation. In addition, a L13a mutant with NLS1 and NLS2 deletion (L13a (1-84) Δ 85-118 + (119-148) Δ 149-203) also fails in nucleolar import.

We further confirmed the nucleolar colocalization of these L13a variants by testing *in vivo* association of L13a proteins with nucleolin protein. We expressed 10 HA-tagged L13a variants (including WT L13a) discussed above in HEK 293T cells followed by cell lysate preparation and immunoprecipitation with anti-HA antibody coated agarose beads. A Western blot using a part of immunoprecipitation input with nucleolin antibody was done to show presence of nucleolin protein in all the IP-lysates before HA-based immunoprecipitation shown in the figure 31.

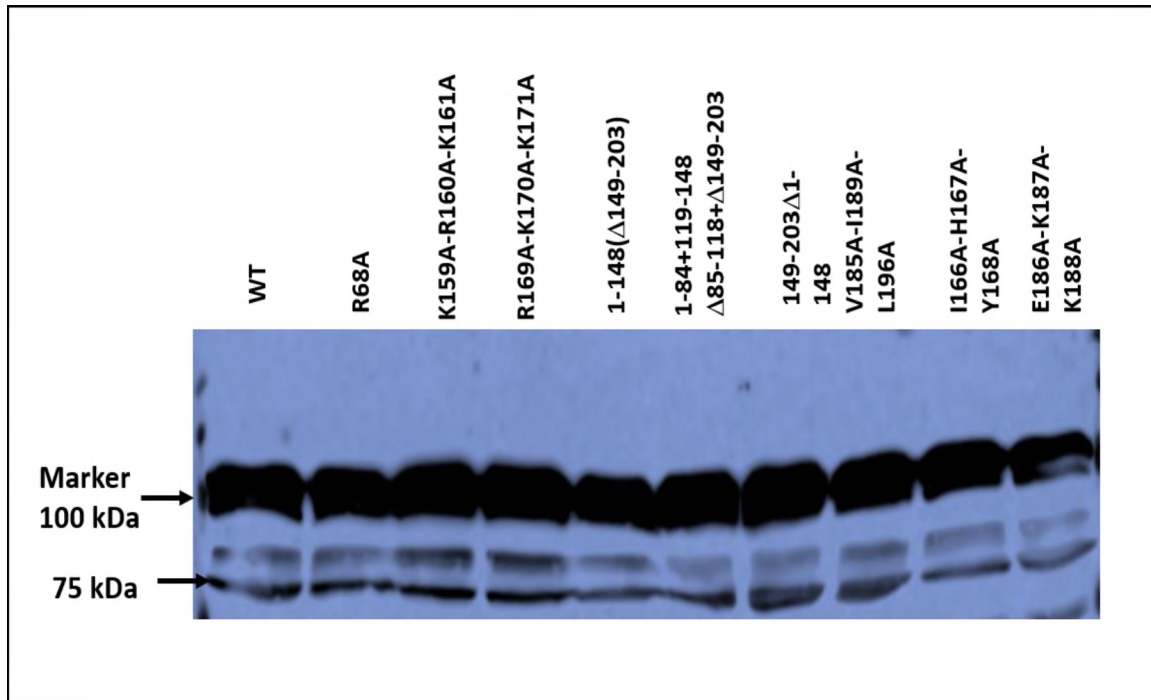


Figure 31: Immunoblot of IP lysates input using anti-nucleolin antibody. 10 μ l of HA-tagged WT/mutant L13a expressing HEK 293T cell lysates were separated by SDS-PAGE followed by immunoblot with anti-nucleolin antibody, showing the presence of nucleolin protein in all the IP lysates.

The presence of nucleolin protein in the L13a immunoprecipitates was detected by immunoblot with anti-nucleolin antibody and used as a proof to show association of L13a and nucleolin protein. As expected, nucleolin was not detected in the K159A-R160A-K171A, L13a 1-148 Δ 149-203, V185A-I189A-L196A, L13a (1-84) Δ 85-118 + (119-148) Δ 149-203 L13a immunoprecipitates. This is in agreement with the nucleolar translocation assay results. All these mutants failed to translocate to the nucleolus and incorporate into

ribosomes. Whereas, ribosome incorporation competent R169A-K170A-K171A, E186A-K187A-K188A, I166A-H167A-Y168A, WT L13a proteins were found to be associated with nucleolin. The C-terminal extension only (L13a 149-203 Δ 1-148) and R68A mutants also showed interaction with nucleolin protein. Both of these proteins successfully colocalizes with the nucleolin in the nucleolus but fail to incorporate into the ribosomes (figure 32a). An immunoblot of L13a immunoprecipitates with anti-HA antibody was also done to check for equal efficiency of HA-based immunoprecipitation (figure 32b). These results support the notion that nucleolar trafficking of ribosomal protein L13a is important for ribosomal incorporation but doesn't ensure its incorporation as is the case with R68A and L13a 149-203 Δ 1-148 mutants.

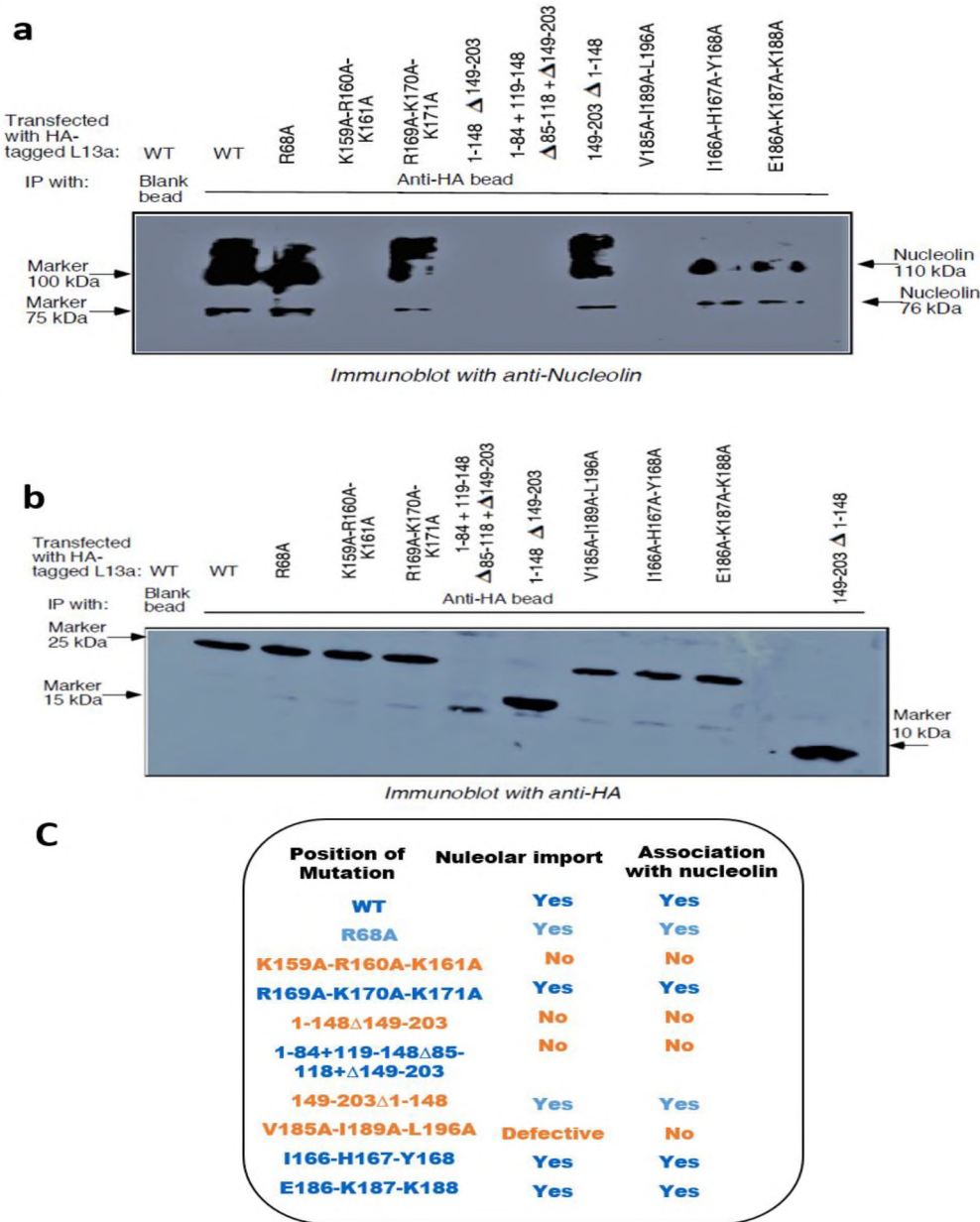


Figure 32: In vivo association of L13a and its mutant variants with nucleolin. Lysates of HEK 293T cells expressing recombinant HA-tagged L13a (wild type or mutant as indicated above each lane) were subjected to immunoprecipitation with anti-HA-coated beads (or non-antibody-coated blank beads as a control). (a) The immunoprecipitates were run on SDS-PAGE gels and immunoblotted with anti-nucleolin antibody and (b) anti-HA antibody. (c) Summary of results of in vivo association of L13a variants with nucleolin, compared with subcellular localization assay results.

2.3.11. Conservation of translational silencing domain and ribosomal incorporation domain in L13a among eukaryotes.

To further gain insights into the evolution of C-terminal extension of L13a and its functional significance, we performed sequence alignment of L13a protein among 7



Figure 33: Amino acid Sequence alignment of uL13 proteins -CLUSTAL O (1.2.4). Amino acid sequence alignment of 7 eukaryotic sequences is shown with the conserved ribosomal incorporation domains arginine 68 and Lysine 159 and 161 indicated by two boxes (red) and translation silencing domain arginine 169, Lysine 170 and 171 (blue box) shown in the above figure.

eukaryotes namely, *C. elegans*, *S. cerevisiae*, *P. mariana*, *D. melanogaster*, *M. musculus*, *H. sapiens* and *B. taurus*.

We observed that N-terminal domain of L13a is more conserved than the C-terminal domain in eukaryotes except in higher eukaryotes i.e. human, mouse and bovine where C-terminal extension shows considerable conservation. Also, amino acid Arg68 previously identified as essential for ribosomal incorporation and amino acids K159, R160 and K161 critical for ribosomal incorporation identified in this study are conserved among all seven eukaryotes. However, the translational silencing domain Arg169, Lys170 and Lys171 is conserved among only 3 higher eukaryotes *H. sapiens*, *M. musculus* and *B. taurus*, suggesting an essential role of evolution of c-terminal extension in higher eukaryotes in translational silencing of inflammatory proteins. Such an endogenous defense mechanism against uncontrolled inflammation has not been reported in the lower eukaryotes like yeast. The sequence alignment results are shown in figure 33.

2.5 Discussion

Ribosome biogenesis in eukaryotes is much more complex than in their prokaryotic counterparts. The rRNA processing and assembly of ribosomes is facilitated by several cofactors, endo- and exonucleases (Chen and Huang, 2001), RNA helicases (O'Day, 1996), SnoRNPs (Ni, Tien and Fournier, 1997) and accessory proteins (Saveanu *et al.*, 2003). The association of rRNA and ribosomal proteins with each other to form functional ribonucleoproteins (RNP) has been a challenging topic under investigation almost since the discovery of ribosomes (Nierhaus, 1980). Ribosomal proteins are important constituents of ribosomes. However, initial investigations were mainly focused on the processing of pre-rRNAs and characterization of the assembly factors involved in ribosome biogenesis, with less emphasis on r-proteins and their functions. Ribosome structure analysis has shown that the PTC (peptidyl transferase center) is devoid of ribosomal proteins and the process of peptide bond formation is catalyzed by rRNA, suggesting r-proteins don't directly participate in the protein synthesis mechanism but might have more indirect roles to play such as rRNA processing and stabilization of ribosomal subunits. Studies in the last 10 years have witnessed an increase in understanding the role of r-proteins being a part of ribosomes in yeast and mammals. In vitro studies suggest that binding of individual r-protein to rRNA occurs in stages. The initial interactions are weak, but they strengthen as assembly proceeds. Ribosomes in prokaryotes and eukaryotes share a common conserved rRNA core and some conserved r-proteins while eukaryotic ribosomes have acquired eukaryote-specific rRNA extensions and r-protein. Some conserved r-proteins have also evolved N- or C-terminal extensions through the course of evolution. In this study, we also identified a eukaryote-specific C-terminal

extension of unknown function in ribosomal protein L13a by sequence and structure alignment of *E. coli* and human L13a. A series of previous studies from our laboratory have identified Arg68 in the N-terminal globular domain of L13a as essential for its ribosomal incorporation (Das *et al.*, 2013). However, the role of the C-terminal domain in ribosomal incorporation or extra-ribosomal functions of L13a was never explored before. Studying the mechanism of incorporation of r-protein L13a into the 60S ribosomal subunit is important to improve our understanding of the complexities of ribosome biogenesis, role of L13a within the ribosome and its extra-ribosomal function in translational silencing and inflammation resolution (Mazumder *et al.*, 2003). Since release of L13a from the ribosomal large subunit is essential for its extra ribosomal function, understanding how L13a incorporates into the ribosomes may also reveal the mechanisms regulating its release for translational silencing activity. In this study, we have done structural and functional analysis of a eukaryote-specific C-terminal extension (amino acids 149-203) in human ribosomal protein L13a. This extension harbors a predicted NLS (Lys159-Lys188) and a predicted RNA-binding domain (Arg169-Lys179). It also contains amino acids which are predicted to interact with another ribosomal protein, L14.

In eukaryotes, ribosomal proteins are translated in the cytoplasm and then imported into the nucleus and nucleolus, where incorporation into the precursor ribosomes takes place. The first question to be asked is how r-proteins are imported into the nucleus prior to their association with rRNA. Studies have shown that there are transporters that facilitate nuclear import of r-proteins by recognizing nuclear localization signals in r-proteins (Bange *et al.*, 2013). In yeast, nascent NLS containing r-proteins are imported into the nucleus via binding to the β -karyopherins such as KAp123, Kap108 and Kap121 (Rout,

Blobel and Aitchison, 1997). Mammals also use similar transporters such as importin β -related transporters e.g. Imp9a and Imp9b import rpS7, rpL18a (Jäkel *et al.*, 2002). Importins recognize specific nuclear localization signals (NLSs) in the cargo proteins. The importins also interact with nucleoporins, which are components of the nuclear pore complex. This interaction allows a facilitated diffusive translocation of the importin-cargo complex through the nuclear pore. Once in the nucleus, the importins bind to Ran:GTP, which triggers cargo (protein) release. The importin-Ran:GTP complex then recycles back to the cytoplasm, where the GTP on Ran is hydrolyzed, and Ran:GDP dissociates from the importins. NLS sequences are usually short sequences of basic amino acids, e.g. the NLS of SV40 large T antigen is 5 amino acids long. However, many ribosomal proteins and other nucleic-acid binding proteins are known to carry longer NLS sequences. One such example is ribosomal protein L23a where importins recognize a domain of 43 residues. One reason for such longer NLSs in ribosomal proteins could be that the importins not only direct cargos to the nucleus but might shield basic proteins against undesired interactions during transit. This assumption goes well with the predicted NLS in L13a C-terminal extension which is also 29 amino acids long. To experimentally validate this predicted NLS, we tested a deletion version of L13a for its ability to traffic to the nucleus. Unfortunately, our study does not provide any evidence whether the predicted NLS of L13a plays any role in nuclear translocation as we do not see retention of L13a protein with NLS deletion in the cytoplasm of human cell lines. Most ribosomal proteins carry more than one NLS-like sequence. One striking example is human large ribosomal protein L7. Its sequence carries basic cluster NLS-like segments within the N-terminal region (within first 54 amino acids) and another in the middle region (156-167 amino acids). NLS deletion and

immunofluorescence-based studies showed that at least one NLS is sufficient for nuclear import of L7 protein (Ko *et al.*, 2006). In silico programs NLS mapper and NLStradamus also predicted bipartite NLS in human L13a: one spanning the region from Arg84-Val115 (NLS1) and the other in the C-terminal domain Lys159-Lys188 (NLS2). However, our immunofluorescence-based studies and deletion of either one NLS or both NLS failed to identify a functional NLS in the L13a. Interestingly, deleting both NLS1 and NLS2 impairs nucleolar import of the protein as well. These studies suggest that L13a may utilize a non-conventional mechanism to enter the nucleus like some other ribosomal proteins like L12, that do not rely upon the NLS for nuclear import. Ribosomal protein L12 uses a distinct nuclear import pathway mediated by importin 11 (Plafker and Macara, 2002). Future studies aimed at identifying the specific importers of human L13a may uncover the mechanism and/or specific sequence of L13a essential for its nuclear import.

The study covered in this thesis has demonstrated the role of C-terminal extension in the ribosomal incorporation of the L13a. Deletion of full-length C-terminal extension (149-203) not only impaired nucleolar import and incorporation into the ribosomes, but also impaired the translational silencing activity of L13a. This finding supports the notion that prokaryotes lack nucleus/nucleolus (site of ribosome biogenesis and ribosomal incorporation of L13a) as well as L13a mediated inflammation control mechanism, therefore, this eukaryote specific C-terminal extension might have evolved for its role in ribosome biogenesis to mediate the nucleolar translocation, ribosomal incorporation and translational silencing activity (extra-ribosomal function of L13a reported in higher eukaryotes). Studies in yeast have shown that the eukaryote-specific carboxy-terminal extension of L16 (homolog of mammalian L13a) is essential for growth

and rRNA processing (27S pre-rRNA to mature 25S and 5.8S rRNA). However, the ribosomal incorporation of L16 is not affected by the deletion of the C-terminal extension (Espinar-Marchena *et al.*, 2016). In human L13a, we have identified amino acid residues within the C-terminal extension that are essential for ribosomal incorporation of L13a. These residues include Lys159, Lys 161, Val185, Ile189 and Leu196. Residues at position 159(K) and 161(K) are essential for nucleolar translocation of the protein and subsequent incorporation of L13a into the ribosomes.

Eukaryotic ribosomes have an extensive network of protein-protein interactions, which involves eukaryote-specific ribosomal proteins or eukaryote-specific extensions of conserved ribosomal proteins. These interactions are thought to stabilize ribosomes. Amino acids Val185, Ile189 and Leu196 in the C-terminal domain of human L13a have been predicted to be involved in an interaction with another ribosomal protein L14. Such an interaction between yeast L16 and L14 also exists. L16 is located on the solvent-side of the 60S subunit in close proximity to L14. While such an interaction is speculated to be important for uL13 incorporation into ribosomes (Klinge *et al.*, 2011)(Ben-Shem *et al.*, 2011), other studies conducted in yeast doesn't support this notion (Espinar-Marchena *et al.*, 2018). The reason is that L16 incorporation is an earlier event than L14 which assembles in the nucleolus with pre-60S r-particles, whereas, L16 incorporates in 90S precursor ribosome in yeast. Therefore, L16 incorporation is not dependent on presence of L14 on the ribosome (Espinar-Marchena *et al.*, 2018). However, conditions might differ in higher eukaryotes such as humans where there are considerable differences in characteristics of L13a and its yeast homolog L16. Structural alignment studies have shown that yeast L16 and human L13a share almost identical structures. However, the amino acid

composition of the eukaryotes -specific C-terminal extension is not identical (figure33). In addition, the molecular environment and the contacts that yeast L16 and human L13a form with rRNA also differs. This difference in contacts made with rRNA is more prominent in C-terminal extensions of both the proteins. Therefore, differences in the structure and function of yeast L16 and human L13a may in part explain the observed differences between the yeast and mammalian systems and outcome of interactions between L13a and L14 in human ribosome. Detailed study of L13a-L14 interaction may provide additional insight into the mechanism of ribosomal incorporation of L13a.

We also observed that all the ribosomal incorporation defective mutants namely K159A-R160A-K161A, V185A-I189A-L196A, L13a 1-148 Δ 149-203, except one L13a 149-203 Δ 1-148 failed to translocate into the nucleolus. Proteins were seen retained in the nucleus. This suggests that multiple or shared amino acid sequences of L13a control its nucleolar import. This implies that nuclear import of ribosomal protein may be prerequisite for its incorporation but doesn't ensure its nucleolar import and subsequent ribosomal incorporation.

An important extra-ribosomal function of L13a has been widely studied where L13a is an essential component of the GAIT protein complex that inhibits the translation of mRNAs encoding inflammatory proteins (Mazumder *et al.*, 2003). However, the precise mechanism and L13a domain critical for this extra-ribosomal function of L13a has not been established yet. In this study, we explored the role of eukaryote-specific C-terminal extension of L13a in translational silencing activity and showed that this extension alone (L13a 149-203) is capable of supporting the GAIT-element mediated translation silencing pathway. Further we showed that amino acids Arg169, Lys 170, L171 within this extension

are essential for the extra-ribosomal function of L13a. Mutating these three residues abrogates silencing. These three amino acid residues are conserved among mouse, human and bovine species but not among lower eukaryotes such as yeast. (figure33). This is consistent with the fact that such this type of translational control has not been reported in yeast. Further, L13a sequence alignment among seven eukaryote species namely *C. elegans*, *S. cerevisiae*, *P. mariana*, *D. melanogaster*, *M. musculus*, *H. sapiens* and *B. taurus* (figure33) shows that the N-terminal globular part of L13a is more conserved than the C-terminal extension among all the seven species. Interestingly, the eukaryote-specific C-terminal extension is more conserved among the higher eukaryotes such as human, mouse and bovine. This supports the idea that this eukaryote-specific C-terminal extension has further evolved in higher eukaryotes to acquire additional and important functions in inflammation resolution in immune cells. This sequence alignment also showed that the translational silencing domain consisting of three amino acids Arg169-Lys170-Lys171 is also conserved among human, mouse and bovine but not in the lower eukaryotes such as yeast. Also, residues K159-R160-K161 (discussed in this manuscript) and R68 (Das *et al.*, 2013), essential for ribosomal incorporation of L13a, are highly conserved among all seven species (figure 33).

It has been shown previously that L13a phosphorylation at Serine77 mediated via DAPK-ZIPK pathway is essential for release of L13a from 60S ribosomal subunit and assembly into the GAIT complex (Mukhopadhyay *et al.*, 2008). We have shown that C-terminal extension alone can silence the translation of GAIT-element bearing reporter mRNA transcript. The obvious question asked here is: How does the C-terminal L13a extension (Tyr149-Val203) assemble into the GAIT complex without the essential

phosphorylation (C-terminal extension lacks phosphorylation site S77) and what is the precise role of serine77 phosphorylation in the release of L13a from the ribosome and assembly into the GAIT complex? We proposed a hypothesis that serine phosphorylation has a role in changing the conformation of L13a on the ribosome in such a way that the residues (Arg68, Lys159-Arg-160-Lys161) making contacts with the rRNA could fail to anchor with the rRNA thus causing its release from the ribosome. Also, this conformational change could also mediate the assembly of L13a into the GAIT complex. Figure 34 shows the spatial proximity of negatively charged amino acids to serine 77. We proposed that phosphorylation mediated addition of negative charge to serine77 residues results in electrostatic repulsion from the negatively charged amino acids in the vicinity, leading to movement of C-terminal helix away from the N-terminal globular domain and this “opening up” of the protein could expose the triad of residues (Arg169-Lys170-Lys171) critical for L13a assembly into the GAIT complex. This hypothesis provides the possible explanation for inability of L13a expressed in bacterial cells to silence translation whereas, the C-terminal extension alone retains this ability, although proteins in both the cases are in unphosphorylated form. This hypothesis needs experimental testing in the future.

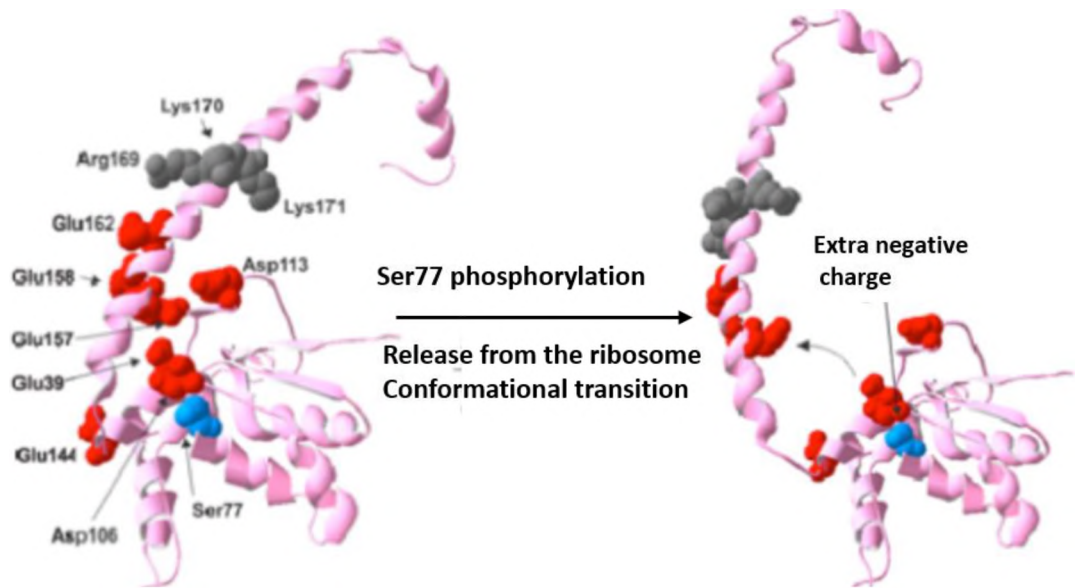


Figure 34: Proposed model for phosphorylation-induced conformational transition of the L13a C-terminal helix. Ser77 of human L13a is located in the vicinity of negatively charged amino acid residues (Glu39 and Asp106), which in turn are surrounded by additional negatively charged residues (Glu144, Glu157 and Glu158). Therefore, the added negative charge resulting from phosphorylation of Ser77 may push the eukaryote-specific C-terminal helix extension away from the globular domain of the protein, which would expose the residues shown to be critical for GAIT element-dependent translational silencing in this study (Arg169, Lys170, Lys171). Human L13a is depicted as a ribbon diagram based on the CryoEM structure of the human ribosome at 3.6 Å resolution (Protein Data Bank code 5T2C). Side chains (Van der Waals radii) of the negatively charged amino acid residues within the vicinity of Ser77 are shown.

In this study we have identified the ribosomal incorporation domain (Lys159-Lys161 and Val185-Ile189-Leu196) and translational silencing domain (Arg169-Lys170-Lys171), which work independently. Results of ribosome incorporation assay and nucleolar translocation assay for various L13a mutants are presented in table 1. Our earlier work has demonstrated the physiological significance of L13a in inflammation resolution in macrophage-specific L13a knock out mice, where the lack of L13a resulted in failure of inflammation resolution and more severe immune response (Poddar *et al.*, 2013)(Poddar *et al.*, 2016). Importantly, it is not possible to study the consequences of the loss of GAIT complex-mediated inflammation resolution mechanisms in a systemic/total L13a knock out mice due to embryonic lethality (discussed in next chapter). Our finding that abrogation of the GAIT element mediated translation silencing by mutating Arg169-Lys170-Lys171 without affecting the ribosomal incorporation presents the possibility of generating a whole body knock-in mouse model to further examine the physiological significance of L13a mediated translational silencing on a systemic level.

L13a variants	Ribosomal Incorporation	Nuclear & Nucleolar Translocation assay	
		Nucleus	Nucleolus
WT	+	-	+
R68A	+	-	+
1-148 Δ 149-203	-	+	-
149-203 Δ 1-148	-	-	+
V185A-I189A	-	+	+
V185A-I189A-L196A	-	+	+
K159A-R160A-K161A	-	+	-
K159A	-	+	-
R160A	+	-	+
K161A	-	+	-
R169A-K170A-K171A	+	-	+
1-84+119-203(Δ 85-118)	N.D.	+	+
1-84+119-148(Δ 85-118 & Δ 149-203)	N.D.	+	-
I166A-H167A-Y168A	+	-	+
K172A	+	-	+
Q173A	+	-	+
M175A	+	-	+
R176A	+	-	+
L177A	+	-	+
K179A-Q180A	+	-	+
R59A-K60A-K61A	-	+	+

Table1: Summarizing results of ribosome incorporation and subcellular localization of L13a mutants.

LEGEND: + and - Indicate presence (+) or absence (-) of L13a protein in the given subcellular organelle. N.D: Not done

CHAPTER III
ROLE OF RIBSOMAL PROTEIN L13a IN EARLY EMBRYONIC
DEVELOPMENT IN MICE

3.1. ABSTRACT

Eukaryotic ribosomal protein L13a belongs to conserved universal ribosomal uL13 protein family. Previous studies in our laboratory showed the essential role of L13a as a physiological defense against uncontrolled inflammation in macrophage-specific knockout mice. To study the consequence of total knockout of L13a, we generated mice harboring the heterozygous knockout (KO) allele for L13a (L13a^{+/-}). These mice are breeding competent and show no visible abnormality under standard animal housing conditions. However, the mice harboring the homozygous KO allele (L13a^{-/-}) are embryonically lethal at an early embryonic stage. Interestingly, we found the survival of the embryo in the pre-implanted morula stage. This suggests an essential role of this protein in early embryonic development. Next Generation Sequencing (NGS) analysis of the pre-implanted embryos and comparing the expression of Differentially Expressed Genes (DEG) with the regression scale of L13a transcript level, we have identified several potential targets showing altered

expressions. These studies also showed specific confinement of L13a in the nucleus only in the early embryonic stage but not in the embryonic fibroblast harvested from the more developed embryo from the uterus.

3.2 Introduction

In our current study, we have elaborated the role of ribosomal protein L13a in the early embryonic development in mammals. Ribosomal protein L13a is one of the proteins that incorporates into the ribosomes at an early stage during ribosome biogenesis in the nucleolus. Previously, we have shown that the loss of L13a in cultured cells of myeloid origin doesn't affect ribosome biogenesis and the primary function of the ribosome (protein translation) (Chaudhuri *et al.*, 2007). In addition, previous studies in our laboratory have also shown that the tissue specific knock out of L13a in macrophages abrogates the L13a mediated translational silencing of inflammatory proteins such as chemokine and chemokine receptors. This results in a more aggressive inflammatory condition in the macrophage- specific L13a knock out mice when challenged with inflammatory stimuli such as LPS, thioglycolate or administration of dextran sodium sulfate as compared to wild type (WT) mice. This severe inflammatory phenotype in the L13a knock out mice is associated with decreased survival and poorer chances of recovery due to failure of inflammation resolution mechanism in the absence of GAIT-mediated translational silencing pathway (Poddar *et al.*, 2013)(Poddar *et al.*, 2016).

Our next goal was a more detailed study about the ribosomal and ribosome-independent functions of L13a. The best way to address this goal was to knock out L13a at systemic level and study its impact on inflammation resolution mechanisms in experimentally induced inflammatory diseases. We generated a mouse heterozygous for the L13a allele by neomycin cassette flanked by LoxP, FRT sites to mediate knock out of one L13a allele. These L13a heterozygous mice are breeding competent, don't show

morphological defects, suggesting that one allele for L13a is sufficient for survival and physiological functions. To study the outcome of systemic loss of L13a, we crossed L13a heterozygous mice to obtain mice homozygous for L13a knock out. To our surprise, L13a total knock out mice were not identified among the new borns as well as post-implantation embryos (6.5 dpc to 18.5 dpc) of the heterozygous parents. This implies an essential role of L13a in embryonic development at an early stage.

Therefore, we dissected the mouse embryos from preimplantation (2.5 dpc) to post-implantation (18.5 dpc) stages for immunostaining or isolation of nucleic acids to do downstream experiments focused on studying the role of L13a in embryonic development and survival.

In this study, we have proposed that ribosomal protein L13a plays a pivotal role in formation and survival of L13a $-/-$ (homozygous knock out) blastocyst stage embryos (3.0 to 3.5 dpc).

3.3 MATERIAL AND METHODS

3.3.1 Generation of L13a heterozygous knock out (L13a^{+/-}) mice

The targeting construct for L13a gene was designed by introducing Neomycin (Neo) cassette flanked by LoxP and FRT sites upstream of exon 2 and downstream of exon 7 so that exons 2 to 7 of the L13a gene could be conditionally targeted. The Targeted iTL IC1 (C57BL/6) embryonic stem cells positive for the above construct were microinjected into Balb/c blastocysts. The Resulting chimeras with a high percentage black coat color were mated to C57BL/6 FLP mice to remove the Neo cassette. Tail DNA was analyzed for identification of mice with Neo deletion. Confirmed Somatic Neo Deleted Mice were set up for mating with C57BL/6N wild-type mice to generate Germline Neo Deleted mice.

3.3.2 Animal housing, breeding and setting up timed mating

All animals (C57BL/6 mice) were housed and bred according to the rules of National Institute of Health (NIH) and the Institutional Animal Care and Use Committee (IACUC) of Cleveland State University. They were supplied with regular drinking water and fed a normal chow diet. L13a heterozygous male and female mice (aged about 6-8) were paired to obtain new borns to maintain the line and to screen the pups for L13a total knock out mice. To screen the embryos for L13a total knock out genotype, timed matings were performed by pairing the L13a^{+/-} male and female mouse after 5:00 PM. Next day, the females were examined visually for the presence of a vaginal plug, an indication of mating. The plug is made of coagulated secretions from the vesicular glands of the male. The females showing vaginal plugs were separated from the males and housed in separate

cages. This is counted as 0.5 dpc (mating is assumed to have happened at 12:00 am). These females were sacrificed at the desired time points to obtain embryos for downstream experiments. Carbon dioxide was used as the euthanizing agent followed by cervical dislocation to confirm the death. This method is consistent with the recommendations of the Panel on Euthanasia of the American Veterinary Medical Association.

3.3.3. PCR- based genotyping strategy

DNA extracted from the tail snipped of 11 day old pups was used in a PCR reaction to confirm the targeted disruption of L13a allele mediated by Neo deletion. Tail (about 3 mm) was digested in 150 μ l DirectPCR Lysis reagent (Viagen Biotech; Catalog No: 101-T) and 5 μ l Proteinase K (ambion) for 12-14 hours. DNA samples were boiled at 85°C for 45 minutes. 1 μ l of DNA lysate was used in the PCR based genotyping assay. Primers NDEL1 and NDEL2 and WT1 were used to screen mice for deletion of Neo cassette. After Neo deletion, one set of LoxP-FRT sites remain (178 bp). Primer set NDEL1 and NDEL2 yields a band with a size of 428 bp indicating Neo deletion. A band with a size of 1.68 kb with NDEL1 and NDEL2 primers indicates the wild type allele. The presence of the Neo cassette is not amplified by this PCR screening because the size is too great. Primers NDEL1 and WT1 gives a PCR product of 599 bp on WT allele. A PCR for each DNA sample was set up in a total volume of 25 μ l reaction volume. Each PCR reaction included 12.5 μ l of EconoTaq Plus Green 2x Master Mix (Lucigen catalog# 30033-1), 11 μ l ddH₂O, .25 μ l of 1 μ M each primer (sequences given below) and 1.0 μ l DNA. After a 2 minute hot

start at 94°C, the samples were run using the PCR conditions given below in a thermocycler. The PCR product was run on a 2% gel with a 100 bp ladder as reference.

Primer Sequences:

NDEL1: 5'- CAA TAG GAA TCC TAT GCC TGC TGA GG -3'

NDEL2: 5'- GTG GTG TGA AAA GAC ACA TGT CAG AGC -3'

WT1: 5'- CCC TTG GAC CCA AGA GCA GAG CAG-3'

PCR parameters:

Step1: 94° C for 2 minutes

Step2: 94° C for 30 seconds, 60°C for 30 seconds, 72°C for 1 minute. (30 cycles)

4°C for ∞

WT mouse yields band of 599 bp and 1.68 bp. Heterozygous L13a mouse shows bands of 428, 599 and 1.68 bp. Whereas, a single band of 428 bp represents homozygous knock out genotype for L13a gene.

3.3.4 Post-implantation embryo harvest and genotyping assay

Embryos (post-implantation) to extract DNA for genotyping were harvested from the uteri of L13a heterozygous pregnant females crossed with L13a heterozygous males at desired time points (6.5 dpc to 18.5 dpc). Each embryo was washed twice in the phosphate saline buffer (1X PBS) to get rid of mother's uterine tissues. A part of embryonic tissue was

digested in DirectPCR Lysis Reagent (Mouse Tail) (Viagen Biotech, Catalog No: 101-T) at 55° C for 12-14 hours. 1µl DNA was used for PCR-based genotyping to screen for WT (L13a^{+/+}), heterozygous (L13a^{+/-}) and homozygous knock out (L13a^{-/-}) embryos.

3.3.5 Induction of super-ovulation

Female mice can be induced to ovulate a greater number of eggs than normal through the administration of gonadotropins. WT and L13a heterozygous L13a female mice (23-25 days old) were injected interperitoneally (IP) with 100 µl (5 IU) of pregnant mare serum (PMS) between 2:00 and 4:00 PM on day 1. On Day 3, forty-two to fifty hours after the PMS injection, the mice received an IP injection of 100 µl (5 IU) of human chorionic gonadotropin (HCG). Immediately following injection, female mice were paired with the appropriate stud males of desired genotype of 8 weeks of age or older. Ovulation occurs approximately 12 hours after HCG injection, at which time the eggs can be fertilized. Females are examined for vaginal plugs on the day after HCG injection and mating. This is counted as 0.5 DPC (days post coitum). PMS was bought from Bio vendor (Cat# RP1782721000) and HCG from Sigma Aldrich (Cat# C1063). Both of the hormones were diluted with PBS/saline to give a final conc. of 5 IU in 100µl. The age of the female to be injected is critical for inducing superovulation depending on the strain of the mouse. In C57BL/6 mouse, 24-25 days old is the optimal age for hormonal injection.

3.3.6 Pre-implantation embryo harvest and genotyping assay

Pre-implantation embryos for PCR-based genotyping were harvested by dissecting pregnant females at 2.0, 2.5, 3.0 and 3.5 dpc to obtain early morula, compact morula and blastocyst stage embryos respectively. 2.0 and 2.5 dpc embryos were harvested by flushing

the oviducts with M2 media (cat# M7167; Sigma-Aldrich) under dissection microscope and 3.5 DPC embryos by flushing the uterine horns with M2 media in 10 mm cell culture dish. Each embryo was transferred to a drop of PBS and washed twice, followed by lysis in 10 μ l of Cells-to-cDNA II Cell Lysis Buffer (Cat# AM8723) and heating the samples at 75° C for 10 minutes. 4 μ l of lysate was used in 25 μ l PCR reaction for genotyping to identify homozygous L13a knock out embryos.

3.3.7. Mouse embryonic fibroblast generation and culture

Mouse embryonic fibroblasts were generated from 13.5 dpc post implantation embryos harvested from L13a heterozygous and WT female to obtain WT and L13a^{+/-} fibroblasts respectively. On thirteenth day of pregnancy, females were euthanized, disinfected with 70% ethanol and transferred to a sterile tissue culture hood. Uteri containing embryos were harvested and washed in PBS twice. Each embryo was washed once in PBS and transferred in 6-well plate with DMEM-10% FBS/PS/50 μ M β -mercaptoethanol. With a sharp blade, the head of each embryo was cut and transferred to an Eppendorf containing DirectPCR lysis buffer to extract DNA for genotyping. Red organs (liver/spleen) were removed with forceps followed by mashing the embryos inside 6 cm-dish (5ml DMEM-10% FBS/PS/50 μ M β -mercaptoethanol) through sieve (BD Falcon Cell strainer 352350, 70 μ m Nylon) using a 5 ml syringe plunger. Cells were allowed to settle down and adhere overnight. The next day, cells were trypsinized and passaged in new 6 cm dishes (labelled as Passage 1) until the cells grow towards confluency. Cells were further passaged once or twice before doing immunofluorescence-based assay (primary MEFs can be used for experiments up to P5).

3.3.8 Immunofluorescence assay of pre-implantation embryos and mouse embryonic fibroblasts

Pre-implantation embryos from 2-cell stage to blastocyst stage were harvested from oviduct and uterus after performing timed mating. Each embryo was washed in PBS, fixed in a drop of 4% PFA (Paraformaldehyde) for 10 minutes, permeabilized by incubating them in 0.1-0.2% TritonX-100 in PBS for 10 -15 minutes (approximately). Embryos were blocked with 3% BSA in PBS for 1 hour. Embryos were incubated in mouse anti-L13a antibody (SantaCruz, Cat# SC-390131) and/or rabbit anti-L26 antibody (abcam; Catalog# ab59567) at a dilution of 1:50 in PBS, overnight at 4° C. The next day, embryos were washed with PBS three times (5 minutes each) and incubated with secondary antibodies Alexa Fluor 594 donkey anti-rabbit IgG (H+L) (cat# A21207 Invitrogen) and Alexa Fluor 488 donkey anti-mouse IgG (H+L) (cat#A21202 Invitrogen) for 1-2 hour at room temperature at a dilution is 1:100 in PBS. All the steps from secondary antibody should be performed in dark at room temperature. Embryos were also incubated in PBS+DAPI to stain nuclei for 10-15 minutes, followed by washings with PBS (twice). Each embryo was mounted in a small drop of Prolong gold antifade reagent in the center of a glass slide. Prepared slides were stored overnight, and images were captured the next day using a Nikon confocal microscope.

3.3.9 RNA extraction and purification

Total RNA was extracted from individual embryos harvested from the intercross of heterozygous L13a mice. Each embryo was washed in PBS and transferred to 10 µl of Cells-to-cDNA II Cell Lysis Buffer (Cat# AM8723) and boiled at 75° C for 10 minutes.

The nucleic acid lysates were centrifuged briefly and transferred immediately to the ice. RNA purification was performed using the PicoPure RNA Isolation Kit (Thermo Fisher Scientific, Catalog# KIT0214) following the user's manual. The RNA was eluted in 15 μ l of elution buffer supplied in the kit. The purified RNA samples were sent for next generation sequencing (NGS) to study the differential pattern of gene expression in WT, heterozygous and KO pre-implantation mouse embryos (morula stage: 3.0 dpc).

3.4 Results:

3.4.1 Generation of mice heterozygous for the disruption of RP L13a:

In order to evaluate the ribosomal and extra-ribosomal functions of L13a in mammals, a mouse model carrying only one allele for L13a was generated and ordered from InGenious Targeting laboratory. The design of the targeting construct is shown in Figure 35a. A neomycin cassette flanked by Lox P and FRT (flippase recognition target) sites was inserted targeting exon 2 to exon 7 of the mouse L13a genomic sequence to facilitate its removal. Embryonic stem (ES) cells from C57BL/6 mice were transfected with the L13a targeting construct and the recombinant embryonic stem (rES) cells were microinjected into Balb/c blastocysts. Resulting chimeras with a high percentage black coat color were mated to C57BL/6 FLP mice to remove the Neo cassette. Tail DNA was analyzed from pups with black coat using primer set NDEL1 and NDEL2 to screen mice for the deletion of the Neo cassette. After Neo deletion, one set of LoxP-FRT sites remain (178 bp). A band with a size of 428 bp indicates Neo deletion and a band with a size of 1.68 kb indicates the wild type allele (figure 35c). The presence of the Neo cassette could

not be amplified by this PCR screening because the size of the full length neo cassette is too great to be amplified and visualized on the agarose gel. Once somatic Neo Deletion was confirmed, mice were set up for mating with C57BL/6N wild-type mice to generate Germline Neo Deleted mice. Resulting pups were genotyped using primer set NDEL1, NDEL2, and WT1 to screen mice for the deletion of the Neo cassette. A band with a size of 428 bp indicates Neo deletion. NDEL1 / WT1 amplifies a band with a size of 599 bp on the wild type allele, and NDEL1 / NDEL 2 amplifies band with a size of 1.68 kb on the wild type allele (figure 36d). The primers within the L13a genomic loci for somatic neo deletion confirmation (NDEL1 and NDEL2) and primers for germline neo deletion (NDEL1, NDEL2 and WT1), PCR parameters are shown in the figure 36b

Primer sequences:

NDEL1: 5'- CAA TAG GAA TCC TAT GCC TGC TGA GG -3'

NDEL2: 5'- GTG GTG TGA AAA GAC ACA TGT CAG AGC -3'

WT1: 5'- CCC TTG GAC CCA AGA GCA GAG CAG-3'

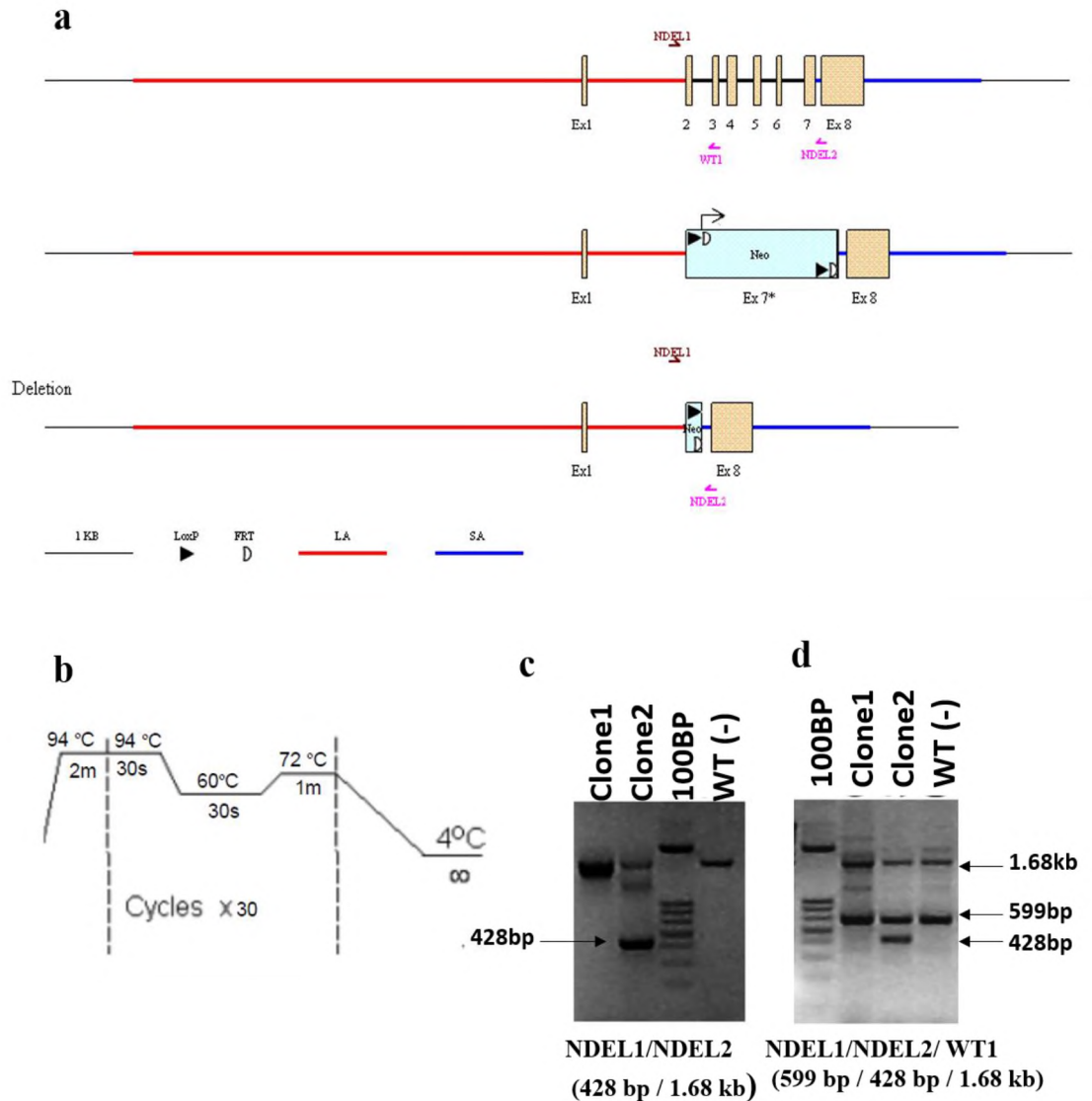


Figure 35: Generation of L13a knock out mouse. (a). Schematic diagram of targeted disruption of L13a allele from exon 2 to exon 7 mediated by neomycin cassette flanked by loxP and FRT sites. (b). PCR Parameters for genotyping. (c). Identification of somatic Neo deletion by PCR-based genotyping. (d). Identification of Neo deletion in germline by PCR-based genotyping.

3.4.2 Absence of L13a homozygous knock out mice among the new born pups from L13a heterozygous male and female intercross:

Previous studies from laboratory have demonstrated an important role of L13a in inflammation resolution in mammals and macrophage specific L13a knock out mice showed poor survival, more pronounced inflammatory disease symptoms in response to experimentally induced inflammatory diseases (Poddar D et al., 2013 and 2016).

In our current study, we wanted to investigate the consequences of total knock out of L13a in a mouse model. Therefore, we crossed mice heterozygous for L13a and screened new born pups by PCR-based genotyping using primers specific to L13a WT allele and knock out allele (neo deletion). Results showed that all the offspring from heterozygotic cross were either WT or heterozygous for L13a. Another important observation we made is the disruption of Mendelian distribution of offspring as demonstrated by more heterozygous pups among new born mice than WT. The number of mice screened, and the genotyping results are shown in the table 2 below:

L13a +/- parents	Genotype			Total number of Pups screened
	+/+	+/-	-/-	
New born pups	37	101	0	138

Table2: Screening of L13a^{+/-} mouse intercross. Genomic DNA extracted from new borns' tails was genotyped by PCR using primers specific for L13a KO allele and WT allele to identify total knock out (L13a^{-/-}) mice.

3.4.3 Absence of L13a homozygous knock out mice in post-implantation embryos from L13a heterozygous intercross:

The observation that no L13a total knock out mouse could be identified among the offspring from heterozygous cross clearly suggests that systemic loss of L13a results in embryonic lethality in mice. In order to get more insights, we considered the following possibilities: embryonic death during (i) post-implantation development (ii) pre-implantation development (iii) failure of egg-sperm fertilization or a defect in gametogenesis. We started with screening the post-implantation stages. The gestation period in mice consists of 20-21 days and implantation of blastocysts in the uterus takes place at day 4.5. To harvest post-implantation embryos, timed mating of L13a^{+/-} heterozygous male and female mice were performed, females were sacrificed at different time points ranging from 18.5 to 6.5 dpc. For each time point, females were sterilized with 70% ethanol followed by dissecting the abdominal cavity to locate the uterus and harvest embryos. Each embryo was washed twice in 1x PBS to remove contaminants (maternal tissue). A small part of embryonic tissue was digested in DirectPCR lysis buffer to isolate DNA for genotyping. L13a total knock out embryos were not identified during the screening of post-implantation embryos from 6.5 to 18.5 dpc, implying an essential role of L13a in early embryonic development (table 3). Also, the embryos don't show morphological defects. We also looked for the resorption sites which are an indication of the embryonic death post implantation and formed as a result of embryo remnants being resorbed by maternal immune cells (figure 36).

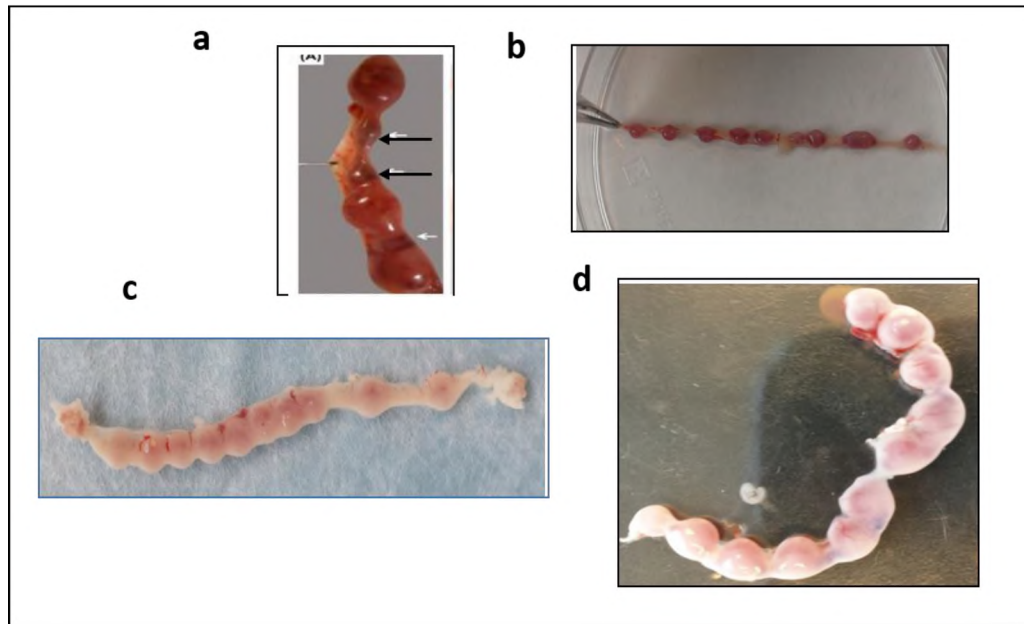


Figure 36: Screening uteri of L13a heterozygous females for resorption sites. (a) A reference image with appearance of resorption sites indicated by arrows. (b,c,d).L13a heterozygous pregnant females' uteri of 6.5 (b), 9.5 (c) and 13.5 (d) dpc screened for resorption sites.

Age (dpc)	Number of mice embryos with indicated genotype			Number of resorptions	Total
	+/+	+/-	-/-		
18.5	4	13	0	0	17
13.5	4	12	0	0	16
10.5	2	8	0	0	10
9.5	3	10	0	0	13
6.5	5	11	0	0	16

Table 3 : Screening of Post-implantation embryos of L13a^{+/-} mice intercross. Embryos from L13a heterozygote females were harvested at 18.5 dpc to 6.5 dpc. DNA extracted from embryos was used for PCR-based genotyping using primers specific to L13a WT and KO allele to identify L13a total knock embryos.

The uteri of L13a^{+/-} females crossed with L13^{+/-} males don't show resorption sites or signs of embryonic death post-implantation. This further implies that L13a total knock out embryos are not implanted in the uterus. We speculated that L13a might be essential for development of either early stage embryos and implantation or gametogenesis i.e. formation of ova and sperms.

3.4.4 Ribosomal protein L13a is essential for blastocyst formation/survival.

To further investigate the role of ribosomal protein L13a in embryonic development in mammals and to identify the specific stage of lethality due to complete loss of ribosomal protein L13a, we screened preimplantation embryos harvested from pregnant females at

different time point starting from blastocyst stage (3.5 dpc) and early morula stage (2.5 dpc). Genomic DNA extracted from individual embryo was genotyped to identify L13a total knock out embryos. We have shown that morula stage embryos (2.0-2.5 dpc) homozygous knock out for L13a survive and don't show morphological defects/changes from WT or heterozygous embryos when observed under the microscope as shown in figure 37a and b. Out of 81 embryos screened, 44 were heterozygous, 25 WT and 12 knock out for L13a as shown in table 4. However, homozygous knock out blastocysts could not be identified by genotyping. All the offspring genotyped showed WT (L13a^{+/+}) or heterozygous (L13a^{+/-}) genotype. These experiments suggest that ribosomal protein L13a may play an essential role in survival and implantation of blastocyst stage embryos (3.5 dpc) or transition of morula stage into blastocyst stage in mice.

Total No. of early Morula embryos Screened (L13a ^{+/-} parents)	Heterozygous (+/-)	WT	Knock out (L13a ^{-/-})
81	44	25	12

Table 4. Screening of pre-implantation embryos for L13a total KO embryos

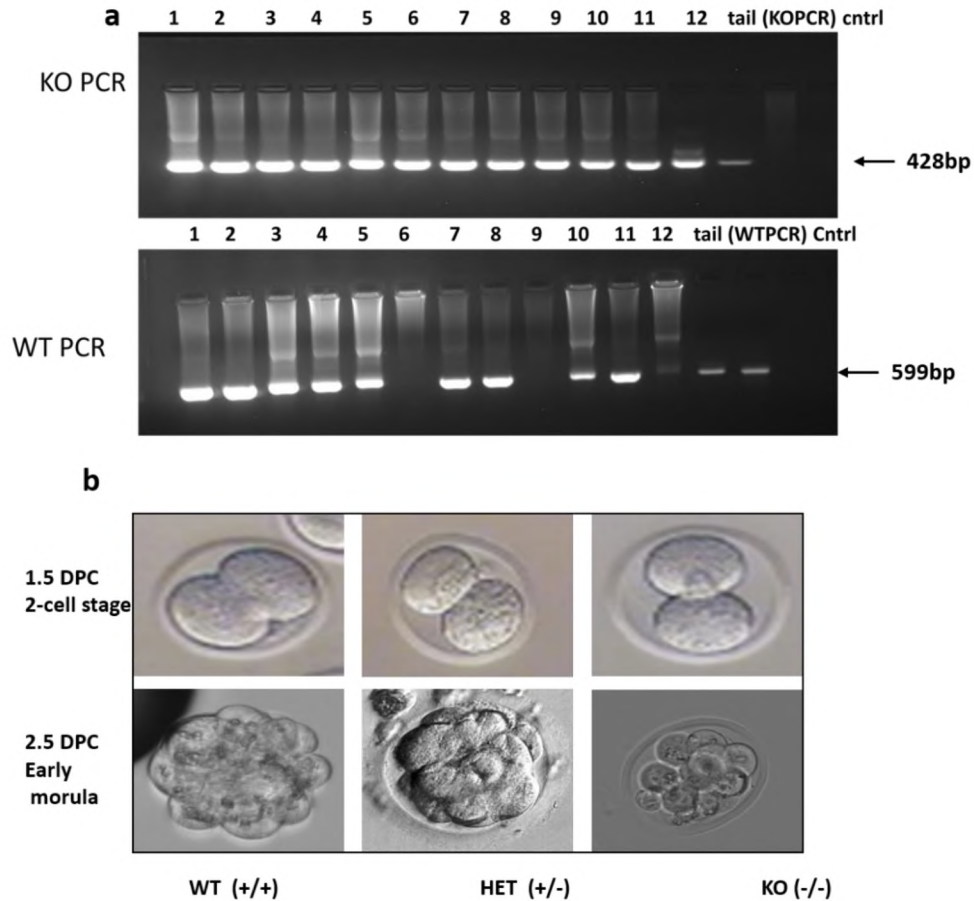


Figure 37: Identification of L13a total KO embryos. (a) Agarose gel image showing PCR amplicons of 2.5-3.0 dpc embryos for KO allele (upper panel) and WT allele (lower panel). Embryo 6 and 9 showed PCR-amplification for KO allele only. (b). WT, heterozygous and KO 2-cell stage and early morula embryos are shown.

3.4.5 Ribosomal protein L13a is localized in the nucleus of pre-implantation stage embryos.

In our current study, we have successfully shown that ribosomal protein L13a is essential for the survival of early embryonic stages in mice. To further gain insights into the role of L13a in embryonic development, we performed

immunofluorescence-based assay to study the subcellular localization of L13a protein from 2-cell stage (1.5 dpc) up to the formation of mature blastocyst (3.5 dpc). The embryos were harvested from the L13a heterozygotes cross at different time points followed by fixing and staining with mouse anti-L13a antibody and a secondary antibody Alexa Fluor 488 donkey anti-mouse IgG. Nuclei were visualized by staining the embryos with DAPI. The images captured by a confocal microscope showed localization of ribosomal protein L13a in the nuclei of all the pre-implantation stages (2.5 to 3.5 dpc), suggesting an important function played by L13a in the nucleus, shown in figure 38.

We also showed that this nuclear localization of L13a is exclusive for L13a protein only, whereas, another 60S ribosomal subunit protein L26 was seen localized in the cytoplasm. Immunostaining of morula and blastocyst stage embryos with antibody for another ribosomal protein L26 showed the localization of L26 in the cytoplasm only, further suggesting that ribosomal protein L13a might play an essential nucleus-specific role in early developmental stages in mammals (figure 39a). In addition, mouse embryonic fibroblasts generated from post-implantation 14.5 dpc WT and heterozygous L13a embryos showed the localization of L13a in both nucleus and cytoplasm (figure 39b). We did not see any difference in the sub-cellular localization of L13a in WT and heterozygous mouse embryonic fibroblasts (MEFs). This experiment showed that L13a is localized in the nucleus in pre-implantation stages and in cytoplasm and nucleus in post-implantation stages, suggesting an essential nuclear function being performed by L13a prior to

or during implantation of late blastocysts in the uterus. The results of immunostaining are shown in figure 39.

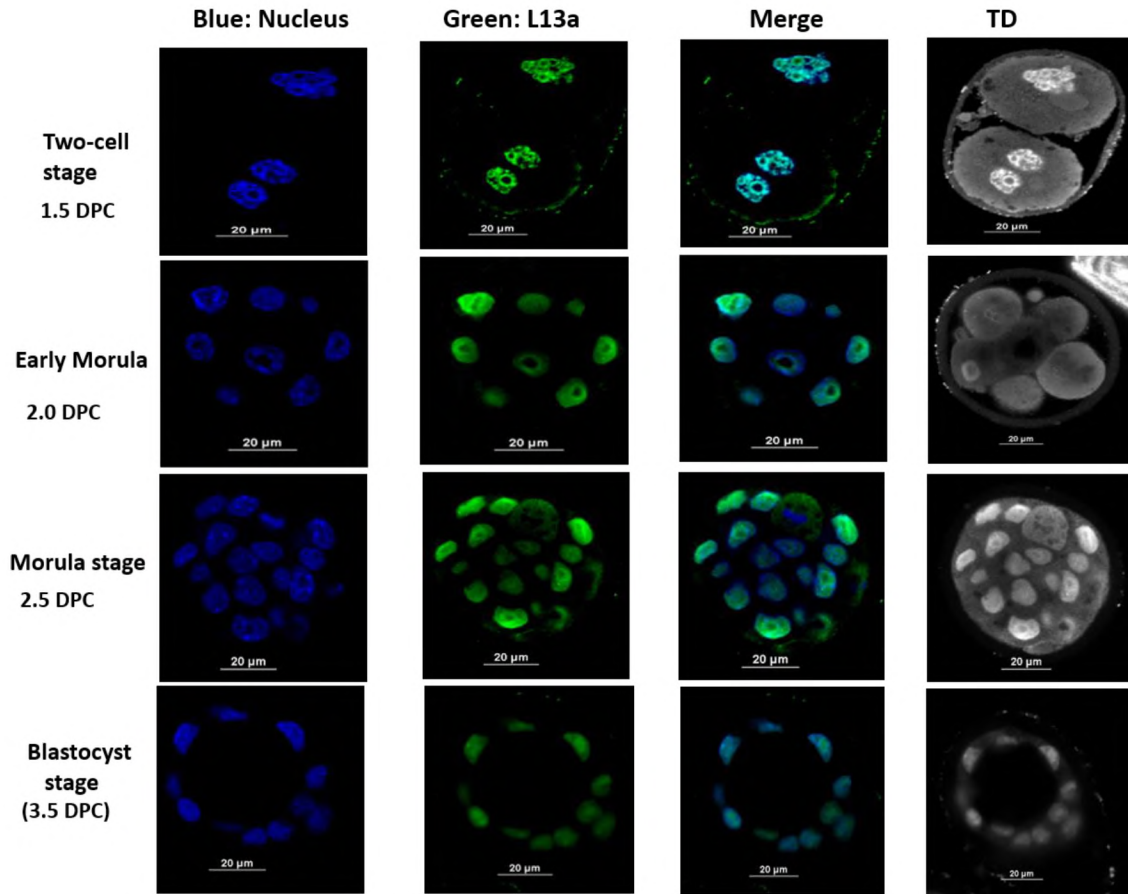


Figure 38: subcellular localization of L13a in pre-implantation embryos. Embryos from 2-cell stage to blastocyst stage were immunostained with mouse L13a antibody and a dye conjugated (green) anti-mouse secondary antibody. Nuclei were stained with DAPI (blue). All the pre-implantation embryos showed nuclear localization of L13a protein.

L13a:Green; Nucleus: Blue; L26:Red

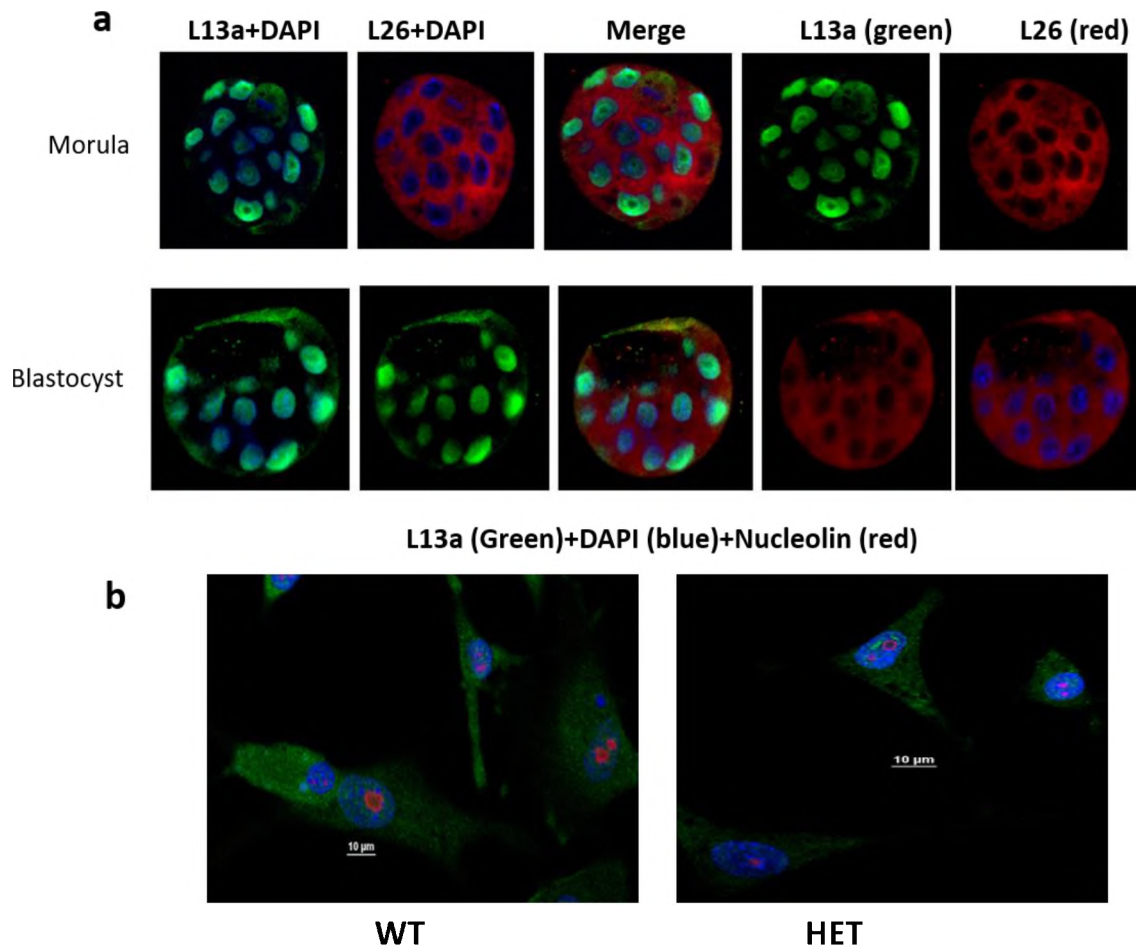


Figure 39: Subcellular localization of L13a and L26 in pre-implantation stage embryos and L13a localization in (post-implantation embryonic cells) MEFs (a). Morula and early blastocyst stage embryos immunostained with L13a antibody (green) and L26 antibody (red). (b). Mouse embryonic fibroblasts (generated from 14.5 dpc) immunostained with L13a antibody (green) and nucleolin antibody (red). Nuclei are stained with DAPI (blue). L13a is localized in nucleus of pre-implantation embryonic cells and in the nucleus and cytoplasm in post-implantation mouse embryonic fibroblasts. L26 is localized in the cytoplasm of both morula and blastocyst stage embryos.

3.4.6 Modulation of inflammatory pathways in pre-implantation embryos homozygous for L13a knock out.

Since we have shown that L13a is essential for survival and implantation of pre-implantation embryos in mice, the underlying mechanism by which L13a regulates the embryonic development at such an early stage needs to be investigated further. Interestingly, we observed that L13a protein is localized in the nucleus in all the pre-implantation stage embryos and as the embryos advance into post-implantation development, L13a is present in the nucleus and in the cytoplasm of the embryonic cells. Therefore, we speculated that L13a may play an important role in the nucleus during early development. To gain more insight, we harvested early morula stage embryos to isolate total RNA. Purified RNA samples were subjected to RNA sequencing. Due to the limitation of the amount of nucleic acid obtained from early stage morula embryos, we chose to do RNA sequencing of random embryos without doing PCR-based genotyping. First, cDNA libraries prepared from individual RNA sample were sequenced to generate a L13a regression scale depending upon the relative abundance of L13a mRNA transcripts (figure 40). The patterns of differentially expressed genes were compared with reference to the Regression scale of L13a (scale of 9 to 2) to identify the genes and underlying pathways modulated in response to L13a expression. The NGS results have shown that several genes show downregulation/upregulation in the absence of L13a when compared with the regression scale of L13a e.g. Ptma, HnrnPa1, Clta, unc50, Gm7056, E2f4, Syce2, CKS2, Wnk1 (figure 40). We also subjected our RNA sequencing data to pathway analysis, which showed L13a transcript abundance is correlated with the modulation of several pathways. One noteworthy pathway is the cytokine and inflammatory pathway. As the

relative abundance of L13a decreases as represented by regression scale of L13a, this pathway shows upregulation indicated by an arrow in the figure 41.

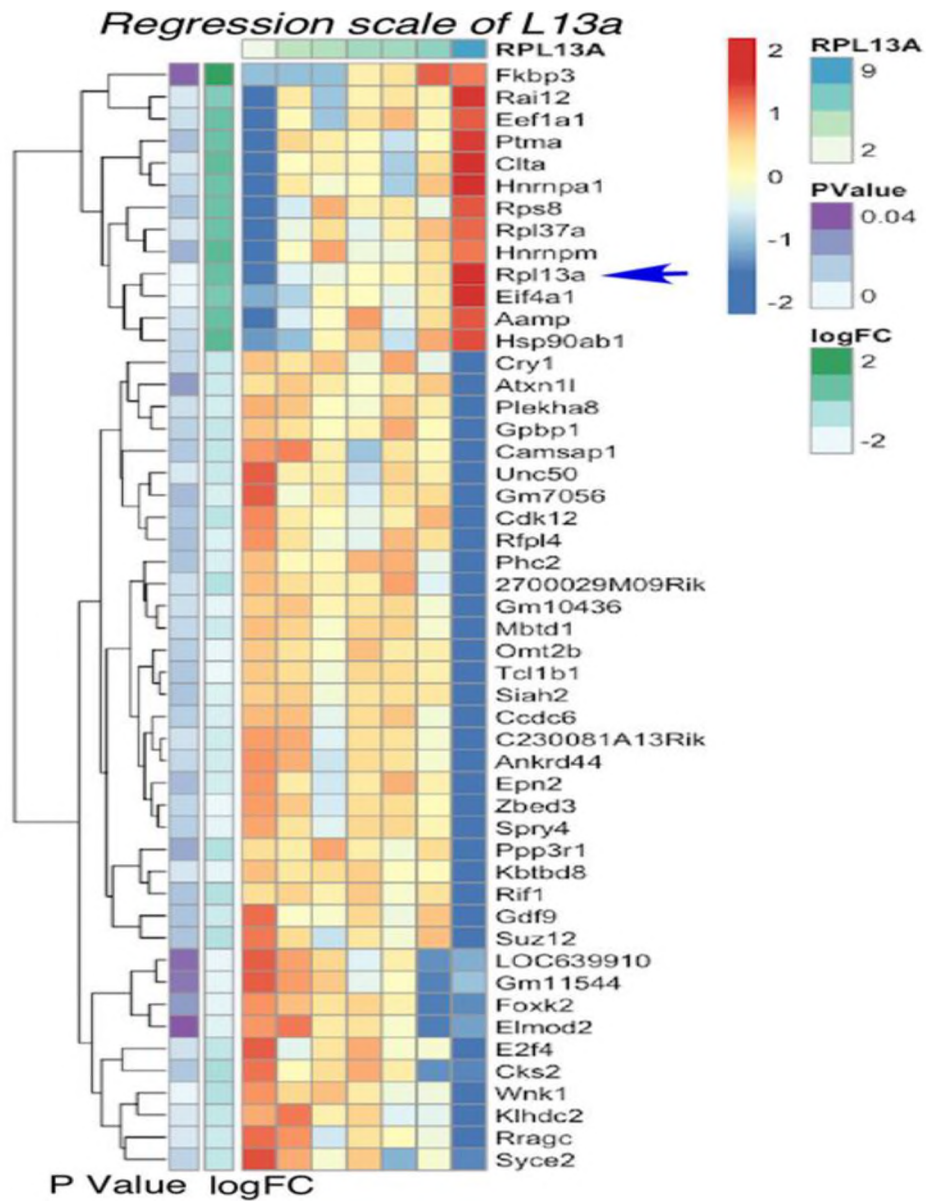


Figure 40: Alteration of gene expression in absence of L13a in early embryogenesis. RNA samples from individual early morula stage (L13a+/- parents cross) subjected to RNA sequencing. RNA sequencing results identified several potential targets modulating in absence of RP L13a in early embryonic stages. The gene expression was compared to the abundance of L13a transcripts (regression scale) and log FC (fold change) and P value is also indicated for each target gene.

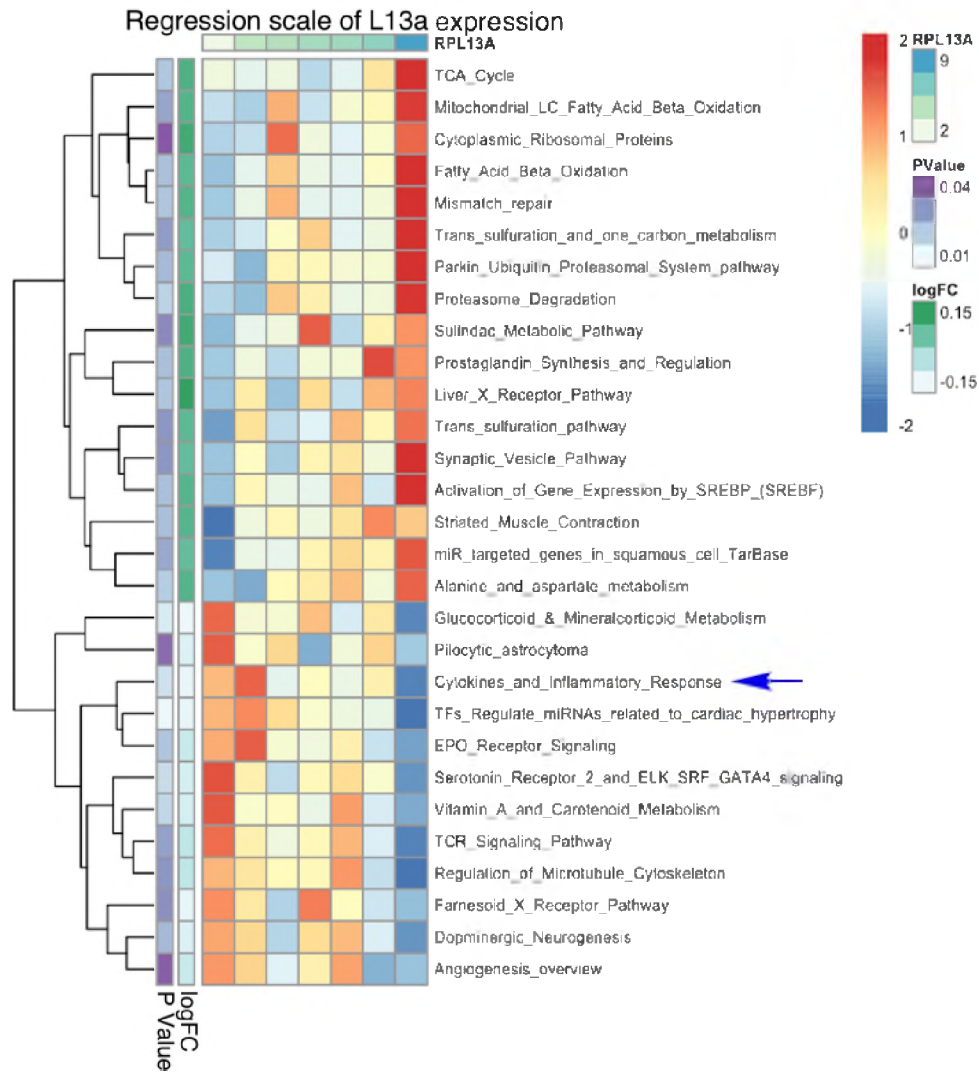


Figure 41: RNA sequencing data revealed a negative correlation between cytokine and inflammatory pathway (indicated by blue arrow in the figure) and the regression scale of L13a. RNA samples from individual embryo from L13a[±] intercross were subjected to NGS to see the relative abundance of mRNA transcript. RNA seq data subjected to pathway analysis identified the pathways modulated in response to L13a absence.

3.5 Discussion:

Ribosomal proteins are well known to play extra-ribosomal functions in addition to their essential role in ribosome assembly and protein translation. Dysfunctions in most RPs induce developmental defects ranging from general translation impairment-related defects to tissue-specific phenotypes. In mammals, RP genes mutations are associated with several tissue-specific abnormalities such as the mouse Tail-short (Ts), Tail-short shionogi (Tss) and Rabortorcido (Rbt) mutants, showing skeletal abnormalities such as short, kinky tails and neural tube defects such as exencephaly, spina bifida and cleft palate etc.(Hustert *et al.*, 1996). Recent studies have shown that the developmental defects in Ts (Tail-short) mutants are caused by mutations in Rpl38. Targeted disruption of small subunit ribosomal protein S19 has been shown to induce embryonic lethality in mice embryos at pre-implantation stage, suggesting an essential role of S19 in development of S19 homozygous knock out zygotes into blastocysts (Matsson *et al.*, 2004). Another example of embryonic lethality in mammals is in ribosomal protein S6-heterozygous embryos, resulting in death at post-implantation stage (gastrulation stage).

The study covered in this thesis also demonstrates a similar role played by ribosomal protein L13a. This study suggests an essential role of L13a in the survival and implantation of L13a total knock out embryos. The RNA sequencing performed on embryos (WT, HET and KO) has identified several genes which are modulated in response to relative abundance of L13a mRNA transcripts. Since L13a as a component of GAIT complex plays a pivotal role in inflammation resolution, we performed pathway analysis using RNA sequencing data. Interestingly, cytokine and inflammatory pathway showed an

inverse correlation with the abundance of L13a mRNA transcripts. Recently, there have been several reports where the role of immune cells and inflammatory proteins have been investigated in blastocyst implantation and embryonic development (Dekel *et al.*, 2014)(Simón *et al.*, 1998). Further studies need to be conducted to understand the role of L13a in embryogenesis in more depth. We have also observed that L13a is exclusively localized in the nucleus during pre-implantation development. However, it tends to be localized in cytoplasm in post-implantation stages. Therefore, we speculated an important role of L13a in the nucleus and that L13a may regulate the expression of a cohort of genes required for developmental progression during blastocyst implantation.

Future studies aiming at selecting and validating potential L13a targets from NGS results will shed more light on the mechanism underlying the role of L13a in mammalian embryogenesis. Since L13a is localized in the nucleus in pre-implantation stages, we also aim at testing the engagement of L13a in the chromatin isolated from morula stage embryos and mouse stem cells generated from inner cell mass based on the speculation that L13a could modulate the expression of target genes at the transcriptional or post-transcriptional level.

CHAPTER IV

CONCLUSION

This thesis covers three main aspects of L13a: its ribosomal function (ribosomal incorporation mechanism), extra-ribosomal function (translational silencing mechanism) and its role in early embryonic development in mice.

Regulation of gene expression at the level of translation can occur by many means and adds considerable richness and sophistication to gene regulation. One of the most interesting features of this mechanism is: these translational regulations are usually reversible, as it is often mediated through reversible protein modifications such as the phosphorylation mediated activation/inactivation of initiation factors. The need for translational control is also apparent for systems where transcriptional control is not possible, such as cells which lack nuclei such as reticulocytes (Lackner and Bähler, 2008). We have demonstrated one such mechanism mediated by a specific domain within the eukaryote specific C-terminal extension of ribosomal protein L13a. Previously, we have shown that L13a, as a component of the GAIT complex, inhibits the translation initiation of target mRNAs, thereby, resolving the inflammation. It is generally considered that a regulated inflammatory response is beneficial to the host; but at the same time a

dysregulated response can result in an autoimmune attack and prove to be lethal for the host. Therefore, timely resolution of inflammation is critical. L13a mediated translational silencing of inflammatory genes has evolved as an endogenous defense against the uncontrolled inflammation. In our current study, we have identified the translational silencing domain (Arg169-Lys170-Lys171) in the C-terminal extension of human L13a protein. We have experimentally shown that mutating this domain abrogates GAIT-pathway mediated translational silencing activity of L13a. We also studied the role of eukaryote-specific C-terminal extension (149-203AA) of human L13a protein. Such eukaryotic-specific extensions are present in human L13a protein and its homologs from yeast to mammals. Deletion of this C-terminal extension results in the loss of ribosomal incorporation as well as the loss of translational silencing activity of L13a. Moreover, the amino acid sequence of the C-terminal helix compared amongst higher eukaryotes such as mouse, human and bovine is more conserved than lower eukaryotes such as yeast. Therefore, we proposed that this C-terminal extension in higher eukaryotes (mammals) has evolved to play an extra-ribosomal function in resolution of inflammation in the cells of myeloid origin, providing a physiological defense against inflammatory diseases. Such a mechanism is missing in lower eukaryotes. In addition, we have also identified amino acid residues within the C-terminal extension which are essential for ribosomal incorporation of L13a and its interaction with another ribosomal protein L14 on the ribosome surface.

Therefore, this study involving structure/function analysis of ribosomal protein L13a has identified a ribosomal incorporation domain (Lys159, Lys161) and translational silencing domain (Arg169, Lys170, Lys171) within the C-terminal extension of L13a. Interestingly, both these domains are mutually exclusive and work independently.

In this study, we have observed that nuclear import of human L13a is resistant to the deletion of predicted NLS sequences and several other mutations encompassing long stretches of L13a sequence. Only nucleolar import was compromised. Therefore, we speculated that L13a might have some important nuclear role that remains unexplored yet. This study aimed at investigating the consequences of a total knock out of L13a in mouse has put forth an essential role of L13a in embryonic development. Systemic loss of L13a induces embryonic lethality at the morula stage (2.5-3.0 dpc). The observation that L13a is localized in the nuclei of mouse pre-implantation embryos further suggests an important role of L13a in the nucleus.

This interesting observation about the subcellular localization of L13a within the nuclei of human cultured cells and mammalian early embryonic cells needs to be investigated further to understand the diverse roles played by L13a.

REFERENCES

- Andersen, J. S. *et al.* (2002) 'Directed Proteomic Analysis of the Human Nucleolus', *Current Biology*, 12(1), pp. 1–11. doi: 10.1016/S0960-9822(01)00650-9.
- Andersen, J. S. *et al.* (2005) 'Nucleolar proteome dynamics', *Nature*, 433(7021), pp. 77–83. doi: 10.1038/nature03207.
- Arif, A. *et al.* (2011) 'Phosphorylation of glutamyl-prolyl tRNA synthetase by cyclin-dependent kinase 5 dictates transcript-selective translational control', *Proceedings of the National Academy of Sciences*, 108(4), pp. 1415–1420. doi: 10.1073/pnas.1011275108.
- Bange, G. *et al.* (2013) 'New twist to nuclear import: When two travel together', *Communicative & Integrative Biology*, 6(4), p. e24792. doi: 10.4161/cib.24792.
- Basu, A. *et al.* (2014) 'Ribosomal Protein L13a Deficiency in Macrophages Promotes Atherosclerosis by Limiting Translation Control-Dependent Retardation of Inflammation', *Arteriosclerosis, Thrombosis, and Vascular Biology*, 34(3), pp. 533–542. doi: 10.1161/ATVBAHA.113.302573.
- Ben-Shem, A. *et al.* (2011) 'The Structure of the Eukaryotic Ribosome at 3.0 Å Resolution', *Science*, 334(6062), pp. 1524–1529. doi: 10.1126/science.1212642.
- Bouvet, P. *et al.* (1998) 'Nucleolin Interacts with Several Ribosomal Proteins through Its RGG Domain', *Journal of Biological Chemistry*, 273(30), pp. 19025–19029. doi: 10.1074/jbc.273.30.19025.
- BUGLER, B. *et al.* (2005) 'Detection and Localization of a Class of Proteins Immunologically Related to a 100-kDa Nucleolar Protein', *European Journal of*

- Biochemistry*, 128(2–3), pp. 475–480. doi: 10.1111/j.1432-1033.1982.tb06989.x.
- Caizergues-Ferrer, M. *et al.* (1987) ‘Phosphorylation of nucleolin by a nucleolar type NII protein kinase’, *Biochemistry*, 26(24), pp. 7876–7883. doi: 10.1021/bi00398a051.
- DEL CAMPO, M. (2004) ‘Crystal structure of the catalytic domain of RluD, the only rRNA pseudouridine synthase required for normal growth of *Escherichia coli*’, *RNA*, 10(2), pp. 231–239. doi: 10.1261/rna.5187404.
- Chaudhuri, S. *et al.* (2007) ‘Human ribosomal protein L13a is dispensable for canonical ribosome function but indispensable for efficient rRNA methylation’, *RNA*, 13(12), pp. 2224–2237. doi: 10.1261/rna.694007.
- Chen, D. and Huang, S. (2001) ‘Nucleolar components involved in ribosome biogenesis cycle between the nucleolus and nucleoplasm in interphase cells’, *Journal of Cell Biology*, 153(1), pp. 169–176. doi: 10.1083/jcb.153.1.169.
- Das, P. *et al.* (2013) ‘Insights into the Mechanism of Ribosomal Incorporation of Mammalian L13a Protein during Ribosome Biogenesis’, *Molecular and Cellular Biology*, 33(15), pp. 2829–2842. doi: 10.1128/MCB.00250-13.
- Dekel, N. *et al.* (2014) ‘The Role of Inflammation for a Successful Implantation’, *American Journal of Reproductive Immunology*, 72(2), pp. 141–147. doi: 10.1111/aji.12266.
- Dever, T. E. and Green, R. (2012) ‘The Elongation, Termination, and Recycling Phases of Translation in Eukaryotes’, *Cold Spring Harbor Perspectives in Biology*, 4(7), pp. a013706–a013706. doi: 10.1101/cshperspect.a013706.
- Dundr, M. and Raška, I. (1993) ‘Nonisotopic ultrastructural mapping of transcription sites within the nucleolus’, *Experimental Cell Research*. doi: 10.1006/excr.1993.1247.
- Espinar-Marchena, F. *et al.* (2018) ‘Ribosomal protein L14 contributes to the early

- assembly of 60S ribosomal subunits in *Saccharomyces cerevisiae*', *Nucleic Acids Research*, 46(9), pp. 4715–4732. doi: 10.1093/nar/gky123.
- Espinar-Marchena, F. J. *et al.* (2016) 'Role of the yeast ribosomal protein L16 in ribosome biogenesis', *The FEBS Journal*, 283(16), pp. 2968–2985. doi: 10.1111/febs.13797.
- GHISOLFI, L. *et al.* (1992) 'Concerted activities of the RNA recognition and the glycine-rich C-terminal domains of nucleolin are required for efficient complex formation with pre-ribosomal RNA', *European Journal of Biochemistry*, 209(2), pp. 541–548. doi: 10.1111/j.1432-1033.1992.tb17318.x.
- Ghosh, A. and Komar, A. A. (2015) 'Eukaryote-specific extensions in ribosomal proteins of the small subunit: Structure and function', *Translation*, 3(1), p. e999576. doi: 10.1080/21690731.2014.999576.
- Glisovic, T. *et al.* (2008) 'RNA-binding proteins and post-transcriptional gene regulation', *FEBS Letters*, 582(14), pp. 1977–1986. doi: 10.1016/j.febslet.2008.03.004.
- Granneman, S. (2004) 'Ribosome biogenesis: of knobs and RNA processing', *Experimental Cell Research*, 296(1), pp. 43–50. doi: 10.1016/j.yexcr.2004.03.016.
- Green, R. and Noller, H. F. (1996) 'In vitro complementation analysis localizes 23S rRNA posttranscriptional modifications that are required for *Escherichia coli* 50S ribosomal subunit assembly and function.', *RNA (New York, N.Y.)*, 2(10), pp. 1011–21. <http://www.ncbi.nlm.nih.gov/pubmed/8849777>.
- Heine, M. A., Rankin, M. L. and DiMario, P. J. (1993) 'The Gly/Arg-rich (GAR) domain of *Xenopus* nucleolin facilitates in vitro nucleic acid binding and in vivo nucleolar localization.', *Molecular Biology of the Cell*, 4(11), pp. 1189–1204. doi: 10.1091/mbc.4.11.1189.

- Hellen, C. U. T. (2018) 'Translation Termination and Ribosome Recycling in Eukaryotes', *Cold Spring Harbor Perspectives in Biology*, 10(10), p. a032656. doi: 10.1101/cshperspect.a032656.
- Hernandez-Verdun, D. *et al.* (2010) 'The nucleolus: structure/function relationship in RNA metabolism', *Wiley Interdisciplinary Reviews: RNA*, 1(3), pp. 415–431. doi: 10.1002/wrna.39.
- Herrera, A. H. and Olson, M. O. J. (1986) 'Association of protein C23 with rapidly labeled nucleolar RNA', *Biochemistry*, 25(20), pp. 6258–6264. doi: 10.1021/bi00368a063.
- Hustert, E. *et al.* (1996) 'Rbt (rabo torcido), a new mouse skeletal mutation involved in anteroposterior patterning of the axial skeleton, maps close to the ts (tail-short) locus and distal to the sox9 locus on chromosome 11', *Mammalian Genome*, 7(12), pp. 881–885. doi: 10.1007/s003359900261.
- Jackson, R. J., Hellen, C. U. T. and Pestova, T. V. (2010) 'The mechanism of eukaryotic translation initiation and principles of its regulation', *Nature Reviews Molecular Cell Biology*, 11(2), pp. 113–127. doi: 10.1038/nrm2838.
- Jäkel, S. *et al.* (2002) 'Importins fulfil a dual function as nuclear import receptors and cytoplasmic chaperones for exposed basic domains', *The EMBO Journal*, 21(3), pp. 377–386. doi: 10.1093/emboj/21.3.377.
- Jansen, R. P. (1991) 'Evolutionary conservation of the human nucleolar protein fibrillarin and its functional expression in yeast', *The Journal of Cell Biology*, 113(4), pp. 715–729. doi: 10.1083/jcb.113.4.715.
- Jia, J. *et al.* (2012) 'Protection of Extraribosomal RPL13a by GAPDH and Dysregulation by S-Nitrosylation', *Molecular Cell*, 47(4), pp. 656–663. doi:

10.1016/j.molcel.2012.06.006.

Junera HR, Masson C and Hernandez-verdum D (1995) 'The three-dimensional organization of ribosomal genes and the architecture of the nucleoli vary with G1, S and G2 phases.', *J Cell science*, 108, pp. 3427–3441.

Kaczanowska, M. and Ryden-Aulin, M. (2007) 'Ribosome Biogenesis and the Translation Process in Escherichia coli', *Microbiology and Molecular Biology Reviews*, 71(3), pp. 477–494. doi: 10.1128/MMBR.00013-07.

Kapasi, P. *et al.* (2007) 'L13a Blocks 48S Assembly: Role of a General Initiation Factor in mRNA-Specific Translational Control', *Molecular Cell*, 25(1), pp. 113–126. doi: 10.1016/j.molcel.2006.11.028.

Klinge, S. *et al.* (2011) 'Crystal Structure of the Eukaryotic 60S Ribosomal Subunit in Complex with Initiation Factor 6', *Science*, 334(6058), pp. 941–948. doi: 10.1126/science.1211204.

Ko, J.-R. *et al.* (2006) 'Mapping the essential structures of human ribosomal protein L7 for nuclear entry, ribosome assembly and function', *FEBS Letters*, 580(16), pp. 3804–3810. doi: 10.1016/j.febslet.2006.05.073.

Komar, A. A. and Hatzoglou, M. (2005) 'Internal Ribosome Entry Sites in Cellular mRNAs: Mystery of Their Existence', *Journal of Biological Chemistry*, 280(25), pp. 23425–23428. doi: 10.1074/jbc.R400041200.

Kornprobst, M. *et al.* (2016) 'Architecture of the 90S Pre-ribosome: A Structural View on the Birth of the Eukaryotic Ribosome', *Cell*, 166(2), pp. 380–393. doi: 10.1016/j.cell.2016.06.014.

Lafontaine, D. L. J. *et al.* (1998) 'The box H⁺ACA snoRNAs carry Cbf5p, the putative

- rRNA pseudouridine synthase', *Genes & Development*, 12(4), pp. 527–537. doi: 10.1101/gad.12.4.527.
- Lam, Y. W. (2005) 'The nucleolus', *Journal of Cell Science*, 118(7), pp. 1335–1337. doi: 10.1242/jcs.01736.
- Leary, D. J. and Huang, S. (2001) 'Regulation of ribosome biogenesis within the nucleolus', *FEBS Letters*, 509(2), pp. 145–150. doi: 10.1016/S0014-5793(01)03143-X.
- Li, Z., Pandit, S. and Deutscher, M. P. (1999) 'RNase G (CafA protein) and RNase E are both required for the 5' maturation of 16S ribosomal RNA', *The EMBO Journal*, 18(10), pp. 2878–2885. doi: 10.1093/emboj/18.10.2878.
- Maden, B. E. H. (1990) 'The Numerous Modified Nucleotides in Eukaryotic Ribosomal RNA', in, pp. 241–303. doi: 10.1016/S0079-6603(08)60629-7.
- Martin-Marcos, P., Hinnebusch, A. G. and Tamame, M. (2007) 'Ribosomal Protein L33 Is Required for Ribosome Biogenesis, Subunit Joining, and Repression of GCN4 Translation', *Molecular and Cellular Biology*, 27(17), pp. 5968–5985. doi: 10.1128/MCB.00019-07.
- Matsson, H. *et al.* (2004) 'Targeted Disruption of the Ribosomal Protein S19 Gene Is Lethal Prior to Implantation', *Molecular and Cellular Biology*, 24(9), pp. 4032–4037. doi: 10.1128/MCB.24.9.4032-4037.2004.
- Mazumder, B. *et al.* (2003) 'Regulated Release of L13a from the 60S Ribosomal Subunit as A Mechanism of Transcript-Specific Translational Control', *Cell*, 115(2), pp. 187–198. doi: 10.1016/S0092-8674(03)00773-6.
- Mazumder, B. and Fox, P. L. (1999) 'Delayed Translational Silencing of Ceruloplasmin

- Transcript in Gamma Interferon-Activated U937 Monocytic Cells: Role of the 3' Untranslated Region', *Molecular and Cellular Biology*, 19(10), pp. 6898–6905. doi: 10.1128/MCB.19.10.6898.
- Melnikov, S. *et al.* (2015) 'Insights into the origin of the nuclear localization signals in conserved ribosomal proteins', *Nature Communications*, 6(1), p. 7382. doi: 10.1038/ncomms8382.
- Mukhopadhyay, R. *et al.* (2008) 'DAPK-ZIPK-L13a Axis Constitutes a Negative-Feedback Module Regulating Inflammatory Gene Expression', *Molecular Cell*, 32(3), pp. 371–382. doi: 10.1016/j.molcel.2008.09.019.
- Ni, J., Tien, A. L. and Fournier, M. J. (1997) 'Small Nucleolar RNAs Direct Site-Specific Synthesis of Pseudouridine in Ribosomal RNA', *Cell*, 89(4), pp. 565–573. doi: 10.1016/S0092-8674(00)80238-X.
- Nierhaus, K. H. (1980) 'The assembly of the prokaryotic ribosome', *Biosystems*, 12(3–4), pp. 273–282. doi: 10.1016/0303-2647(80)90024-6.
- O'Day, C. (1996) '18S rRNA processing requires the RNA helicase-like protein Rrp3', *Nucleic Acids Research*, 24(16), pp. 3201–3207. doi: 10.1093/nar/24.16.3201.
- Ofengand, J. and Bakin, A. (1997) 'Mapping to nucleotide resolution of pseudouridine residues in large subunit ribosomal RNAs from representative eukaryotes, prokaryotes, archaeobacteria, mitochondria and chloroplasts 1 Edited by D. E. Draper', *Journal of Molecular Biology*, 266(2), pp. 246–268. doi: 10.1006/jmbi.1996.0737.
- Olson, M. O. J., Hingorani, K. and Szebeni, A. (2002) 'Conventional and nonconventional roles of the nucleolus.', *International review of cytology*, 219, pp. 199–266.

Available at: <http://www.ncbi.nlm.nih.gov/pubmed/12211630>.

- Østergaard, P. *et al.* (1998) 'Assembly of proteins and 5 S rRNA to transcripts of the major structural domains of 23 S rRNA 1 Edited by D. E. Draper', *Journal of Molecular Biology*, 284(2), pp. 227–240. doi: 10.1006/jmbi.1998.2185.
- P. Bouvet *et al.* (1999) 'Structure and functions of nucleolin', *Journal of Cell Science* .
- Pederson, T. (1998) 'Growth factors in the nucleolus?', *The Journal of cell biology*, 143(2), pp. 279–81. doi: 10.1083/jcb.143.2.279.
- Plafker, S. M. and Macara, I. G. (2002) 'Ribosomal Protein L12 Uses a Distinct Nuclear Import Pathway Mediated by Importin 11', *Molecular and Cellular Biology*, 22(4), pp. 1266–1275. doi: 10.1128/MCB.22.4.1266-1275.2002.
- Poddar, D. *et al.* (2013) 'An Extraribosomal Function of Ribosomal Protein L13a in Macrophages Resolves Inflammation', *The Journal of Immunology*, 190(7), pp. 3600–3612. doi: 10.4049/jimmunol.1201933.
- Poddar, D. *et al.* (2016) 'L13a-dependent translational control in macrophages limits the pathogenesis of colitis', *Cellular & Molecular Immunology*, 13(6), pp. 816–827. doi: 10.1038/cmi.2015.53.
- Powers, T., Daubresse, G. and Noller, H. F. (1993) 'Dynamics of In Vitro Assembly of 16S rRNA into 30S Ribosomal Subunits', *Journal of Molecular Biology*, 232(2), pp. 362–374. doi: 10.1006/jmbi.1993.1396.
- Roussel, P. (1996) 'The rDNA transcription machinery is assembled during mitosis in active NORs and absent in inactive NORs', *The Journal of Cell Biology*, 133(2), pp. 235–246. doi: 10.1083/jcb.133.2.235.
- Rout, M. P., Blobel, G. and Aitchison, J. D. (1997) 'A Distinct Nuclear Import Pathway

- Used by Ribosomal Proteins', *Cell*, 89(5), pp. 715–725. doi: 10.1016/S0092-8674(00)80254-8.
- Sampath, P. *et al.* (2003) 'Transcript-Selective Translational Silencing by Gamma Interferon Is Directed by a Novel Structural Element in the Ceruloplasmin mRNA 3' Untranslated Region', *Molecular and Cellular Biology*, 23(5), pp. 1509–1519. doi: 10.1128/MCB.23.5.1509-1519.2003.
- Sampath, P. *et al.* (2004) 'Noncanonical Function of Glutamyl-Prolyl-tRNA Synthetase', *Cell*, 119(2), pp. 195–208. doi: 10.1016/j.cell.2004.09.030.
- Sansam, C. L., Wells, K. S. and Emeson, R. B. (2003) 'Modulation of RNA editing by functional nucleolar sequestration of ADAR2', *Proceedings of the National Academy of Sciences*, 100(24), pp. 14018–14023. doi: 10.1073/pnas.2336131100.
- Saveanu, C. *et al.* (2003) 'Sequential Protein Association with Nascent 60S Ribosomal Particles', *Molecular and Cellular Biology*, 23(13), pp. 4449–4460. doi: 10.1128/MCB.23.13.4449-4460.2003.
- Scheer, U., Thiry, M. and Goessens, G. (1993) 'Structure, function and assembly of the nucleolus', *Trends in Cell Biology*. doi: 10.1016/0962-8924(93)90123-I.
- Scherl, A. *et al.* (2002) 'Functional Proteomic Analysis of Human Nucleolus', *Molecular Biology of the Cell*. Edited by J. Gall, 13(11), pp. 4100–4109. doi: 10.1091/mbc.e02-05-0271.
- Schwarzacher, H. G. and Mosgoeller, W. (2000) 'Ribosome biogenesis in man: Current views on nucleolar structures and function', *Cytogenetic and Genome Research*. doi: 10.1159/000056853.
- Simón, C. *et al.* (1998) 'Cytokines and embryo implantation.', *Journal of reproductive*

immunology, 39(1–2), pp. 117–31. Available at:
<http://www.ncbi.nlm.nih.gov/pubmed/9786457>.

Snow, M. H. L. (1977) ‘Gastrulation in the mouse: Growth and regionalization of the epiblast’. doi: 42: 293-303.

Sonenberg, N. and Hinnebusch, A. G. (2009) ‘Regulation of Translation Initiation in Eukaryotes: Mechanisms and Biological Targets’, *Cell*, 136(4), pp. 731–745. doi: 10.1016/j.cell.2009.01.042.

Stagg, S. M., Mears, J. A. and Harvey, S. C. (2003) ‘A Structural Model for the Assembly of the 30S Subunit of the Ribosome’, *Journal of Molecular Biology*, 328(1), pp. 49–61. doi: 10.1016/S0022-2836(03)00174-8.

Tollervey, D. *et al.* (1993) ‘Temperature-sensitive mutations demonstrate roles for yeast fibrillarin in pre-rRNA processing, pre-rRNA methylation, and ribosome assembly’, *Cell*. doi: 10.1016/0092-8674(93)90120-F.

Tollervey, D. and Kiss, T. (1997) ‘Function and synthesis of small nucleolar RNAs’, *Current Opinion in Cell Biology*, 9(3), pp. 337–342. doi: 10.1016/S0955-0674(97)80005-1.

Tutuncuoglu, B. *et al.* (2016) ‘The N-terminal extension of yeast ribosomal protein L8 is involved in two major remodeling events during late nuclear stages of 60S ribosomal subunit assembly’, *RNA*, 22(9), pp. 1386–1399. doi: 10.1261/rna.055798.115.

Vyas, K. *et al.* (2009) ‘Genome-Wide Polysome Profiling Reveals an Inflammation-Responsive Posttranscriptional Operon in Gamma Interferon-Activated Monocytes’, *Molecular and Cellular Biology*, 29(2), pp. 458–470. doi:

10.1128/MCB.00824-08.

Zatsepina, O. V. *et al.* (1993) 'The RNA polymerase I-specific transcription initiation factor UBF is associated with transcriptionally active and inactive ribosomal genes', *Chromosoma*. Springer-Verlag, 102(9), pp. 599–611. doi: 10.1007/BF00352307.